Graduate School Form 30
(Revised 08/14)

PURDUE UNIVERSITY
GRADUATE SCHOOL
Thesis/Dissertation Acceptance

This is to certify that the thesis/dissertation prepared

By Danika M. Tumbleson

Entitled
Treatment and Genetic Analysis of Craniofacial Deficits Associated with Down Syndrome

For the degree of Master of Science

Is approved by the final examining committee:

Randall J. Roper

Teri Belecky-Adams

Robert Yost

Christine Picard

To the best of my knowledge and as understood by the student in the Thesis/Dissertation Agreement, Publication Delay, and Certification/Disclaimer (Graduate School Form 32), this thesis/dissertation adheres to the provisions of Purdue University's "Policy on Integrity in Research" and the use of copyrighted material.

Randall J. Roper

Approved by Major Professor(s): _____

_____

Approved by: Simon Atkinson 11/20/2014

Head of the Department Graduate Program Date

TREATMENT AND GENETIC ANALYSIS OF CRANIOFACIAL DEFICITS ASSOCIATED WITH DOWN SYNDROME

A Thesis

Submitted to the Faculty

of

Purdue University

by

Danika M. Tumbleson

In Partial Fulfillment of the

Requirements for the Degree

of

Master of Science

December 2014

Purdue University

Indianapolis, Indiana

To my husband and family, for your unvarying encouragement, love and support that continually inspire me to grow and achieve.

ACKNOWLEDGMENTS

I would like to thank my advisor, Dr. Randall Roper, for his mentoring, guidance, teaching, and enthusiasm for science. During my graduate studies, I have become a better critical thinker, researcher, teacher, and mentor because of his example. I would also like to acknowledge Dr. Kathleen Marrs, for her past mentorship during the GK-12 Education Program and for her continued support during my time as a graduate student. Under her mentorship, I found a passion for teaching and through her found the resources to improve and refine those skills. I would also like to thank the many others who helped with this reseach, including Samantha Deitz, Alex Chom, Emily Haley, Mariyamou Diallo, Gracelyn Bose, Susanna Angermeier, Rachel Novack for your hard work and more importantly your friendship.

TABLE OF CONTENTS

Page

Page

Page

LIST OF TABLES

LIST OF FIGURES

Figure Page

ABSTRACT

Tumbleson, Danika M. M.S., Purdue University, December 2014. Treatment and Genetic Analysis of Craniofacial Deficits Associated With Down Syndrome. Major Professor: Randall J. Roper.

Down syndrome (DS) is caused by trisomy of human chromosome 21 (Hsa21) and occurs in ~1 of every 700 live births. Individuals with DS present craniofacial abnormalities, specifically an undersized, dysmorphic mandible which may lead to difficulty with eating, breathing, and speech. Using the Ts65Dn DS mouse model, which mirrors these phenotypes and contains three copies of ~50% Hsa21 homologues, our lab has traced the mandibular deficit to a neural crest cell (NCC) deficiency in the first pharyngeal arch (PA1 or mandibular precursor) at embryonic day 9.5 (E9.5). At E9.5, the PA1 is reduced in size and contains fewer cells due to fewer NCC populating the PA1 from the neural tube (NT) as well as reduced cellular proliferation in the PA1. We hypothesize that both the deficits in NCC migration and proliferation may cause the reduction in size of the PA1. To identify potential genetic mechanisms responsible for trisomic PA1 deficits, we generated RNA-sequence (RNA-seq) data from euploid and trisomic E9.25 NT and E9.5 PA1 (time points occurring before and after observed deficits) using a next-generation sequencing platform. Analysis of RNA-seq data revealed differential trisomic expression of 53 genes from E9.25 NT and 364 genes from E9.5 PA1, five of which are present in three copies in Ts65Dn. We also further analyzed

the data to find that fewer alternative splicing events occur in trisomic tissues compared to euploid tissues and in PA1 tissue compared to NT tissue. In a subsequent study, to test gene-specific treatments to rescue PA1 deficits, we targeted *Dyrk1A*, an overexpressed DS candidate gene implicated in many DS phenotypes and predicted to cause the NCC and PA1 deficiencies. We hypothesize that treatment of pregnant Ts65Dn mothers with Epigallocatechin gallate (EGCG), a known Dyrk1A inhibitor, will correct NCC deficits and rescue the undersized PA1 in trisomic E9.5 embryos. To test our hypothesis, we treated pregnant Ts65Dn mothers with EGCG from either gestational day 7 (G7) to G8 or G0 to G9.5. Our study found an increase in PA1 volume and NCC number in trisomic E9.5 embryos after treatment on G7 and G8, but observed no significant improvements in NCC deficits following G0-G9.5 treatment. We also observed a developmental delay of embryos from trisomic mothers treated with EGCG from G0-G9.5. Together, these data show that timing and sufficient dosage of EGCG treatment is most effective during the developmental window the few days before NCC deficits arise, during G7 and G8, and may be ineffective or harmful when administered at earlier developmental time points. Together, the findings of both studies offer a better understanding of potential mechanisms altered by trisomy as well as preclinical evidence for EGCG as a potential prenatal therapy for craniofacial disorders linked to DS.

CHAPTER 1. INTRODUCTION

1.1 Overview of Down Syndrome

Down syndrome (DS) occurs in ~1/700 live births (Parker *et al.* 2010) and is caused by trisomy of human chromosome 21 (Hsa21). DS is the most common live born chromosomal aneuploidy and the most common genetic cause of intellectual disability (ID). In addition to this phenotype, individuals display alterations in many tissues and organ systems including varied facial features, congenital heart defects, skeletal deficiencies, hypotonia, gastrointestinal disease, and shortened stature. However, these phenotypes present with varying penetrance and severity. The mechanism by which Trisomy 21 causes variability in the expression of phenotypes is not fully understood. However, current research has made progress in identifying genotype-phenotype correlations in DS.

Down syndrome was first described in 1846 by Édouard Onésimus Séguin, who later became the first president of the American Association for Mental Deficiency. He was a founder of methods for educating those in France and the United States to those considered to display mental retardation. Although he was the first to describe the disorder, evidence of DS exists in the archaeological record as early as 500 A.D. in Mexican terra-cotta (Martinez-Frias 2005) and in many European paintings from 1500

A.D. onward (Berg and Korossy 2001). In 1866, John Langdon Down, for whom DS is named, described the group of phenotypes that were later named after him. He correctly described several of the characteristic facial features including a 'face that is flat and broad', has a 'very narrow palpebral fissure', and a tongue that 'is long, thick, and much roughened' (Down 1866; Neri and Opitz 2009). It was not until almost 100 years later, following the development of karyotyping technology, that Jerome Lejeune and Patricia Jacobs identified an extra copy of chromosome 21 as the genetic cause of DS (Lejeune *et al.* 1959a; Lejeune *et al.* 1959b). Since the genetic cause of DS was identified, great progress has been made in DS research including a better characterization of phenotypes, creation of mouse models of trisomy, and the sequencing of chromosome 21 in 2000 (Hattori *et al.* 2000; Megarbane *et al.* 2009). This progress, along with improvements in medical care and increased socialization over the last several decades, have led to an increased life expectancy of over 50 years of age for individuals with DS (Coppus 2013).

1.2 Genetic Basis and Incidence of Trisomy 21

Trisomy 21 most commonly develops as a result of non-disjunction of a whole or part of Hsa21 during Meiosis I or II in the developing gametes. Trisomy occurs most often when chromosomes do not separate properly and remain together in the same oocyte or sperm (Figure 1.1). In 88% of cases, the gamete carrying the extra chromosome is transmitted from the oocyte, while only 8% of cases originate from the sperm, and 4% originate mitotically (Antonarakis 1991; Muller *et al.* 2000). Although more rare, Trisomy 21 can also be caused by translocation of Hsa21 or display as a

mosaicism where the genome consists of a mix of trisosmic and euploid cells. Trisomy 21 occurs randomly and its incidence is not heritable in most cases. Any heritability in Trisomy 21 usually occurs when the trisomy is caused by a translocation of Hsa21.

The only factor correlated with an increased incidence of DS is advanced maternal age (Allen *et al.* 2009). No correlation has been made between Trisomy 21 pregnancies within any particular ethnicity, socio-economic status, or with smoking or alcohol consumption habits during pregnancy. However, more babies with DS are born in certain countries and within certain ethnic groups because of discrepancies in choice to terminate the fetus following a DS diagnosis (Guedj and Bianchi 2013). It is hypothesized that higher rates of DS occur in mothers over 35 years of age because the cellular machinery in the egg breaks down as the age of the egg increases. Although incidence of DS increases with maternal age, the overall birth rate of babies with DS is higher in younger women, since more babies are born to women under 35 (Huether *et al.* 1998; Driscoll and Gross 2009).

1.3 Prenatal Diagnosis of Down Syndrome

Prenatal testing is commonly practiced with the purpose of detecting fetal aneuploidies, specifically trisomies 13, 18, 21 and aneuploidies related to the X and Y chromosome (Gorzelnik *et al.* 2013; Lim *et al.* 2013). The majority of aneuploidies result in natural fetal termination, usually within the first trimester. However, Trisomy 21

displays the highest survival rate, affecting 1 in 700 live births (Parker *et al.* 2010). For this reason, prenatal testing is most utilized in detection of Trisomy 21 (Lim *et al.* 2013).

Currently, several procedures exist to detect Trisomy 21 and include both prenatal screening and prenatal testing procedures. Prenatal screening tests such as the nuchal translucency test and non-invasive prenatal testing (NIPT) are used to provide initial risk assessment of fetal chromosomal abnormalities. They are easy to perform, present negligible risk to the fetus or mother, and are non-invasive (Lim *et al.* 2013). Although these screening tests do not provide a definitive diagnosis, they are powerful tools in helping to make a decision whether to undergo further invasive testing to obtain a diagnosis. To establish a Trisomy 21 diagnosis, prenatal diagnostic testing procedures such as chorionic villus sampling (CVS) or amniocentesis are routinely used. These tests, however, are invasive and present a small risk to the fetus. When making decisions about prenatal screening or diagnostic testing, it is common for patients to be referred for genetic counseling to facilitate the decision making process.

1.3.1 Nuchal Translucency Test

Prenatal screening tests are usually performed in the first trimester. Nuchal translucency testing in particular is performed at 11-14 weeks during pregnancy. This test uses ultrasound to assess the quantity of fluid in the tissue at the nape of the fetus's neck. Fetuses with DS tend to have a greater amount of fluid around the neck. This test is often combined with analysis of maternal age and maternal plasma to detect pregnancy

associated plasma protein-A (PAPP-A) and free beta-human chorionic gonadotropin (β-hCG) to provide a more accurate risk estimation for chromosomal aneuploidy (Malone *et al.* 2005). Although these prenatal screening tests cannot confirm a DS diagnosis, they are valuable tools as they identify more than 90% of DS cases with a 5% false positive rate (Lim *et al.* 2013).

1.3.2 Non-invasive Prenatal Testing

As a more potent screening test for DS, NIPT is rapidly evolving as a prenatal diagnostic tool for DS with the advent of next-generation sequencing technologies. It requires only a blood sample from the mother and can be performed easily, at low cost, and at negligible risk to the fetus (Daley *et al.* 2014). The test measures low levels of cell-free fetal DNA (cffDNA) circulating freely in the maternal bloodstream. DNA in the blood is sequenced and ratios of DNA from Hsa21 analyzed. A mother carrying a fetus with DS will show higher levels of DNA from Hsa21 relative to that of other chromosomes. Although this test provides advantages over invasive procedures in cost and fetal risk, it is limited by the amount of cffDNA detectable in maternal blood, which is usually only 3-5%. However, NIPT has been reported to detect cases of DS as early as 6-10 weeks during pregnancy and has a high detection rate for DS (99-100%) with a low false positive rate (<1%) (Bianchi *et al.* 2012; Norton *et al.* 2012; Palomaki *et al.* 2012). This test is becoming more widely used and with continued development may replace invasive tests such as amniocentesis and CVS in the future.

1.3.3 Amniocentesis and Chorionic Villus Sampling

Once prenatal screening tests have indicated the fetus is at risk for a chromosomal aneuploidy, invasive testing using amniocentesis or chorionic villus sampling (CVS) can be performed to provide a definitive diagnosis. Amniocentesis is performed by taking a small amount of amniotic fluid from the placenta through a fine needle inserted through the abdomen. CVS is performed by taking a small sample of cells from the amniotic sac where it attaches to the wall of the uterus. These tests carry several disadvantages; however, amniocentesis and CVS sampling both carry significant risks of damaging a healthy fetus. They have a 1% miscarriage rate, are costly, and require expert technicians (Lim *et al.* 2013). Despite these risks, amniocentesis and CVS are estimated to be 98-99% accurate in the diagnosis of DS (ACOG Practice Bulletin No. 88, 2007; Wilson *et al.* 2013). These tests are most often used to confirm a DS diagnosis after NIPT and nuchal translucency tests have indicated the fetus has a high risk of carrying DS.

1.3.4 Current Trends in Prenatal Testing for Down Syndrome

The importance of prenatal screening and testing procedures in DS is growing as it provides the basis of decisions regarding future fetal and prenatal care. Several studies have noted both positive and negative effects of the increased commonality of prenatal diagnostics in DS. With the increase in average maternal age observed in the last 10-15 years worldwide, there has also been an increase in the prevalence of DS cases, which includes still births, live births and terminated affected pregnancies (Loane *et al.* 2013).

However, with increased availability of prenatal screening and testing, the number of DS live births has remained largely unchanged as there is a growing trend in choice to terminate an affected pregnancy following a DS diagnosis. This trend holds true in many European countries where prenatal screening and testing is readily available, but does not hold true in all countries worldwide; the percentage of DS live births per DS case vary widely between countries depending on availability of testing, government policy, ethnicity and attitudes towards fetal termination (Morris and Alberman 2009; Cocchi *et al.* 2010; van Gameren-Oosterom *et al.* 2012; Loane *et al.* 2013). Although there has been an overall growing trend towards increased termination of DS pregnancies, there are still many mothers who opt to carry a DS pregnancy to term and raise a child with DS. Studies of mothers who chose to keep their child with DS and had a DS prenatal diagnosis indicate that the diagnosis was beneficial for them during their pregnancy. Mothers who chose to keep their child with DS who did not have a prenatal diagnosis but received one at their child's birth also indicated that an early diagnosis would have been beneficial during their pregnancy (Ralston *et al.* 2001).

In the future with continued research, early diagnosis of a DS pregnancy may offer an opportunity for prenatal treatment of an affected fetus during a small window of development where phenotypes associated with DS can be preventatively improved. Many studies have already found that such prenatal treatment can positively impact brain development and improve postnatal neurocognition and behavior in DS mouse models (Guedj and Bianchi 2013). The importance of prenatal diagnosis will continue to increase

as further study and development of prenatal treatments may provide additional options for those carrying a fetus with DS.

1.4 Gene Dosage Imbalance in Trisomy 21

The mechanism by which gene dosage imbalance in Trisomy 21 causes characteristic DS phenotypes is not well understood. However, the presence of an extra copy of Hsa21 is known to disrupt developmental gene pathways in DS. In particular, the increased gene copy number of the triplicated ~350 protein-coding Hsa21 genes causes dysregulation of both trisomic and non-trisomic genes in related downstream pathways (Kahlem *et al.* 2004; Chou *et al.* 2008; Billingsley *et al.* 2013; Letourneau *et al.* 2014) and often in genes involved in regulating developmental processes. Current research has focused on identifying genotype-phenotype correlations. This has proved difficult as individuals carrying complete Trisomy 21 display many phenotypes with widely varying severity. However, progress has been made in identifying genotype-phenotype correlations. These approaches have included mapping of human partial Trisomy 21 cases (Korbel *et al.* 2009), construction of partial trisomy mouse models, and gene expression analysis studies in cells and tissues of individuals with DS and in mouse models of DS (Lyle *et al.* 2009).

1.5 Down Syndrome Phenotype

Individuals with DS may display over 80 clinical phenotypes that vary widely in severity. Some features are common to all individuals with DS to varying degrees including characteristic facial dysmorphology, intellectual disability, a small, hypocellular brain, and early onset Alzheimer's disease (Roper & Reeves 2006). There is also an increased risk for many other conditions including congenital heart defects (40-50% of cases), incidence of childhood leukemia, and Hirschsprung disease. Many individuals also display skeletal deficiencies and hypotonia, or low muscle tone. At birth, hypotonia is often used as an indicator of DS if the condition was undetected during pregnancy. Although many of the phenotypes associated with DS present challenges, higher rates in the suppression of solid tumor growth is observed and the incidence rate of many cancers is significantly reduced in the DS population (Sussan *et al.* 2008; Baek *et al.* 2009)

1.5.1 Craniofacial Phenotype

All individuals with DS display some form of characteristic facial dysmorphology (Roper and Reeves, 2006). This characteristic dysmorphology of the face results mainly from malformation of the underlying craniofacial skeleton (Richtsmeier *et al.* 2002). Compared to humans with a normal chromosome compliment, DS craniofacial structure is characterized by an overall reduction in head size, flattened occiput, a small midface and reduced facial height, flattened nasal bridge, mediolaterally reduced orbital region, reduced bizygomatic breadth, small maxilla and mandible, brachycephaly, and dental anomalies (Richtsmeier *et al.* 2000; Richtsmeier *et al.* 2002; Shott 2006; Starbuck *et al.*

2013). These alterations in craniofacial structures contribute to differences in soft tissue structure including upslanting palpebral fissures and inner epicanthic folds (Epstein 2001). Although these phenotypes are displayed in all individuals with DS, there is a great deal of individual variability in the severity of expression of these phenotypes.

Altered structure of the craniofacial skeleton in DS, particularly the small jaw and oral cavity, impacts the structure or function of many orofacial structures including the airways and tongue, causing impaired eating, breathing, and speech (Hennequin *et al.* 1999; Shott 2006; Faulks *et al.* 2008; Billingsley *et al.* 2013). In particular, individuals with DS often display tongue hyper portrusion as a result of the reduced size of the mandible causing a relative macroglossia. (Hennequin *et al.* 1999; Guimaraes *et al.* 2008). The relative macroglossia and reduced oral cavity contribute to complications with the development of suckling, mastication, swallowing and speech (Hennequin *et al.* 1999). It is reported that 57-68% of newborns and children with DS have feeding problems (Spender *et al.* 1996; Spahis and Wilson 1999) which may persist through adulthood with as many as 25% of adults with DS reporting eating difficulties (Hennequin *et al.* 2000). Orofacial alterations can also lead to a constricted airway which can cause subglottic stenosis and obstructive sleep apnea (Shott 2006). This can result in fatigue during the day which has been reported to cause additional challenges in learning ability. Speech development is also hindered in part by orofacial alterations, and additionally by learning disabilities and hearing loss in some cases (Kent and Vorperian 2013). Together, these alterations can prevent individuals with DS from reaching their full developmental potential and reduce their quality of life.

1.6 Mouse Models of Down Syndrome

Animal models have been of great use in understanding growth and early development in DS. Because mammals share conserved gene homology, research with animals has led to a greater understanding of genotype-phenotype correlations in humans. Knowledge of these correlations has aided in the discovery of underlying causes of many genetic disorders and various diseases and have led to proposed treatments. Mouse models in particular are used to model many human conditions because of conserved gene homology, low cost of maintenance, and high fecundity, allowing developmental progression to be studied at a quickened rate (Frick *et al.* 2013).

The trisomic genes found on Hsa21 are also found grouped on three chromosomes in the mouse. In particular, the long arm of Hsa21 is 33.7 Mb in size and contains approximately 444 genes with homologues on mouse chromosomes 10, 16, and 17 (Sturgeon and Gardiner 2011). Of the 444 Hsa21 genes, about two-thirds have a gene homologue on Mmu16, while the remaining third can be found on Mmu10 and Mmu 17. Several mouse models have been created that provide partial trisomies modeling DS. The Ts65Dn mouse model, containing segmental trisomy of ~104 Hsa21 genes, is the most utilized mouse model and mirrors many of the phenotypes associated with DS including the craniofacial phenotype. Other less utilized models such as the Ts1Cje, Ms1Ts65, Ts1Rhr, Dp1Yey, Dp2Yey, and Dp3Yey also contain genes at dosage imbalance and but display less of the characteristic DS phenotypes (Sérégaza *et al.* 2006; Moore and Roper 2007; Rueda *et al.* 2012).

Another model, the Tc1 mouse, contains ~90% of Hsa21, but displays the extra chromosome only mosaically (Moore and Roper 2007; Rueda *et al.* 2012).

1.6.1 Ts65Dn Mouse Model

The Ts65Dn mouse model contains an extra chromosome carrying the telomeric end of mouse chromosome 16 (Mmu16) attached to the small centromeric end of Mmu17 (Davisson *et al.* 1993; Reeves *et al.* 1995) (Figure 1.2). The Ts65Dn mouse model was created by Muriel Davisson and colleagues at the Jackson Laboratory by producing reciprocal translocations through irradiation of the testes of male DBA/2J (D2) mice. After breeding males with C57BL/6J (B6) females, F1 offspring were screened for specific chromosome aberrations until a significant translocation was identified (Davisson *et al.* 1990). The specific translocation identified contained the extra chromosome carrying the telomeric end of Mmu16 attached to the small centromeric end of Mmu17 (Davisson *et al.* 1993; Reeves *et al.* 1995). This extra chromosome contains 12-15 Mb of Mmu16, a region conserved with the Hsa21 region 21q21-22.3 (Reeves *et al.* 1995; Baxter *et al.* 2000). Together, this produces a segmental trisomy which contains ~104 Hsa21 homologues, making the Ts65Dn mouse at dosage imbalance for ~50% of total Hsa21 genes (Reeves *et al.* 1995; Hattori *et al.* 2000) (Figure 1.2).

1.6.1.1 Ts65Dn Phenotypes

Many studies have been performed to evaluate how the Ts65Dn mouse models human DS phenotypes. Thus far, the Ts65Dn mouse has been shown to mirror DS phenotypes in neurologic and brain deficiencies (Baxter *et al.* 2000), learning, memory and hearing deficits (Reeves *et al.* 1995), reduced birth weight (Roper *et al.* 2006b), a weakened skeletal phenotype (Blazek *et al.* 2011), heart malformations (MOORE 2006), and alterations in craniofacial morphology (Richtsmeier *et al.* 2000; Richtsmeier *et al.* 2002). Using 3D morphometric analysis, it has been shown that Ts65Dn mice mirror specific craniofacial dysmorphologies displayed in humans with DS including an overall reduction in head dimensions, a small midface, mediolaterally reduced orbital region, reduced maxilla and mandible, and brachycephaly (Figure1.3) (Richtsmeier *et al.* 2000). Ts65Dn mice also display brain deficiencies including a hypocellular brain, adisproportionately reduced cerebellum, and several neuropathological changes including a reduced number of Purkinje cells and granule cell neurons and reduced cell proliferation in the dentate gyrus (Insausti *et al.* 1998; Belichenko *et al.* 2004; Roper *et al.* 2006a). Ts65Dn female mice also display reduced fertility and male mice are functionally sterile. Increased perinatal lethality is also present in Ts65Dn mice (Roper *et al.* 2006b). Although on average, ~50% of pups in each litter are trisomic at birth, many trisomic pups die after birth, leaving only ~30% of trisomic pups in each litter by three weeks postnatally (Reeves *et al.* 1995; Moore 2006; Roper *et al.* 2006b).

1.7 Neural Crest and Craniofacial Development

Neural crest cells (NCC) are a pluripotent cell population that differentiates into a variety of cell types and provides the main source of craniofacial mesenchyme for the formation of the craniofacial skeleton. In mammals, NCC originate from the tip or 'crest' of the open neural fold which closes to become the neural tube (NT) (Santagati and Rijli 2003)(Figure 1.4). Depending on the region of the NT from which NCC emigrate, NCC will become cranial, cardiac, trunk, or vagal NCC, each of which will differentiate to become diverse sets of tissue types. In order for NCC to form their intended tissue types, several steps must occur including migration of sufficient NCC from the NT to their intended destination, differentiation into intended cell types, and successful proliferation of the cells in the developing tissue (Figure 1.5). In order for cells to differentiate and become a specified cell type, cells must be induced to a specific cell fate by an extracellular inductive signal such as bone morphogenic protein (BMP) or fibroblast growth factor (FGF) (Knecht and Bronner-Fraser 2002). These signals differ between developing environments and make possible the development of multiple cell and tissue types from uniform pluripotent NCC lines. NCC migrating from the region of the NT near the developing head arise from the diencephalon, midbrain, and hindbrain to form cranial NCC. Cranial NCC have the ability to differentiate into various mesenchymal derivatives such as cartilage, bone and connective tissue in the head, in addition to neurons and glia cells of the peripheral nervous system (Knecht and Bronner-Fraser 2002; Zhao *et al.* 2006). Rostral cranial NCC form the frontonasal skeleton while cranial NCC migrating to the pharyngeal arches differentiate to form the cartilage and bone of

the jaw, middle ear, and neck (Santagati and Rijli 2003) (Figure 1.6). In the formation of the mandible, cells travel from the NT to populate the first pharyngeal arch (PA1), the closest pharyngeal arch to the developing head (Roper and Reeves 2006) (Figure 1.7). Understanding the role of NCC in craniofacial development may help to identify the origins of NCC-related deficiencies causing many of the DS phenotypes.

1.7.1 Mandibular and First Pharyngeal Arch Phenotype

Individuals with DS display a dysmorphic, undersized mandible compared to normal individuals that causes difficulties with eating, breathing, speech, and sleep (Richtsmeier *et al.* 2000). In Ts65Dn mice, the PA1, the NCC derived structure that develops into the mandible, is smaller in trisomic embryos by embryonic day 9.5 (E9.5) (Figure 1.8). In Ts65Dn embryos aged 9.25 days from conception (E9.25), the size of the PA1 is comparable to euploid littermates. However, by E9.5 (six hours later) the size of the PA1 in trisomic embryos becomes reduced in both the number of NCC and overall volume of the PA1 (Roper *et al.* 2009). This deficiency is present from E9.5 onward, persists at E13.5, and is never recovered. These deficiencies arise from a decrease in the number of NCC migrating from the neural tube, a reduction in number of proliferating cells, and generation of new cells within the PA1 (Roper *et al.* 2009). These findings suggest that gene dosage imbalance caused by trisomy occurring in the 6 hour window of development between E9.25 and E9.5 alters development of NCC-derived tissues through the altering gene networks involved in NCC migration and proliferation.

1.8 *DYRK1A*: A Candidate Gene for Down Syndrome

Much of the recent DS research has focused on identifying candidate genes or gene regions found on Hsa21 as the cause of specific DS phenotypes. Dual-specificity tyrosine phosphorylation kinase 1A (*DYRK1A*) is a DS candidate gene found in three copies and located on the 21q22.2 region of Hsa21. It has been implicated to contribute to many of the DS phenotypes, specifically to alterations in brain and intellectual ability associated with DS (Courcet *et al.* 2012). *DYRK1A* is a serine-threonine kinase known to phosphorylate several transcription factors and functions as a cell cycle regulator (Soppa *et al.* 2014). Specifically, it regulates proteins involved in brain and neuronal development (Tejedor and Hammerle 2011) including neuronal differentiation and has been linked to several neurodegenerative diseases including Alzheimer's disease (Wegiel *et al.* 2011; Mazur-Kolecka *et al.* 2012). *DYRK1A* is overexpressed ~1.5-fold in many tissues including human DS fetal brains and its homologue in mice has been shown to be overexpressed in a temporal spatial dependent manner in many developing tissues in Ts65Dn mice and embryos including the Ts65Dn E9.5 PA1 (Deitz, S. Unpublished Data). Overexpression of *Dyrk1a* in mice has been shown to lead to learning and memory deficits (Altafaj *et al.* 2001) and brain developmental abnormalities (BRANCHI *et al.* 2004), including delayed neuronal differentiation (Kurabayashi and Sanada 2013), and altered neurogenesis (Thomazeau *et al.* 2014). It has also been implicated to cause alterations in cell cycle regulation (Branchi *et al.* 2004; Chen *et al.* 2013; Soppa *et al.* 2014) cause motor dysfunction (Martinez de Lagran *et al.* 2004), and potentially alter craniofacial development (Solzak *et al.* 2013). Research suggests that overexpression of

Dyrk1a protein destabilizes gene pathways involved in development and cell cycle regulation resulting in these phenotypes. In particular, overexpression of Dyrk1a protein is thought to destabilize an important developmental regulatory circuit involving NFATc, a nuclear factor of activated T-cells (Arron *et al.* 2006) (Figure 1.9). NFATc is a regulator of vertebrate development with known roles in development of cardiac tissue, muscle, nervous system, and in certain immune responses. The 1.5-fold overexpression of Dyrk1a is thought to prevent nuclear occupancy of NFATc, causing a failure to activate NFATc transcription factors involved in development. Tests in NFATc deficient mice suggest reduced NFATc levels cause many of the DS phenotypes. In addition to NFATc, Dyrk1a also phosphorylates other proteins including APP and TAU, known to be involved in Alzheimer pathogenesis, and CYCLINL2, involved in cell cycle regulation (Figure 1.10). A great deal of recent research has focused on correcting Dyrk1a overexpression in mice to test the hypothesis that Dyrk1a overexpression is sufficient to induce many of the DS phenotypes. By normalizing Dyrk1a levels through alterations of *Dyrk1a* copy number or Dyrk1a protein expression in transgenic mice, many studies have reported improved learning (Souchet *et al.* 2014) improved or corrected brain phenotypes (Altafaj *et al.* 2013; Pons-Espinal *et al.* 2013) and motor alterations (Ortiz-Abalia *et al.* 2008). Together these studies implicate that normalization of Dyrk1a protein overexpression has the potential to improve not only brain, learning, and motor deficits, but other less-studied DS phenotypes as well.

1.9 EGCG as a *Dyrk1a* Inhibitor to Correct Down Syndrome Phenotypes

Epigallocatechin-3 gallate (EGCG) is a small molecule inhibitor of the DYRK1A protein, and has been tested as a clinically translatable way to normalize DYRK1A overexpression and correct phenotypes associated with DS (Bain *et al.* 2003). EGCG is the major polyphenol found in green tea and constitutes 9-13% of its total dry weight (Dufresne and Farnworth 2001) (Figure 1.11). EGCG has well known health benefits due to its antioxidant properties and protection from metabolic syndrome, many types of cancers, neuroprotection, improvements in cognitive function, bone health, and reduced risk for cardiovascular disease (Nagle *et al.* 2006; Hodgson and Croft 2010; Williamson *et al.* 2011). EGCG has recently been investigated as a potential therapeutic for DS phenotypes as it is able to inhibit DYRK1A protein activity and potentially normalize DYRK1A levels (Bain *et al.* 2003; Adayev *et al.* 2006; De la Torre *et al.* 2014). There are conflicting hypotheses as to how EGCG inactivates DYRK1A. Some studies suggest that EGCG inhibits DYRK1A protein activity by binding the ATP pocket of the protein, preventing it from phosphorylating its downstream targets (WANG *ET AL.* 2012) while others suggest it is a non-competitive inhibitor with EGCG and that it binds to the X-XI kinase domain (Adayev *et al.* 2006). Studies have shown that EGCG is able to increase proliferation rates in Dyrk1a overexpressing cells from Ts65Dn embryos making it a useful treatment *in vitro.* EGCG is also able to cross the blood-brain and placental barriers making it a viable treatment to correct effects of Dyrk1a overexpression *in vivo*. *In vivo* studies with mice have shown that EGCG can correct brain and cognitive deficits in mice overexpressing Dyrk1a (Adayev *et al.* 2006; Guedj *et al.* 2009; Wang *et al.* 2012;

Pons-Espinal *et al.* 2013; De la Torre *et al.* 2014) suggesting it may be effective as a modifier of phenotypes linked to Dyrk1a overexpression.

Harmine, another small molecule DYRK1A inhibitor, has also been investigated for its ability to inhibit DYRK1A protein activity. This molecule has been found to inhibit DYRK1A activity and Tau phosphorylation at multiple Alzheimer's disease related sites (Frost *et al.* 2011). However, harmine is toxic *in vitro* and causes chromosomal alterations even at low levels and would not provide a clinically translatable therapy to normalize phenotypes related to the overexpression of DYRK1A (Boeira *et al.* 2001). EGCG has emerged as one of the most safe inhibitors of DYRK1A compared to other screened kinase inhibitors (Adayev *et al.* 2006).

1.10 Next Generation Sequencing

Next generation sequencing (NGS) is a recent and growing technology that allows the DNA or RNA to be sequenced to determine the order of nucleotide bases. This technology has been revolutionary in identifying biological structure and function, creating maps of evolutionary conservation, identifying gene transcription, chromatin structure, methylation patterns, genetic variation, association to inherited diseases, and gene alterations in cancer, in addition to better defining the roles of protein-coding genes, non-coding RNAs and regulatory sequences (Lander 2011). Genome-wide expression analyses (RNA-seq) have been especially utilized in DS to identify how gene expression in DS varies (Marguerat and Bahler 2010) from both DS and non-DS samples matched in

as many parameters as possible such as age, gender and tissue type to compare gene expression levels. Previous microarray studies have found that gene expression varies widely across tissue types and indicate that both trisomic and non-trisomic genes are dysregulated in DS to some degree in trisomic tissues (Li *et al.* 2012). More recent NGS studies have additionally suggested that other genomic elements may play a role in causing dysregulation of developmental pathways in DS including non-coding RNA species such as snoRNAs and microRNAs (Costa *et al.* 2011). There is also evidence that trisomy may cause the alternative splicing of genes which may further alter gene dysregulation (Toiber *et al.* 2010; Wegiel *et al.* 2011). Together, this research provides a background for comparison of future gene expression studies in various tissue-specific and temporally dependent gene expression profiles of DS. The continuation of gene expression analysis in DS provides further understanding of genotype-phenotype correlations which may aid in development of gene-targeted therapies for DS phenotypes.

1.11 Hypothesis

We hypothesize that Dyrk1a plays a role in causing deficient cell numbers in the E9.5 trisomic PA1, and is a key gene in the development of the small dysmorphic mandible displayed in DS. Because Dyrk1A is overexpressed ~1.5-fold in E9.5 trisomic PA1 and NT, we hypothesize it may contribute to NCC migration and proliferation deficits in the PA1 due to gene-dosage imbalance. We hypothesize that cell deficits in Ts65Dn E9.5 PA1 will be ameliorated when pregnant Ts65Dn mothers are treated orally with a low dose of EGCG from G0 – G9.5.

CHAPTER 2. MATERIALS AND METHODS

2.1 Animal Housing

Female B6EiC3Sn a/A-Ts(1716)65Dn (Ts65Dn) and female and male C57Bl/6J (B6) and C3H/HeJ (C3H) mice were purchased from the Jackson Laboratory (Bar Harbor, ME). B6C3F1 mice were bred by crossing B6 females with C3H males. A colony of Ts65Dn males and females were generated and maintained at Indiana University-Purdue University Indianapolis (IUPUI) by crossing Ts65Dn females with B6C3F1 males. Ts65Dn females and B6C3F1 females were also used in embryonic studies. Male B6CBA-Tg(Wnt1-lacZ)206Amc/J (Wnt1-LacZ) mice were also purchased from the Jackson Laboratory and maintained at IUPUI for embryonic studies. All Ts65Dn embryos and offspring were genotyped using PCR as described below. All animal housing and other experimental procedures conformed to IACUC regulations.

2.2 Genotyping of Ts65Dn Mice and Embryos

Ts65Dn mice and embryos were genotyped using the breakpoint PCR genotyping protocol described by Reinholdt et al., 2011. Since the trisomic translocated chromosome is the distinguishing factor between Ts65Dn and euploid mice, the PCR detects the

translocation breakpoint between the telomeric end of Mmu16 attached to the centromeric end of Mmu17. The forward primer binding on the Mmu17 side of the translocation site was Chr17fwd: 5'-GTGGCAAGAGACTCAAATTCAAC-3' and the reverse primer binding on the Mmu16 side Chr16rev: 5'-TGGCTTATTATTATCAGGGCATTT-3'. This primer set amplifies a 275 bp product from the translocation site. Positive control primers IMR1781: 5'-TGTCTGAAGGGCAATGACTG-3' and IMR1782: 5'-GCTGATCCGTGGCATCTATT-3' were used to amplify a 544 bp product. All four primers were obtained from Invitrogen (Carlsbad, CA). In a 25 µl reaction total, primers were used at a final concentration of 0.4 µM each. 1.5 µl of DNA at a concentration of 75-125 ng/µl was used in each sample for both mouse and embryo DNA. PCR cycling conditions were 94°C for 2 minutes, and 35 cycles at 94°C for 45 seconds, 55°C for 45 seconds, and 72°C for 60 seconds, with a 72°C for 7 minutes extension, and 4°C hold (REINHOLDT *et al.* 2011). PCR products were separated for 25 min at 105 volts on a 1.5% agarose gel containing SYBR Gold DNA Staining Solution (Invitrogen, Carlsbad, CA).

2.3 Generation of Ts65Dn Embryos

Female Ts65Dn mice were checked for estrus and bred to either B6C3F1 or homozygous Wnt1-LacZ males. To perform matings, Ts65Dn females were placed in a male mouse's cage overnight for 15-20 hours. Females were checked for a vaginal plug the next morning, with 12:00 pm on the day of the mating identified as E0.5 to ensure timed mating. Females were then removed from breeding partners and single-housed for

nine days after the plug was identified, when embryos were staged at embryonic day 9.5 (E9.5). After nine days, mothers were euthanized with isoflurane (Vedco, Inc., St. Joseph, MO) between 10am and 2pm and cervical dislocation performed to ensure brain function was severed and the mouse was deceased. Before embryos were removed, the mother's abdomenal region around the removal site was sprayed with 70% ethanol. Embryos were removed and placed in 1% Phosphate-Buffered Saline (PBS) (Mediatech, Inc., Manassas, VA) in a petri dish and placed on ice to induce hypothermia. Embryos were dissected in individual petri dishes containing PBS using forceps and a dissecting microscope. Yolk-sac tissue was removed for genotyping at time of dissection as the tissue is fetally, not maternally, derived and allows embryonic tissue to be left intact. Somite numbers of each embryo were counted along the dorsal side of the embryo at time of dissection and used to determine developmental stage. Somites are derived from the mesoderm and differentiate to become cartilage, bone, muscle, and dermis throughout the body (Christ and Ordahl 1995) and can be used to stage the intrinsic development of the embryo (Venters *et al.* 2008). This is helpful as the 15-20 hour breeding period leaves room for variation in the embryo's developmental stage reached by E9.5. Better comparison of developmental processes is achieved when embryos are somite-matched. Embryos were processed as described below and embryos with 21-24 somites used for comparison in our studies. A small group of 18-20 somite embryos were included in our study; however data for these embryos were analyzed and presented separately.

2.4 *In-Vivo* EGCG Treatment

To assess the effects of prenatal EGCG on correcting NCC deficits in the developing PA1, pregnant Ts65Dn mothers were treated with EGCG and embryos were removed at E9.5 for tissue specific analysis following treatment to observe its effects on PA1 development.

2.4.1 Preparation of EGCG

30 g of purified EGCG (>95%) (Sigma-Aldrich, St. Louis, MO) was dissolved in 2 mL PBS to create a 15 mg/mL solution. Pregnant Ts65Dn and euploid mice bred to either Wnt1-LacZ males or B6C3F1 males were treated with EGCG orally using one of two treatment regimens. Mice were treated with EGCG at concentrations well below established genotoxicity levels (Isbrucker *et al.* 2006).

2.4.2 G7-G8 EGCG Treatment

Female Ts65Dn and euploid mice bred to Wnt1-LacZ males were weighed at time vaginal plug was observed. Females gaining at least 1-1.5 grams by seven days after the plug was observed were considered pregnant and were treated with EGCG or PBS as a control. Treatment was administered by oral gavage with a 22-gauge needle on gestational day 7 and day 8 (G7- G8) after the plug was observed and given twice daily with approximately 8 hours between treatments for a total of 4 treatment administrations.

Either PBS was administered as a control treatment or EGCG was administered at a concentration 200mg EGCG/kg body weight (a dose equivalent to 100 times the average daily EGCG dose in green tea) twice per day for a total of 400mg/kg/day. Mice were monitored before, during and after treatment. Treatment was discontinued in cases where mice appeared to be lethargic or less responsive following treatment and mice were removed from the study. On G9.5, mothers were sacrificed and embryos dissected out for processing as described below.

2.4.3 G0-G9.5 EGCG Treatment

Female Ts65Dn and euploid mice were bred to Wnt1-LacZ or B6C3F1 males. At the start of the study, only Wnt1-lacZ euploid males were used for embryo generation, however, it became both difficult to generate embryos using these males and to generate embryos that were of sufficient developmental age. To continue our study, B6C3F1 euploid males, used to maintain the Ts65Dn colony, were bred with Ts65Dn females to produce Ts65Dn/B6C3F1 embryos. Data generated from embryos fathered by each set of male mice was analyzed separately, as differences in genetic background can influence developmental phenotypes (DEITZ and ROPER 2011). Female mice were weighed at the time the vaginal plug was observed at G0.5 and at subsequent days 7, 8, and 9. EGCG treatment was prepared by dissolving 124 µL of 15mg/mL EGCG prepared as described above, into 20mL of tap water (a dose equivalent to 10 times the average daily EGCG dose in green tea) for a final concentration of 0.094mg EGCG/ml and administered *ad libitum* from G0-G9.5 following observation of the vaginal plug. Treatment was changed

every two days, at which time the amount of treatment consumed was measured and recorded. Mothers gaining at least 1-1.5g by day 8 and an additional ~0.5g from G8 to G9 were sacrificed on G9.5 and embryos dissected out as described above. Because EGCG is known to degrade rapidly at room temperature (Table 2.1), rate of degradation was included in calculations of the average amount of EGCG consumed by mothers treated from G0 – G9.5 (Table 3.1). In other studies in our lab, phosphoric acid has been routinely added to EGCG treatment as a pH-lowering stabilizing agent, significantly reducing the natural degradation of EGCG in solution. However upon starting this stabilized EGCG treatment, normally fecundate mothers yielded no embryos at G9.5 over a period of several months. Hence, the addition of phosphoric acid to EGCG treatment was discontinued, and all mothers included in the study were treated with EGCG only dissolved in water as described previously.

2.5 Embryo Processing

2.5.1 DNA Isolation of Yolk Sacs

Yolk sacs were removed during embryo dissection and placed in yolk sac lysis buffer (150mM NaCl, 20mM Tris-HCl ph 7.5, 5mM EDTA, 0.5% SDS, in ddH_2O) with Proteinase K (12.5 µl of Proteinase K per 1 ml of yolk sac lysis buffer, 50 µL per yolk sac) (Bioline, Taunton, MA) and incubated overnight at 55°C. To each sample, 12.5 µl 5M NaCl was added, each sample vortexed, then centrifuged at 13K rpm for 5 minutes. The supernatant was removed and placed in a new tube, 50 µl isopropanol was added,

and the sample was incubated for 5 minutes at room temperature before centrifuging at 13K for 15 minutes. The supernatant was removed and discarded, 50 µl of cold 70% was added to the pellet, and the sample vortexed before centrifuging at 13K for one additional minute. Samples were turned upside-down and gently blotted on a paper towel to remove the supernatant. Samples were dried upside down on a fresh paper towel for 10-15 minutes. After samples were dry, 20 µl ddH_2O was added to each sample and samples stored at 4°C until analyzed by PCR.

2.5.2 Embryo Fixing and Embedding

Whole embryos were dissected out and placed in PBS in individual tubes until processing 0-3 hours later. To fix embryos, PBS was removed from each sample and the embryo washed with 500 µl of 0.1M phosphate buffer. Phosphate buffer was removed, 500 µl fixing solution (0.2% gluteraldehyde with 5 mM EGTA and 2 mM $MgCl_2$ in 0.1M phosphate buffer) added before incubating for 15-20 minutes depending on embryo size. Afterwards, fix solution was removed and embryos were washed three times for five minutes each in wash buffer (2 mM $MgCl_2$, 0.02% Nonidet P-40 in 0.1 M phosphate buffer). Ts65Dn/Wnt1-lacZ embryos were stained with 0.025% 5-bromo-4-chloro-3-indoyl-β-D-galactopyranoside in 5 mM potassium ferricyanide, 5 mM potassium ferrocyanide for 1.5 hours at 37°C. Embryos were then postfixed (Ts65Dn/B6C3F1 embryos immediately following the three washes) with 4% paraformaldehyde overnight at 4°C. The next day, embryos were processed through a series of 500 µl washes. Embryos underwent dehydration washes in alcohol (10 min each in 50%, 70%, 70%,

95%, 95%, 100%, and 100% ethanol), clearing with xylenes (10 min each in 1:1 xyelene:100% ethanol, xylene, xylene), and infiltration with paraplast (20 min each in 1:1 xylene:paraplast, paraplast, paraplast). Embryos were then embedded parasagitally in paraffin and cured for one week at 4°C.

2.5.3 Embryo Histology

Embryos were sectioned with a microtome in 18µm sections with 5 sections per microscope slide. The embryo sections were placed on a slide warmer overnight at 37°C and melted at 55°C for 1 hour to ensure sections adhered to the slides. The sections were further processed through washes in CitriSolv (Fisher Scientific, Kalamazoo, MI) in three 4 minute washes or until all paraffin wax was cleared from the slides, two 2 minute washes in 100% ethanol, 1 minute in 95% ethanol, and 1 minute in 70% ethanol. The slides were counterstained for 1 minute in 0.1% eosin (Fisher Scientific, Kalamazoo, MI) in 100% ethanol, two 10 and 15 second washes in 95% ethanol, two 2 minute washes in 100% ethanol, and three 3 minute washes in CitriSolv. Slides were removed from the fluid solution and coverslipped using 24 x 60 mm glass (Fisher Scientific, Kalamazoo, MI) and mounted with DPX mountant (VWR, West Chester, PA). Slides were cured for one week at room temperature before completing unbiased stereology.

2.6 Unbiased Stereology

Unbiased stereology was used to measure the volume of structures and tissues through systematic random sampling of the tissue. This was accomplished using Stereologer 2000 software and a Nikon Eclipse 80i microscope with moving stage (Japan). Unbiased stereology was used to quantify total embryo volume, PA1 volume and number of NCC in the PA1 of embryos. Unless otherwise stated, only embryos with 21-24 somites were used for stereological analysis. Cured slides with embryo sections were observed under a dissecting microscope to identify sections containing PA1 tissue and to identify any incomplete or missing sections before completing stereology. Parameters were adapted from (Mouton 2002) to measure PA1 volume, NCC count, and total embryo volume. PA1 volume was measured by sampling every other PA1 section starting with either the first or second section of PA1 tissue, chosen by a random number generator. As each sampled section thickness was assessed, NCC in the PA1 were quantified by counting the number of cells within a dissector spaced at intervals of 60 µm with dimensions of 150 µm² area and 8 µm depth with a 2 µm guard height. Embryo volume was calculated by sampling every fourth section, with the start section from one to four determined by a random number generator. Dimensions were set as a frame area of 25 μm^2, 10 µm frame height, 2 µm guard height, 200 µm from spacing, 8000 μm^2 area per point. Average CE values for PA1 volume, NCC number, and embryo volume measurements were required to be <0.1 to be included in calculations. Statistical differences were calculated using a one-tailed Student's t-test.

2.7 Next Generation Sequencing and Analysis of RNA Isolates from Neural Tube and PA1 Tissue

To identify the effects of trisomy on differential gene expression during the origin of the NCC migration and proliferation deficits in the PA1 initiated between E9.25-E9.5, next generation sequencing was implemented from RNA isolates taken from the E9.25 NT and E9.5 PA1 tissue of euploid and trisomic Ts65Dn embryos.

2.7.1 RNA Isolation and Sample Pooling

Pregnant Ts65Dn trisomic mothers were sacrificed at G9.25 or at G9.5 and embryos removed and placed in PBS. Neural tube (NT) and first pharyngeal arch (PA1) tissue from E9.25 and E9.5 embryos, respectively, was dissected out in PBS using 30G needles. Total RNA was extracted from each sample using the Purifying RNA from Animal Tissues protocol found in the Pure Link Micro Kit from Invitrogen (Carlsbad, CA). RNA was treated with Ribominus to reduce rRNA.

Due to low RNA quantity of individual samples, 3 RNA samples were pooled in each library (1 E9.5 Ts65Dn pool had 4 samples) to provide the ~300ng/pool of RNA needed for sequencing. Samples were pooled based on similar developmental stages as compared by numbers of somites and using littermates where possible to limit variation between pools. Four libraries with 3-4 pooled RNA samples each were created in each of the following groups: E9.5 Trisomic PA1, E9.5 Euploid PA, E9.25 Trisomic NT, E9.25 Euploid NT.

2.7.2 Sequencing, Quality Analysis, and Alignment

RNA extracts (concentration ~300 ng/pool) were prepared for sequencing using EZBead E120 Prep (Life Technologies). Sequencing, using 75bp read lengths, was performed on a SOLiD 5500XL sequencer at the Center for Medical Genomics in the Indiana University School of Medicine. Analysis of RNA-sequence data was performed by Douglas Baumann and R.W. Doerge of the Department of Statistics at Purdue University using package edgeR (Robinson *et al.* 2010). Six data files were produced from the sequencing process, each representing one lane of a sequencing flow-cell, upon which 16 mRNA libraries (representing 16 biological samples) were barcoded and sequenced. The six data files produced from sequencing were presented in eXtensible SeQuence (.xsq) format, the Applied BioSystems proprietary data format for SOLiD sequencers. These files include a binary-style respresentaion of the base call (in SOLiD color-space) and a quality score for the base call. A Python library was used to convert and separate the data into CSFASTA and QUAL files to represent the base calls and quality scores respectively. A quality score was recorded for every base sequenced. Phred Quality Scoring was used to determine bases with a high probability of being called incorrectly. One sample showed slightly diminished quality compared to other samples, however, the design of the experiment (using barcoded samples sequenced on each available lane) allowed any potential resulting bias to be accounted for in the downstream modeling framework. Reads were aligned to mouse reference genome (mm9) by Hai Lin and Yunlong Liu from the Center for Computational Biology and Bioinformatics at Indiana University-Purdue University Indianapolis (IUPUI).

2.7.3 Differential Expression Analysis

Differential expession analysis of the 22,813 genes detected by next generation sequencing was performed by Douglas Baumann and R.W. Doerge of the Department of Statistics at Purdue University. Because many of the genes detected demonstrated too little expression to be used for valid statistical analysis, all genes with average counts less than 5 across the samples within each embryonic day value were filtered out to yield a more powerful analysis. To test for differential expression of each gene, Package edgeR (Robinson *et al.* 2010) was used, which uses a moderated negative binomial distribution to model the count data from the NGS experiment. The negative binomial model was used as it has the potential to accurately model discrete count data seen in NGS applications and allows more flexibility than other commonly used models such as a Poisson distribution. The negative binomial model was used to test for differential expression between the trisomic and euploid samples from E9.5 PA1 and E9.25NT separately. Following the differential expression analysis, the number of transcript variants for differentailly expressed Mmu trisomic genes on Hsa21 was identified by searching both Ensembl and NCBI/GenBank databases. Using Ingenuity Pathway Analysis (IPA) software, functional analysis of differentially expressed genes and their potential relationship in related gene pathways was also performed.

2.7.4 MISO Analysis of Alternative Splicing Events

To identify alternative splicing (AS) events and gene isoforms, differentially expressed genes from our previous analysis were analyzed using a bioinformatic analysis called MISO (Managing Information for Sequence Operations). To perform the MISO analysis RNA-seq reads were aligned to mm9 genome (version 9 of the mouse genome) and sorted. All the .bam files from the differential expression analysis of the same tissue were merged and indexed by samtools. A GFF file with annotations of alternative events was provided by MISO and .bam files were fed into MISO. Since reads in our RNA-seq data were single-end reads, we chose exon-centric analysis. MISO calculated exon/isoform expression levels ("Psi" / Ψ values) in each sample along with confidence intervals. We then used MISO comparison to compute the differences of expressed exons across samples and Bayes factors to determine significance of changes (Δ Ψ).

CHAPTER 3. RESULTS: EFFECTS OF *IN-VIVO* TREATMENT WITH EGCG

3.1 G7-G8 Treatment but Not G0-G9.5 Treatment with EGCG Improves Ts65Dn NCC Deficits

Previously, our lab showed that *in vitro,* trisomic PA1 and NT cells treated with EGCG proliferated more than untreated cells in a dose-dependent manner (Deitz, *Unpublished* data) (Figure 3.1). Further experiments also showed i*n vivo* oral treatment of Ts65Dn mothers with 400mg/kg/day of EGCG at G7 and G8 (gestational day 7 and 8) was sufficient to increase the increase the number of NCC in the PA1 and the size of the PA1 to near-euploid levels in E9.5 trisomic embryos (Figures 3.2, 3.3, 3.4)

We hypothesized that treatment of pregnant Ts65Dn mothers with a lower dose of EGCG from the start of pregnancy to G9.5 would also correct NCC deficits in the PA1, the size of the PA1, and overall size deficits of developing trisomic embryos. This treatment was designed to evaluate the safety and efficacy of EGCG as a potential prenatal supplement for human mothers and fetuses when taken at the start of pregnancy. We used B6C3F1 euploid fathers to breed with Ts65Dn females after difficulties with generation of embryos from Wnt1-LacZ euploid fathers. We found that treatment with EGCG administered to Ts65Dn mothers at a concentration of ~12.2 mg/kg/day on average (Table 3.1) did not correct deficits in the PA1 of trisomic E9.5 embryos.

Average dosage of G0-G9.5 EGCG received through *ad libitum* treatment is detailed in Table 3.1 and Figures 3.5, 3.6. Pregnant, non-pregnant, trisomic and euploid mothers all drank similar volumes of both EGCG and H_2O. After treatment, there were no significant differences between the number of NCC in the PA1 or total embryo volume of trisomic embryos compared to those treated with water (Figures 3.7, 3.9). There was however a significant increase in PA1 volume in euploid embryos from trisomic mothers (Eu/(Ts)) compared to untreated embryos of the same genotype (p=0.046)(Figure 3.8).

There are several slight changes in trisomic EGCG treated embryos. There was a slight, but not significant decrease in EGCG treated Ts/(Ts) embryos compared to untreated embryos in both NCC number (p=0.061) and PA1 volume (p=0.058) compared to control embryos. We attributed this difference to a reduced average somite number in trisomic embryos from trisomic mothers (Ts/(Ts)) treated with EGCG with an average of 21.5 somites while the average somite number of all other groups ranged from 22.5-23.4. This implies that trisomic EGCG treated embryos may have been delayed during development, causing the lower NCC number due to a lapse in development. There was also a slight but non-significant increase in embryo volume of Eu/(Ts) + EGCG embryos compared to untreated Eu/(Ts) embryos (p=0.089).

Together, these results suggest that prenatal treatment with EGCG is sufficient to normalize NCC deficits when given twice in two days at G7 and G8 at a concentration of 400 mg/kg/day, but not when administered continually at a concentration of ~12.2 mg/kg/day from time of pregnancy.

3.2 G0 – G9.5 EGCG Treatment May Cause Developmental Delay in Embryos from Trisomic Mothers

Somites are paired blocks of mesoderm developing on the dorsal side of the embryo and are used to measure developmental time (VENTERS *et al.* 2008). To ensure embryos analyzed were at a similar developmental stage at E9.5, somite numbers were counted along the dorsal side of each embryo. We analyzed the staging of all embryos in each litter used for our study to assess the effects of EGCG on developmental progression. We observed several interesting differences in somite number depending on treatment and genetic background of the embryos. First, we found that Ts/(Ts) and Eu/(Ts) embryos, from both Wnt1-LacZ and B6C3F1 fathers, treated with EGCG from G0 – G9.5 showed significantly lower ($p \leq 0.05$) somite numbers compared to untreated embryos of the same genotype and Eu/(Eu) embryos in the same treatment group (Figure 3.10). No differences in somite numbers were observed in any embryos treated with PBS or EGCG from G7 – G8. The data suggest that EGCG may slow development in embryos from trisomic mothers when given at an earlier time point or for a longer duration. In euploid embryos from euploid mothers, average somite numbers were similar in both control and EGCG treatment groups suggesting EGCG does not affect developmental growth of embryos from euploid mothers.

We also observed subtle differences in somite averages between embryos depending on their genetic background (Figure 3.10). Embryos from Wnt1-LacZ fathers generally showed lower somite averages with more variation than embryos in similar treatment groups from B6C3F1 fathers. Although significantly lowered somite numbers

were observed in G0 – G9.5 EGCG treatment groups in embryos of both backgrounds, the effect was also significantly more pronounced in Wnt1-LacZ embryos from trisomic mothers. Wnt1-LacZ trisomic embryos from trisomic mothers had only 19.0 somites on average with only one embryo at 22 somites reaching the 21-24 somite stage needed to compare stereological data from embryos in other groups. For this reason, Wnt1-LacZ trisomic embryos were not included in further stereologic analysis. However, a comparison of 18-20 somite embryos (Figures 3.11, 3.12, 3.13) was made between EGCG treated Wnt1-LacZ trisomic and euploid embryos to assess differences between trisomic and euploid embryos. Embryos from different paternal backgrounds (Wnt1-LacZ and B6C3F1) were both used in our study as embryos became difficult to generate from Wnt1-LacZ males after a number of months. B6C3F1 males replaced Wnt1-LacZ males in production of embryos from Ts65Dn and euploid mothers. Data collected on embryos of both backgrounds was analyzed and compared separately to avoid confounding differences in data resulting from subtle but known differences attributed to genetic background (Deitz and Roper 2011).

3.3 No Differences Observed in 18-20 Somite Embryos Treated with EGCG

Because trisomic embryos treated with high-dose EGCG displayed lower somite numbers than all euploid and untreated embryos, especially in Wnt1-LacZ embryos, data from this group could not be compared to the stereological data collected in our study from 21-24 somite embryos as embryos were not as developed. We used embryos in this group to instead analyze data from 18-20 somite embryos only. Embryos displaying 18-

20 somites are typically representative of embryos staged prior to E9.5 as E9.5 embryos normally display 21-24 somites. After E9.5, the PA1 volume and NCC count are proportionately smaller in trisomic embryos (Figure 1.8) permanently diverging from that of their euploid littermates. Consistent with this trend, we observed no differences in NCC number, PA1 volume, or embryo volume (Figures 3.11, 3.12, 3.13) between trisomic and euploid 18-20 somite embryos treated with EGCG. These findings suggest that trisomic NCC deficits in the PA1 begin to develop during the period between the 18-20 somite and 21-24 somite developmental time points. These findings support previous research that no differences in trisomic and euploid PA1 exist at E9.25 but are present by E9.5 (ROPER *et al.* 2009). Together, this data suggest that developmental changes that occur specifically between these somite ranges may lead to the altered trisomic PA1. Because these changes happen during this specific range, it provides an optimal window for treatment of embryos with EGCG to reduce or prevent NCC and PA1 deficits in trisomic embryos.

CHAPTER 4. RESULTS: ANALYSIS OF NEXT GENERATION SEQUENCING DATA

4.1 Differential Expression Analysis of Trisomic and Euploid NT and PA1 Tissue

We performed next-generation sequencing of RNA isolates from trisomic and euploid E9.25 NT and E9.5 PA1 tissue to assess the gene expression differences occurring before and after NCC deficits arise in the trisomic PA1. After low-count filtering, NGS detected expression of 13,883 E9.25 NT genes and 13,406 E9.5 PA1 genes. A differential expression analysis was performed on each of these tissue groups to identify differences in gene expression between trisomic and euploid samples in both E9.25 NT and E9.5 PA1. The purpose of this analysis was to identify potential genes and gene pathways specifically altered by trisomy. Of the 13,883 E9.25NT genes that passed the low-count filtering step, only 42 were differentially expressed between the trisomic and euploid samples (Table 4.1). Of the 13,406 E9.5PA1 genes, 336 genes were differentially expressed between the trisomic and euploid samples (Table 4.2). Of the 42 E9.25NT and 336 E9.5PA1 differentially expressed genes, none were found in common between the two embryonic days.

4.1.1 Filtering of Mmu16 and Hsa21 Differentially Expressed Genes

Following the differential expression analysis, we filtered out differentially expressed genes found in 3 copies in our Ts65Dn mice or that had homologues on Hsa21. The purpose of this search was to identify which genes found in 3 copies may play a role in NCC deficits. We also wanted to evaluate whether trisomy results in dysregulation of only genes found in 3 copies or is sufficient to cause dysregulation of both trisomic and non-trisomic genes. Of the 42 E9.25 NT differentially expressed genes, we found no trisomic genes in Ts65Dn or with homologues on Hsa21. All 42 differentially expressed genes are found on non-triplicated portions of the genome in 2 copies both in Ts65Dn and humans. Of the 336 E9.5 PA1 differentially expressed genes, 5 genes triplicated in Ts65Dn contained homologues on Hsa21 while the remaining 331 genes were found non-trisomic portions of the genome in 2 copies in Ts65Dn and humans. The 5 genes containing Hsa21 homologues were *Tiam1*, *Erg*, *Sh3bgr*, *Cldn8*, and *Mrap*.

We also included the Mmu16 genes *Dyrk1a* and *Rcan1* in future transcript variant and MISO analysis as they are of particular interest to our research and have been shown to be differentially expressed in trisomic tissues by qPCR. However, differential expression of either gene was not detected in our NGS analysis.

4.2 Transcript Variant Search for Differentially Expressed Trisomic Genes

Transcript variants of a gene arise when a gene is spliced and different combinations of exons are included in the final gene product in a process called

alternative splicing. To further analyze the 5 trisomic E9.5 PA1 genes found in triplicate in Ts65Dn (*Tiam1, Erg, Sh3bgr, Cldn8, Mrap*) detected by the differential expression analysis, we searched for unique transcript variants of each gene. We also included *Dyrk1a* and *Rcan1* in our searches as they remain DS candidate genes in our study. In detecting transcript variants, we aimed to examine whether trisomy of Mmu16 was also able to cause differential splicing and expression of transcript variants in addition to its ability to induce differential gene expression. Differential splicing and transcript variant expression induced trisomy may serve as a potential explanation for the variability in incidence and severity of trisomy-associated phenotypes in Ts65Dn and in the human DS population.

Searches were performed using both Ensembl and NCBI Gene/GenBank databases as the number of unique transcript variants listed for each gene differed between databases (Table 4.3). Ensembl usually yielded a greater number of unique transcript variants which often included non-coding and putative transcripts while NCBI Gene/GenBank entries yielded the most well-established protein-coding transcripts form(s) of the gene. We found multiple transcript variants for 4 out of 5 of the differentially expressed trisomic genes, and in both *Dyrk1a* (Figure 4.1) and *Rcan1*. The highest number of transcript variants found was in *Tiam1* with 15 unique transcript variants using Ensembl and 3 using NCBI/Genbank.

4.3 MISO Analysis: Detection of Alternative Splicing Events

After finding transcript variants of dysregulated trisomic genes, we further analyzed our NGS data to look for alternative splicing (AS) events that could lead to potential expression of a variety of transcript variants in both trisomic and non-trisomic differentially expressed genes. We used MISO to search for potential AS events among these genes. We performed 4 comparisons to search for AS events among differentially expressed genes (Figure 4.3): (1) euploid and trisomic E9.5 PA1, (2) euploid and trisomic E9.25 NT, (3) euploid E9.25 NT and E9.5 PA1, (4) trisomic E9.25 NT and E9.5 PA1. For each comparison we found (1) 51 AS events that differed between trisomic and euploid E9.25 NT, (2) 24 AS events between trisomic and euploid E9.5 PA1, (3) 54 AS events between trisomic NT and PA1, and (4) 31 AS events between euploid NT and PA1. Between comparisons 1 and 2, only one of the AS events was shared between trisomic and euploid NT and PA1 tissues within the gene *Cdc14b*. *Cdc14b* is involved in cell cycle regulation and dephosphorylation of oncogene TP53. Interestingly, *Cdc14b* displayed different AS patterns between trisomic and euploid tissues. Higher psi values of alternative splicing events in trisomic tissues indicated that longer isoforms of the gene were being transcribed. During the development of euploid PA1, levels of the longer *Cdc14b* isoform decreased, while their levels were maintained at relatively high levels in trisomic PA1 tissue. In addition to *Cdc14b*, two AS events were shared between comparisons 3 and 4. These two genes found within both trisomic NT/PA1 and euploid NT/PA1 were *Fgfr1op2* and *Dph3*. Although transcript variants exist for the 4 of the 5 trisomic E9.5 genes including *Tiam1, Erg, Sh3bgr, Mrap* and for *Dyrk1a* and *Rcan1,* we

did not find evidence of AS for any of these potential DS candidate genes. However, our analysis did reveal AS events and the expression of multiple transcripts from single genes throughout the genome between trisomic and euploid E9.25 NT and E9.5 PA1 tissue that may be of interest to future research efforts (Table 4.4).

CHAPTER 5. DISCUSSION: EFFECTS OF *IN-VIVO* TREATMENT WITH EGCG

5.1 Sufficient Dose of EGCG Required to Ameliorate Trisomic Neural Crest Cell Deficits

We hypothesized that prenatal treatment with EGCG could prophylactically improve or correct adverse phenotypes in Ts65Dn embryos while leaving euploid embryos unaffected. We found that short-term treatment during G7 and G8 with 400 mg/kg/day of EGCG was able to improve NCC deficits in the mandibular precursor. However, longer-term treatment from G0-G9.5 at a lower dose, ~12.2 mg/kg/day EGCG, was unable to improve the trisomic NCC deficits in the mandibular precursor. Evidence from our lab suggests that a higher dosage of EGCG administered at an optimal time point between G7-G8, as opposed to lower dosage administered for longer duration, is what likely improves trisomic phenotypes. In unpublished research from our lab, we have found that 3 week old Ts65Dn mice treated with ~12.2 mg/kg/day of EGCG, comparable to our G0-G9.5 EGCG treatment regimen, for three weeks also yields no changes in cognitive abilities of Ts65Dn mice. However, our lab has also shown that EGCG at a similar dose has been shown to improve the bone phenotype adolescent Ts65Dn mice aged 3-6 weeks. Although EGCG given at ~12.2 mg/kg/day did not improve the cognitive or E9.5 PA1 deficits of Ts65Dn mice and embryos, respectively, a

recent study similar to the cognitive study completed by our lab (DE LA TORRE *et al.* 2014) presented evidence that cognitive abilities of Ts65Dn mice were improved when treated with 90 mg/kg/day EGCG, higher than our low-dose of EGCG treatment. Other research of embryonic development conducted with fetal alcohol syndrome (FAS), which has been shown to share similar developmental gene pathways and phenotypes to DS (Solzak *et al.* 2013), showed that reduced embryonic size in FAS mice can be improved in E9.5 embryos using the same dose (400 mg/kg/day) of EGCG and treatment duration as our G7-G8 EGCG regimen (Long *et al.* 2010). In this study, altered expression of neuronal marker genes in FAS was corrected with this EGCG treatment. Together these results provide evidence that EGCG has the ability to improve NCC deficits associated with DS in mice when treated prenatally at a sufficient dose of EGCG.

5.2 EGCG May Alter Embryonic Developmental Processes

After quantifying somite numbers upon embryo removal to assess developmental staging of embryos, we observed that embryos from trisomic mothers treated with EGCG from G0- G9.5, but not from G7-G8, displayed lowered somite numbers compared to untreated embryos (Figure 3.10). These results suggest that EGCG may alter the progression of development during embryonic growth before E9.5. Because the dose given with our G0-G9.5 treatment was less than that given from G7- G8, EGCG, when administered too early or for too long, has the potential to slow the progression of embryos and potentially alter developmental pathways. Previous research from our lab has confirmed that EGCG may alter gene expression of important developmental genes

such as *Rcan1, Shh, Ptch1,* and *Ets2* in addition to *Dyrk1a* (Figure 5.1). Together this evidence suggests that EGCG may have the ability to affect other developmental pathways, in addition to its ability to potentially normalize Dyrk1a protein overexpression. Although developmental size is decreased in embryos from trisomic mothers at G9.5, offspring have been born and seem to develop normally although no extensive phenotypic data have been collected. Both positive and negative outcomes of the global effects of EGCG treatment will be better understood with future research.

5.3 Translational Value of EGCG Research

The purpose of our study with EGCG in mice was to test its effect on pregnant mice to evaluate its safety and efficacy as a potential prenatal treatment to be taken by human mothers to improve DS phenotypes. It is imperative that EGCG be able to alter DS phenotypes while having no adverse effects on a normally developing fetus as a prenatal supplement would need to be taken before diagnostic testing for DS could be performed. The NCC deficits that lead to craniofacial abnormalities, including the small mandible that contributes to impaired speech, breathing, and eating, arise by 4 weeks of pregnancy in humans, equivalent to G9.5 in Ts65Dn mice. By this time, a mother may either not yet know she is pregnant or be unable to obtain diagnostic testing for DS until 9-10 weeks at the earliest.

When extending the results of our study in Ts65Dn mice to the potential treatment of human fetuses, we show that EGCG does have the potential to be effective in

ameliorating NCC deficits in the mandibular precursor. However, our results showing that EGCG treated euploid mouse embryos from trisomic mothers display a larger PA1 than untreated embryos, suggest that EGCG may have the potential to affect both fetuses with and without DS. Our results showing that EGCG may slow embryonic developmental processes in embryos from trisomic mothers suggests that there is an effect of the trisomic maternal environment which affects the development of the embryos immediately before and at G9.5. When translating this effect to a developing human fetus, the developmental delay effect displayed with EGCG treatment may not be of concern as the maternal uterine environment will most often be euploid, not trisomic. Despite these results, viable pups have been born to trisomic and euploid mouse mothers treated with either of our EGCG treatment regimens, suggesting that the increase in PA1 size or the developmental delay may not be detrimental to developing embryos or their mothers. Future research would be beneficial to determine any undetected genotype-independent effects of EGCG that may be detrimental to a developing euploid embryo or mother to ultimately minimize risks of potentially harming a normally developing human fetus.

CHAPTER 6. DISCUSSION: ANALYSIS OF NEXT-GENERATION SEQUENCING DATA

6.1 Detection of Trisomic and Euploid Differentially Expressed Genes on Mmu16 and Hsa21

Although there are triplicated gene copies of only the genes found on Hsa21 in DS, there are conflicting theories about whether only trisomic genes are dysregulated in DS, or whether trisomic genes also cause the more global dysregulation of non-trisomic genes found in two copies. Various studies have provided evidence of the global dysregulation theory in both Ts65Dn mice and humans. These studies have shown dysregulation of both trisomic and non-trisomic genes in Ts65Dn cerebellum (Saran *et al.* 2003), Ts65Dn E13.5 mandibular tissue (Billingsley *et al.* 2013), human DS fetal fibroblast cells (Letourneau *et al.* 2014) and in human endothelial progenitor cells (Costa *et al.* 2011). Based on this and other research, we hypothesized that trisomy also causes global dysregulation of both trisomic and non-trisomic genes throughout the genome in Ts65Dn E9.25 NT and E9.5 PA1 tissue and may cause NCC deficits leading to the undersized mandible. Our differential expression analysis of NGS data of RNA isolates from both of the aforementioned tissues revealed differential expression of 53 non-trisomic E9.25 NT genes, 364 non-trisomic E9.5 PA1 genes, and 5 trisomic E9.5 NT

genes. Because trisomy is the catalyzing event causing the gene dysregulation and the set of DS-like phenotypes, the evidence suggests that primary dysregulation of trisomic genes causes a secondary dysregulation of non-trisomic genes involved together in similar gene pathways. Together, this evidence suggests that gene dosage imbalance resulting from trisomy, causes global dysregulation of genes that is likely responsible for the array of variably expressed phenotypes that characterize DS.

This analysis also identified 5 additional trisomic candidate genes (*Tiam1, Erg, Sh3bgr, Cldn8, Mrap*) that may play a role in the dysregulation of genes contributing to the NCC deficits in the E9.5 mandibular precursor. Because these genes were the only genes found in triplicate in our analysis, while all other dysregulated genes were found in two copies in both trisomic and euploid tissues, it suggests that *Tiam1, Sh3bgr, Erg, Cldn8,* and *Mrap* may play a role as the start of a gene cascade that causes more global dysregulation of genes throughout the genome. Of the 5 genes, several have been linked to preexisting phenotypes associated with DS. *Tiam1* and *Sh3bgr* have been linked to congenital heart defects in DS (Egeo *et al.* 2000; Liu *et al.* 2014), although there remains some debate about the involvement of *Sh3bgr* in DS heart defects. In addition, *Erg* has been linked to the acute megakaryoblastic leukemia that has a higher incidence in individuals with DS (Stankiewicz and Crispino 2013). Although not found in three copies, we also found altered expression of *Gata1*, a gene also implicated in acute megakaryoblastic leukemia in DS. Further investigation into the role of these genes will help to understand how trisomy may cause global gene dysregulation leading to NCC deficits in the PA1.

Although previous qPCR performed in our lab has indicated that the DS candidate gene *Dyrk1a* is upregulated 1.5-fold in E9.5 PA1, dysregulation of this gene was not detected in our differential expression analysis as we hypothesized. We predict that these conflicting results may be due to in part to descrepancies in the qPCR performed. The probe used to detect the *Dyrk1a* transcript(s) binds to the junction between one set of exons only. Isoforms of the gene with this exon junction may be overexpressed ~1.5x in trisomic tissues. Any alternative isoforms of *Dyk1a* with the same exons spliced out may have been detected by RNA-seq, but not by qPCR suggesting that only specific isoforms of *Dyrk1a* may be overexpressed in trisomic tissues.

6.2 Analysis of Transcript Variants and Alternative Splicing Events

There is extensive evidence indicating that alternative splicing (AS) of some DS candidate genes may play a role in causing the variability in the expression of DS phenotypes. An alternatively spliced gene has the potential to produce an altered protein with altered structure. This may affect its function and interaction with other proteins, ultimately leading to the possibility of an altered phenotype. Specifically, one study found that increased dosage of *Dyrk1a* can cause alternative splicing of *Tau* transcripts, a gene known to play a role in neurogenesis and in Alzheimer's disease (Toiber *et al.* 2010). We attempted to detect whether the 5 E9.5 PA1 trisomic genes we detected in our differential expression analysis could be expressed as multiple transcript variants and found that 4 out of 5 of these genes did have multiple known transcript variants. We also found known transcript variants of both *Dyrk1a* and *Rcan1* (Figures 4.1, 4.2).

Although our MISO analysis revealed no AS of *Tiam1, Sh3bgr, Erg, Cldn8, Mrap, Dyrk1a, or Rcan1,* the analysis did reveal that AS is occurring in other genes between trisomic and euploid E9.25 NT and E9.5 PA1 tissue (Table 4.4). With this analysis, we found approximately twice the number of AS events in the PA1 tissue compared to NT tissue when comparing trisomic and euploid tissues (Figure 4.3, Table 4.4). MISO analysis also revealed less AS events between trisomic NT and PA1 tissues than euploid NT and PA1, suggesting that more AS events are occurring in euploid tissues. This suggests that trisomy may decrease the number of AS events. This provides another mechanism whereby trisomy may lead to an altered phenotype in Ts65Dn mice and individuals with DS.

Although more alternative splicing events seemed to occur in euploid and E9.5 PA1 tissue, very few of the genes in which the AS events were occurring, were shared between these comparison groups. However, three genes were shared between multiple comparison groups: *Fgfr1op2, Dph3,* and *Cdc14b.* Previous studies have shown that SNPs in the *Fgfr1op2* gene are associated with long-term atrophy of the mandible (Suwanwela *et al.* 2011). MISO analysis showed that *Fgfr1op2* displays similar patterns of AS during mandible development in both trisomic and euploid mice indicating that this gene may play an important role in the development of the mandible. The *Dph3* gene however, displayed different AS patterns between trisomic and euploid PA1 tissue. We predict that this difference in *Dph3* gene splicing may contribute to NCC deficiencies in the PA1. The *Cdc14b* gene also displayed different AS patterns between trisomic and euploid tissues with longer isoforms being expressed in trisomic tissues. Because *Cdc14b*

has known involvement in cell cycle regulation, it is likely that alternative splicing of this gene may contribute to the decreased levels of NCC proliferation in the trisomic E9.5 PA1. Together this analysis provides additional genes of interest for future research that have the potential to further understanding of the mechanisms by which trisomy causes the global gene dysregulation and the altered phenotypes of DS.

6.3 Future Research

Based on the research presented here, there are several opportunities for continued research. Because EGCG treatment at G7 and G8 provides an optimal window in which to correct deficiencies and phenotypes associated with trisomy, continuation of the *in vivo* work with EGCG would be beneficial. To continue this research, postnatal assessment of pups whose mothers received EGCG on G7 and G8 at 400 mg/kg/day could establish whether the NCC improvements observed in the E9.5 PA1 translate to a normalized mandible postnatally and throughout adulthood. Pups treated prenatally with EGCG also provide optimal test subjects for cognitive, bone, and other phenotypic tests to assess alternative outcomes of prenatal EGCG treatment.

Because the effects of EGCG were often not genotype specific, a more thorough assessment of EGCG's effects on euploid embryos would be beneficial to future translational studies in humans. It would be valuable to collect data on birth weight, vitals, bone structure, cognitive abilities, heart health and changes in gene expression at specific time points to determine the effects EGCG treatment could have on a normally

developing human fetus. It would also be useful to understand how prenatal EGCG treatment affects mothers independent of developing embryos.

To utilize the RNA sequence data and accompanying analyses performed here, a continued study of how transcript variants are affected by trisomy and lead to an altered phenotype would be valuable. qPCR can be utilized to better characterize differing expression of *Dyrk1a* transcript variants in trisomic and euploid tissues. Although *Dyrk1a* poses the greatest candidate for study, a study of the expression of other variable transcripts in DS genes of interest, including *Tiam1, Sh3bgr, Erg, Cldn8, Mrap,* or *Rcan1* would likely yield interesting findings about the trisomy-induced expression landscape.

The RNA-seqeunce data, specifically the differential expression analysis, also provides a great deal of information with which to discover alternate gene networks involved in the alteration of trisomic phenotypes. Because *Tiam1, Sh3bgr, Erg, Cldn8,* and *Mrap* were the only detected differentially expressed genes found in triplicate, finding other associated gene targets and pathways also dysregulated by trisomy will help to provide a more comprehensive understanding of additional gene networks that may be altered by trisomy. A functional analysis of differentially expressed genes and pathways would also be useful. Together with this continued research, we can better link altered mechanisms to associated phenotypes in trisomy. Success of this research may provide new or better understood targets for gene therapy in efforts to normalize DS phenotypes and provide the opportunity for enhanced quality of life for individuals with DS.

LIST OF REFERENCES

LIST OF REFERENCES

Adayev, T., M. C. Chen-Hwang, N. Murakami, J. Wegiel and Y. W. Hwang, 2006 Kinetic properties of a MNB/DYRK1A mutant suitable for the elucidation of biochemical pathways. Biochemistry **45:** 12011-12019.

Allen, E. G., S. B. Freeman, C. Druschel, C. A. Hobbs, L. A. O'Leary *et al.*, 2009 Maternal age and risk for trisomy 21 assessed by the origin of chromosome nondisjunction: a report from the Atlanta and National Down Syndrome Projects. Hum Genet **125:** 41-52.

Altafaj, X., M. Dierssen, C. Baamonde, E. Marti, J. Visa *et al.*, 2001 Neurodevelopmental delay, motor abnormalities and cognitive deficits in transgenic mice overexpressing Dyrk1A (minibrain), a murine model of Down's syndrome. Hum Mol Genet **10:** 1915-1923.

Altafaj, X., E. D. Martin, J. Ortiz-Abalia, A. Valderrama, C. Lao-Peregrin *et al.*, 2013 Normalization of Dyrk1A expression by AAV2/1-shDyrk1A attenuates hippocampal-dependent defects in the Ts65Dn mouse model of Down syndrome. Neurobiol Dis **52:** 117-127.

Antonarakis, S. E., 1991 Parental origin of the extra chromosome in trisomy 21 as indicated by analysis of DNA polymorphisms. Down Syndrome Collaborative Group. N Engl J Med **324:** 872-876.

Arron, J. R., M. M. Winslow, A. Polleri, C.-P. Chang, H. Wu *et al.*, 2006 NFAT dysregulation by increased dosage of DSCR1 and DYRK1A on chromosome 21. Nature **441:** 595-600.

Baek, K.-H., A. Zaslavsky, R. C. Lynch, C. Britt, Y. Okada *et al.*, 2009 Down's syndrome suppression of tumour growth and the role of the calcineurin inhibitor DSCR1. Nature **459:** 1126-1130.

Bain, J., H. McLauchlan, M. Elliott and P. Cohen, 2003 The specificities of protein kinase inhibitors: an update. Biochem J **371:** 199-204.

Baxter, L. L., T. H. Moran, J. T. Richtsmeier, J. Troncoso and R. H. Reeves, 2000 Discovery and genetic localization of Down syndrome cerebellar phenotypes using the Ts65Dn mouse. Hum Mol Genet **9:** 195-202.

Belichenko, P. V., E. Masliah, A. M. Kleschevnikov, A. J. Villar, C. J. Epstein *et al.*, 2004 Synaptic structural abnormalities in the Ts65Dn mouse model of down syndrome. The Journal of Comparative Neurology **480:** 281-298.

Berg, J. M., and M. Korossy, 2001 Down syndrome before Down: a retrospect. Am J Med Genet **102:** 205-211.

Bianchi, D. W., L. D. Platt, J. D. Goldberg, A. Z. Abuhamad, A. J. Sehnert *et al.*, 2012 Genome-wide fetal aneuploidy detection by maternal plasma DNA sequencing. Obstet Gynecol **119:** 890-901.

Billingsley, C. N., J. R. Allen, D. D. Baumann, S. L. Deitz, J. D. Blazek *et al.*, 2013 Non-trisomic homeobox gene expression during craniofacial development in the Ts65Dn mouse model of Down syndrome. American Journal of Medical Genetics Part A **161:** 1866-1874.

Blazek, J. D., A. Gaddy, R. Meyer, R. J. Roper and J. Li, 2011 Disruption of bone development and homeostasis by trisomy in Ts65Dn Down syndrome mice. Bone **48:** 275-280.

Boeira, J. M., J. da Silva, B. Erdtmann and J. A. Henriques, 2001 Genotoxic effects of the alkaloids harman and harmine assessed by comet assay and chromosome aberration test in mammalian cells in vitro. Pharmacol Toxicol **89:** 287-294.

Branchi, I., Z. Bichler, L. Minghetti, J. M. Delabar, F. Malchiodi-Albedi *et al.*, 2004 Transgenic mouse in vivo library of human Down syndrome critical region 1: association between DYRK1A overexpression, brain development abnormalities, and cell cycle protein alteration. J Neuropathol Exp Neurol **63:** 429-440.

Chen, J. Y., J. R. Lin, F. C. Tsai and T. Meyer, 2013 Dosage of Dyrk1a shifts cells within a p21-cyclin D1 signaling map to control the decision to enter the cell cycle. Mol Cell **52:** 87-100.

Chou, C. Y., L. Y. Liu, C. Y. Chen, C. H. Tsai, H. L. Hwa *et al.*, 2008 Gene expression variation increase in trisomy 21 tissues. Mamm Genome **19:** 398-405.

Christ, B., and C. P. Ordahl, 1995 Early stages of chick somite development. Anat Embryol (Berl) **191:** 381-396.

Cocchi, G., S. Gualdi, C. Bower, J. Halliday, B. Jonsson *et al.*, 2010 International trends of Down syndrome 1993-2004: Births in relation to maternal age and terminations of pregnancies. Birth Defects Res A Clin Mol Teratol **88:** 474-479.

Coppus, A. M., 2013 People with intellectual disability: what do we know about adulthood and life expectancy? Dev Disabil Res Rev **18:** 6-16.

Costa, V., C. Angelini, L. D'Apice, M. Mutarelli, A. Casamassimi *et al.*, 2011 Massive-scale RNA-Seq analysis of non ribosomal transcriptome in human trisomy 21. PLoS One **6:** e18493.

Courcet, J. B., L. Faivre, P. Malzac, A. Masurel-Paulet, E. Lopez *et al.*, 2012 The DYRK1A gene is a cause of syndromic intellectual disability with severe microcephaly and epilepsy. J Med Genet **49:** 731-736.

Daley, R., M. Hill and L. S. Chitty, 2014 Non-invasive prenatal diagnosis: progress and potential. Arch Dis Child Fetal Neonatal Ed **99**:F426-30.

Davisson, M. T., C. Schmidt and E. C. Akeson, 1990 Segmental trisomy of murine chromosome 16: a new model system for studying Down syndrome. Prog Clin Biol Res **360:** 263-280.

Davisson, M. T., C. Schmidt, R. H. Reeves, N. G. Irving, E. C. Akeson *et al.*, 1993 Segmental trisomy as a mouse model for Down syndrome. Prog Clin Biol Res **384:** 117-133.

De la Torre, R., S. De Sola, M. Pons, A. Duchon, M. M. de Lagran *et al.*, 2014 Epigallocatechin-3-gallate, a DYRK1A inhibitor, rescues cognitive deficits in Down syndrome mouse models and in humans. Mol Nutr Food Res **58:** 278-288.

Deitz, S. L., and R. J. Roper, 2011 Trisomic and allelic differences influence phenotypic variability during development of Down syndrome mice. Genetics **189:** 1487-1495.

Down, J. L., 1866 Observations on an ethnic classification of idiots. Ment Retard **33:** 54-56.

Driscoll, D. A., and S. Gross, 2009 Clinical practice. Prenatal screening for aneuploidy. N Engl J Med **360:** 2556-2562.

Dufresne, C. J., and E. R. Farnworth, 2001 A review of latest research findings on the health promotion properties of tea. J Nutr Biochem **12:** 404-421.

Egeo, A., R. Di Lisi, C. Sandri, M. Mazzocco, M. Lapide *et al.*, 2000 Developmental expression of the SH3BGR gene, mapping to the Down syndrome heart critical region. Mech Dev **90:** 313-316.

Epstein, C. J., 2001 Down syndrome (trisomy 21), pp. 1223–1256 in *The Metabolic and Melocular Bases of Inherited Disease*, edited by C. Scriver, A. Beaudet, W. Sly and D. Valle. McGraw-Hill, New York.

Faulks, D., V. Collado, M. N. Mazille, J. L. Veyrune and M. Hennequin, 2008 Masticatory dysfunction in persons with Down's syndrome. Part 1: aetiology and incidence. Journal of Oral Rehabilitation **35:** 854-862.

Frick, A., O. Suzuki, N. Butz, E. Chan and T. Wiltshire, 2013 In vitro and in vivo mouse models for pharmacogenetic studies. Methods Mol Biol **1015:** 263-278.

Frost, D., B. Meechoovet, T. Wang, S. Gately, M. Giorgetti *et al.*, 2011 Beta-carboline compounds, including harmine, inhibit DYRK1A and tau phosphorylation at multiple Alzheimer's disease-related sites. PLoS One **6:** e19264.

Gorzelnik, K., J. Bijok, J. G. Zimowski, G. Jakiel and T. Roszkowski, 2013 Noninvasive prenatal diagnosis of trisomy 21, 18 and 13 using cell-free fetal DNA. Ginekol Pol **84:** 714-719.

Guedj, F., and D. W. Bianchi, 2013 Noninvasive prenatal testing creates an opportunity for antenatal treatment of Down syndrome. Prenatal Diagnosis **33:** 614-618.

Guedj, F., C. Sebrie, I. Rivals, A. Ledru, E. Paly *et al.*, 2009 Green tea polyphenols rescue of brain defects induced by overexpression of DYRK1A. PLoS One **4:** e4606.

Guimaraes, C. V., L. F. Donnelly, S. R. Shott, R. S. Amin and M. Kalra, 2008 Relative rather than absolute macroglossia in patients with Down syndrome: implications for treatment of obstructive sleep apnea. Pediatr Radiol **38:** 1062-1067.

Hattori, M., A. Fujiyama, T. D. Taylor, H. Watanabe, T. Yada *et al.*, 2000 The DNA sequence of human chromosome 21. Nature **405:** 311-319.

Hennequin, M., P. J. Allison and J. L. Veyrune, 2000 Prevalence of oral health problems in a group of individuals with Down syndrome in France. Developmental Medicine & Child Neurology **42:** 691-698.

Hennequin, M., D. Faulks, J. L. Veyrune and P. Bourdiol, 1999 Significance of oral health in persons with Down syndrome: a literature review. Developmental Medicine & Child Neurology **41:** 275-283.

Hodgson, J. M., and K. D. Croft, 2010 Tea flavonoids and cardiovascular health. Mol Aspects Med **31:** 495-502.

Huether, C. A., J. Ivanovich, B. S. Goodwin, E. L. Krivchenia, V. S. Hertzberg *et al.*, 1998 Maternal age specific risk rate estimates for Down syndrome among live births in whites and other races from Ohio and metropolitan Atlanta, 1970-1989. J Med Genet **35:** 482-490.

Insausti, A. M., M. Megias, D. Crespo, L. M. Cruz-Orive, M. Dierssen *et al.*, 1998 Hippocampal volume and neuronal number in Ts65Dn mice: a murine model of Down syndrome. Neurosci Lett **253:** 175-178.

Isbrucker, R. A., J. Bausch, J. A. Edwards and E. Wolz, 2006 Safety studies on epigallocatechin gallate (EGCG) preparations. Part 1: genotoxicity. Food Chem Toxicol **44:** 626-635.

Kahlem, P., M. Sultan, R. Herwig, M. Steinfath, D. Balzereit *et al.*, 2004 Transcript level alterations reflect gene dosage effects across multiple tissues in a mouse model of down syndrome. Genome Res **14:** 1258-1267.

Kent, R. D., and H. K. Vorperian, 2013 Speech Impairment in Down Syndrome: A Review. Journal of Speech, Language, and Hearing Research **56:** 178-210.

Knecht, A. K., and M. Bronner-Fraser, 2002 Induction of the neural crest: a multigene process. Nat Rev Genet **3:** 453-461.

Korbel, J. O., T. Tirosh-Wagner, A. E. Urban, X. N. Chen, M. Kasowski *et al.*, 2009 The genetic architecture of Down syndrome phenotypes revealed by high-resolution analysis of human segmental trisomies. Proc Natl Acad Sci U S A **106:** 12031-12036.

Kurabayashi, N., and K. Sanada, 2013 Increased dosage of DYRK1A and DSCR1 delays neuronal differentiation in neocortical progenitor cells. Genes Dev **27:** 2708-2721.

Lander, E. S., 2011 Initial impact of the sequencing of the human genome. Nature **470:** 187-197.

Lejeune, J., R. Turpin and M. Gautier, 1959a Chromosomic diagnosis of mongolism. Arch Fr Pediatr **16:** 962-963.

Lejeune, J., R. Turpin and M. Gautier, 1959b Mongolism; a chromosomal disease (trisomy). Bull Acad Natl Med **143:** 256-265.

Letourneau, A., F. A. Santoni, X. Bonilla, M. R. Sailani, D. Gonzalez *et al.*, 2014 Domains of genome-wide gene expression dysregulation in Down's syndrome. Nature **508:** 345-350.

Li, C., L. Jin, Y. Bai, Q. Chen, L. Fu *et al.*, 2012 Genome-wide expression analysis in Down syndrome: insight into immunodeficiency. PLoS One **7:** e49130.

Lim, J. H., S. Y. Park and H. M. Ryu, 2013 Non-invasive prenatal diagnosis of fetal trisomy 21 using cell-free fetal DNA in maternal blood. Obstet Gynecol Sci **56:** 58-66.

Liu, C., M. Morishima, X. Jiang, T. Yu, K. Meng *et al.*, 2014 Engineered chromosome-based genetic mapping establishes a 3.7 Mb critical genomic region for Down syndrome-associated heart defects in mice. Hum Genet **133:** 743-753.

Loane, M., J. K. Morris, M. C. Addor, L. Arriola, J. Budd *et al.*, 2013 Twenty-year trends in the prevalence of Down syndrome and other trisomies in Europe: impact of maternal age and prenatal screening. Eur J Hum Genet **21:** 27-33.

Long, L., Y. Li, Y. D. Wang, Q. Y. He, M. Li *et al.*, 2010 The preventive effect of oral EGCG in a fetal alcohol spectrum disorder mouse model. Alcohol Clin Exp Res **34:** 1929-1936.

Lyle, R., F. Bena, S. Gagos, C. Gehrig, G. Lopez *et al.*, 2009 Genotype-phenotype correlations in Down syndrome identified by array CGH in 30 cases of partial trisomy and partial monosomy chromosome 21. Eur J Hum Genet **17:** 454-466.

Malone, F. D., J. A. Canick, R. H. Ball, D. A. Nyberg, C. H. Comstock *et al.*, 2005 First-trimester or second-trimester screening, or both, for Down's syndrome. N Engl J Med **353:** 2001-2011.

Marguerat, S., and J. Bahler, 2010 RNA-seq: from technology to biology. Cell Mol Life Sci **67:** 569-579.

Martinez-Frias, M. L., 2005 The real earliest historical evidence of Down syndrome. Am J Med Genet A **132a:** 231.

Martinez de Lagran, M., X. Altafaj, X. Gallego, E. Marti, X. Estivill *et al.*, 2004 Motor phenotypic alterations in TgDyrk1a transgenic mice implicate DYRK1A in Down syndrome motor dysfunction. Neurobiol Dis **15:** 132-142.

Mazur-Kolecka, B., A. Golabek, E. Kida, A. Rabe, Y. W. Hwang *et al.*, 2012 Effect of DYRK1A activity inhibition on development of neuronal progenitors isolated from Ts65Dn mice. J Neurosci Res **90:** 999-1010.

Megarbane, A., A. Ravel, C. Mircher, F. Sturtz, Y. Grattau *et al.*, 2009 The 50th anniversary of the discovery of trisomy 21: the past, present, and future of research and treatment of Down syndrome. Genet Med **11:** 611-616.

Moore, C. S., 2006 Postnatal lethality and cardiac anomalies in the Ts65Dn Down syndrome mouse model. Mamm Genome **17:** 1005-1012.

Moore, C. S., and R. J. Roper, 2007 The power of comparative and developmental studies for mouse models of Down syndrome. Mamm Genome **18:** 431-443.

Morris, J. K., and E. Alberman, 2009 Trends in Down's syndrome live births and antenatal diagnoses in England and Wales from 1989 to 2008: analysis of data from the National Down Syndrome Cytogenetic Register. Bmj **339:** b3794.

Mouton, P. R., 2002 *Principles and practices of unbiased stereology: an introduction for bioscientists Johns Hopkins University Press*, Baltimore.

Muller, F., M. Rebiffe, A. Taillandier, J. F. Oury and E. Mornet, 2000 Parental origin of the extra chromosome in prenatally diagnosed fetal trisomy 21. Hum Genet **106:** 340-344.

Nagle, D. G., D. Ferreira and Y. D. Zhou, 2006 Epigallocatechin-3-gallate (EGCG): chemical and biomedical perspectives. Phytochemistry **67:** 1849-1855.

Neri, G., and J. M. Opitz, 2009 Down syndrome: comments and reflections on the 50th anniversary of Lejeune's discovery. Am J Med Genet A **149a:** 2647-2654.

Norton, M. E., H. Brar, J. Weiss, A. Karimi, L. C. Laurent *et al.*, 2012 Non-Invasive Chromosomal Evaluation (NICE) Study: results of a multicenter prospective cohort study for detection of fetal trisomy 21 and trisomy 18. Am J Obstet Gynecol **207:** 137.e131-138.

Ortiz-Abalia, J., I. Sahun, X. Altafaj, N. Andreu, X. Estivill *et al.*, 2008 Targeting Dyrk1A with AAVshRNA attenuates motor alterations in TgDyrk1A, a mouse model of Down syndrome. Am J Hum Genet **83:** 479-488.

Palomaki, G. E., C. Deciu, E. M. Kloza, G. M. Lambert-Messerlian, J. E. Haddow *et al.*, 2012 DNA sequencing of maternal plasma reliably identifies trisomy 18 and trisomy 13 as well as Down syndrome: an international collaborative study. Genet Med **14:** 296-305.

Parker, S. E., C. T. Mai, M. A. Canfield, R. Rickard, Y. Wang *et al.*, 2010 Updated National Birth Prevalence estimates for selected birth defects in the United States, 2004-2006. Birth Defects Res A Clin Mol Teratol **88:** 1008-1016.

Pons-Espinal, M., M. Martinez de Lagran and M. Dierssen, 2013 Environmental enrichment rescues DYRK1A activity and hippocampal adult neurogenesis in TgDyrk1A. Neurobiol Dis **60:** 18-31.

Ralston, S. J., D. Wertz, D. Chelmow, S. D. Craigo and D. W. Bianchi, 2001 Pregnancy outcomes after prenatal diagnosis of aneuploidy. Obstet Gynecol **97:** 729-733.

Reeves, R. H., N. G. Irving, T. H. Moran, A. Wohn, C. Kitt *et al.*, 1995 A mouse model for Down syndrome exhibits learning and behaviour deficits. Nat Genet **11:** 177-184.

Reinholdt, L., Y. Ding, G. Gilbert, A. Czechanski, J. Solzak *et al.*, 2011 Molecular characterization of the translocation breakpoints in the Down syndrome mouse model Ts65Dn. Mammalian Genome **22:** 685-691.

Richtsmeier, J. T., L. Baxter and R. H. Reeves, 2000 Parallels of craniofacial maldevelopment in Down Syndrome and Ts65Dn mice. Developmental Dynamics **217:** 137-145.

Richtsmeier, J. T., A. Zumwalt, E. J. Carlson, C. J. Epstein and R. H. Reeves, 2002 Craniofacial phenotypes in segmentally trisomic mouse models for Down syndrome. American Journal of Medical Genetics **107:** 317-324.

Robinson, M. D., D. J. McCarthy and G. K. Smyth, 2010 edgeR: a Bioconductor package for differential expression analysis of digital gene expression data. Bioinformatics **26:** 139-140.

Roper, R. J., L. L. Baxter, N. G. Saran, D. K. Klinedinst, P. A. Beachy *et al.*, 2006a Defective cerebellar response to mitogenic Hedgehog signaling in Down [corrected] syndrome mice. Proc Natl Acad Sci U S A **103:** 1452-1456.

Roper, R. J., and R. H. Reeves, 2006 Understanding the Basis for Down Syndrome Phenotypes. PLoS Genet **2:** e50.

Roper, R. J., H. K. St John, J. Philip, A. Lawler and R. H. Reeves, 2006b Perinatal loss of Ts65Dn Down syndrome mice. Genetics **172:** 437-443.

Roper, R. J., J. F. VanHorn, C. C. Cain and R. H. Reeves, 2009 A neural crest deficit in Down syndrome mice is associated with deficient mitotic response to Sonic hedgehog. Mechanisms of Development **126:** 212-219.

Rueda, N., J. Florez and C. Martinez-Cue, 2012 Mouse models of Down syndrome as a tool to unravel the causes of mental disabilities. Neural Plast **2012:** 584071.

Santagati, F., and F. M. Rijli, 2003 Cranial neural crest and the building of the vertebrate head. Nat Rev Neurosci **4:** 806-818.

Saran, N. G., M. T. Pletcher, J. E. Natale, Y. Cheng and R. H. Reeves, 2003 Global disruption of the cerebellar transcriptome in a Down syndrome mouse model. Hum Mol Genet **12:** 2013-2019.

Sérégaza, Z., P. L. Roubertoux, M. Jamon and B. Soumireu-Mourat, 2006 Mouse Models of Cognitive Disorders in Trisomy 21: A Review. Behavior Genetics **36:** 387-404.

Shott, S. R., 2006 Down syndrome: Common otolaryngologic manifestations. American Journal of Medical Genetics Part C: Seminars in Medical Genetics **142C:** 131-140.

Solzak, J. P., Y. Liang, F. C. Zhou and R. J. Roper, 2013 Commonality in Down and fetal alcohol syndromes. Birth Defects Res A Clin Mol Teratol **97:** 187-197.

Soppa, U., J. Schumacher, V. Florencio Ortiz, T. Pasqualon, F. J. Tejedor *et al.*, 2014 The Down syndrome-related protein kinase DYRK1A phosphorylates p27 and Cyclin D1 and induces cell cycle exit and neuronal differentiation. Cell Cycle **13**.

Souchet, B., F. Guedj, I. Sahun, A. Duchon, F. Daubigney *et al.*, 2014 Excitation/inhibition balance and learning are modified by Dyrk1a gene dosage. Neurobiol Dis.

Spahis, J. K., and G. N. Wilson, 1999 Down syndrome: perinatal complications and counseling experiences in 216 patients. Am J Med Genet **89:** 96-99.

Spender, Q., A. Stein, J. Dennis, S. Reilly, E. Percy *et al.*, 1996 An exploration of feeding difficulties in children with Down syndrome. Dev Med Child Neurol **38:** 681-694.

Stankiewicz, M. J., and J. D. Crispino, 2013 AKT collaborates with ERG and Gata1s to dysregulate megakaryopoiesis and promote AMKL. Leukemia **27:** 1339-1347.

Starbuck, J. M., T. M. Cole, 3rd, R. H. Reeves and J. T. Richtsmeier, 2013 Trisomy 21 and facial developmental instability. Am J Phys Anthropol **151:** 49-57.

Sturgeon, X., and K. J. Gardiner, 2011 Transcript catalogs of human chromosome 21 and orthologous chimpanzee and mouse regions. Mamm Genome **22:** 261-271.

Sussan, T. E., A. Yang, F. Li, M. C. Ostrowski and R. H. Reeves, 2008 Trisomy represses Apc(Min)-mediated tumours in mouse models of Down's syndrome. Nature **451:** 73-75.

Suwanwela, J., J. Lee, A. Lin, T. C. Ucer, H. Devlin *et al.*, 2011 A genetic association study of single nucleotide polymorphisms in FGFR1OP2/wit3.0 and long-term atrophy of edentulous mandible. PLoS One **6:** e16204.

Tejedor, F. J., and B. Hammerle, 2011 MNB/DYRK1A as a multiple regulator of neuronal development. FEBS J **278:** 223-235.

Thomazeau, A., O. Lassalle, J. Iafrati, B. Souchet, F. Guedj *et al.*, 2014 Prefrontal deficits in a murine model overexpressing the down syndrome candidate gene dyrk1a. J Neurosci **34:** 1138-1147.

Toiber, D., G. Azkona, S. Ben-Ari, N. Toran, H. Soreq *et al.*, 2010 Engineering DYRK1A overdosage yields Down syndrome-characteristic cortical splicing aberrations. Neurobiol Dis **40:** 348-359.

van Gameren-Oosterom, H. B., S. E. Buitendijk, C. M. Bilardo, K. M. van der Pal-de Bruin, J. P. Van Wouwe *et al.*, 2012 Unchanged prevalence of Down syndrome in the Netherlands: results from an 11-year nationwide birth cohort. Prenat Diagn **32:** 1035-1040.

Venters, S. J., M. L. Hultner and C. P. Ordahl, 2008 Somite cell cycle analysis using somite-staging to measure intrinsic developmental time. Dev Dyn **237:** 377-392.

Wang, D., F. Wang, Y. Tan, L. Dong, L. Chen *et al.*, 2012 Discovery of potent small molecule inhibitors of DYRK1A by structure-based virtual screening and bioassay. Bioorg Med Chem Lett **22:** 168-171.

Wegiel, J., C. X. Gong and Y. W. Hwang, 2011 The role of DYRK1A in neurodegenerative diseases. Febs j **278:** 236-245.

Williamson, G., F. Dionisi and M. Renouf, 2011 Flavanols from green tea and phenolic acids from coffee: critical quantitative evaluation of the pharmacokinetic data in humans after consumption of single doses of beverages. Mol Nutr Food Res **55:** 864-873.

Wilson, K. L., J. L. Czerwinski, J. M. Hoskovec, S. J. Noblin, C. M. Sullivan *et al.*, 2013 NSGC practice guideline: prenatal screening and diagnostic testing options for chromosome aneuploidy. J Genet Couns **22:** 4-15.

Wiseman, F. K., K. A. Alford, V. L. Tybulewicz, and E. M. Fisher, 2013 Down syndrome--recent progress and future prospects. Hum Mol Genet **18:** 75-83.

Zhao, H., P. Bringas, Jr. and Y. Chai, 2006 An in vitro model for characterizing the post-migratory cranial neural crest cells of the first branchial arch. Dev Dyn **235:** 1433-1440.

TABLES

Table 2.1: Degradation Analysis of EGCG by HPLC-MS

Chemical composition of EGCG prepared as described for the G0-G9.5 i*n-vivo ad libitum* treatment was tested by HPLC-MS analysis after sitting at room temperature for 1, 24, and 48 hours. Data show that EGCG degrades rapidly at room temperature dissolved in water and undergoes significant reductions in concentration over time (Abeysekera, Roper, *Unpublished data*).

Treatment	Time point (hours)	Expected Concentration (mg/mL)	Calculated concentration (mg/mL)
EGCG	1	1	1.001 ±0.0015
	24	1	0.3349 ±0.014
	48	1	0.1699 ±0.013

Table 3.1: G0 – G9.5 *In-vivo* Water and EGCG *Ad libitum* Treatment Data

Father Genotype	Mother Genotype	Treatment Type	Pregnant at G9.5	n	Average body weight at G9.5 (g)	Average total treatment consumed G0-G9.5 (mL) (Figure 3.5)	Average mL treatment consumed per g body weight	Average overall EGCG consumed G0-G9.5 (mg)	mg EGCG/kg/day	Estimated mg EGCG/kg/day with EGCG degratation (Figure 3.6)
B6C3F1	Trisomic	H20	Yes	16	26.838	63.25	2.36	-	-	
B6C3F1	Trisomic	H20	No	7	22.371	61.214	2.74	-	-	
B6C3F1	Trisomic	EGCG	Yes	4	27.540	71.125	2.58	6.615	26.769	12.318
B6C3F1	Trisomic	EGCG	No	3	22.633	64.833	2.86	6.030	29.649	13.644
B6C3F1	Euploid	H20	Yes	9	27.433	66.833	2.44	-	-	
B6C3F1	Euploid	H20	No	2	22.950	81.500	3.55	-	-	
B6C3F1	Euploid	EGCG	Yes	3	27.967	63.00	2.25	5.859	23.367	10.753
B6C3F1	Euploid	EGCG	-	-	-	-		-	-	
									Average	**12.238**
									Standard Deviation*	**2.195**
									Standard Error of the Mean (SEM)*	**0.732**

* Calculated using individual sample values rather than group averages

Table 4.1: Differential Expression Analysis of Trisomic and Euploid E9.25 NT

Gene	Human Chromosome Homologue	Gene Description	logConc	logFC	P.Value	adj.P.Val
Ak2	1	adenylate kinase 2	-12.7943	0.213929	2.04E-06	0.007295
Mrpl9	1	mitochondrial ribosomal protein L9	-13.5808	0.248396	2.14E-06	0.007295
Stil	1	SCL/TAL1 interrupting locus	-13.656	-0.2503	3.15E-06	0.007295
Ubiad1	1	UbiA prenyltransferase domain containing 1	-14.9877	0.317282	2.33E-05	0.018553
Dhcr24	1	24-dehydrocholesterol reductase	-11.3304	0.141935	0.000151	0.049889
Usp48	1	ubiquitin specific peptidase 48	-12.6019	-0.16291	0.000191	0.054019
Aff3	2	AF4/FMR2 family, member 3	-13.6731	-0.39374	1.43E-05	0.017997
Alms1	2	Alstrom syndrome 1	-12.4493	-0.18336	1.75E-05	0.018553
Id2	2	inhibitor of DNA binding 2, dominant negative helix-loop-helix protein	-12.435	-0.17623	3.65E-05	0.020333
Snrpg	2	small nuclear ribonucleoprotein polypeptide G	-15.7556	-0.3554	0.000173	0.053513
Tbccd1	3	TBCC domain containing 1	-14.7609	0.282969	7.88E-05	0.035298
Smarcad1	4	SWI/SNF-related, matrix-associated actin-dependent regulator of chromatin, subfamily a, containing DEAD/H box 1	-12.3527	-0.20872	7.93E-07	0.005504

Table 4.1, continued

Ostc	4	oligosaccharyltransferase complex subunit	-12.9873	0.175576	0.000181	0.053811
Lin54	4	lin-54 homolog (C. elegans)	-13.8964	-0.21105	0.000216	0.05668
Dap	5	death-associated protein	-16.2402	-0.46654	3.11E-05	0.019717
Pim1	6	pim-1 oncogene	-14.1993	0.391914	3.93E-05	0.020333
Fam120b	6	family with sequence similarity 120B	-15.0223	-0.30018	8.40E-05	0.036428
Ier3	6	immediate early response 3	-20.3423	1.661395	0.000207	0.056385
Zfp788	7	zinc finger protein 788	-14.8817	-0.34162	3.09E-06	0.007295
Ephb6	7	Eph receptor B6	-15.6419	0.422153	4.95E-06	0.009821
Mios	7	missing oocyte, meiosis regulator, homolog (Drosophila)	-13.9587	-0.22248	0.000108	0.039944
Ncapg2	7	non-SMC condensin II complex, subunit G2	-12.3973	-0.15811	0.000182	0.053811
Efha2	8	EF-hand domain family, member A2	-16.82	-0.5728	2.18E-05	0.018553
Lrrcc1	8	leucine rich repeat and coiled-coil centrosomal protein 1	-13.8255	-0.22052	7.36E-05	0.034055
Inpp5e	9	inositol polyphosphate-5-phosphatase, 72 kDa	-14.6541	-0.42584	2.51E-05	0.018553
Chmp5	9	charged multivesicular body protein 5	-13.9686	0.244407	2.67E-05	0.018553
Igsf9b	11	immunoglobulin superfamily, member 9B	-15.4905	-0.39395	7.72E-06	0.013396

Table 4.1, continued

Prkcdbp	11	protein kinase C, delta binding protein	-17.2982	0.880583	1.05E-05	0.016273
Nfrkb	11	nuclear factor related to kappaB binding protein	-14.2859	-0.25835	4.10E-05	0.020333
Sdhd	11	succinate dehydrogenase complex, subunit D, integral membrane protein	-13.3573	0.196824	0.000103	0.0398
Pitpnm1	11	phosphatidylinositol transfer protein, membrane-associated 1	-16.9881	0.722254	0.000129	0.044707
Adipor2	12	adiponectin receptor 2	-12.7504	0.189551	2.57E-05	0.018553
Dynll1	12	dynein, light chain, LC8-type 1	-11.9128	0.165497	3.35E-05	0.020208
Mlec	12	malectin	-10.4517	0.137748	8.98E-05	0.036428
Uhrf1bp1l	12	UHRF1 (ICBP90) binding protein 1-like	-13.4865	-0.19601	0.000146	0.049312
Kntc1	12	kinetochore associated 1	-12.5547	-0.16332	0.000193	0.054019
Srsf9	12	serine/arginine-rich splicing factor 9	-13.1778	0.177621	0.000216	0.05668
Akap11	13	A kinase (PRKA) anchor protein 11	-11.676	-0.21352	3.60E-08	0.0005
Zdhhc20	13	zinc finger, DHHC-type containing 20	-13.093	-0.20282	2.22E-05	0.018553
Idh3a	15	isocitrate dehydrogenase 3 (NAD+) alpha	-13.5238	0.218021	3.12E-05	0.019717
Mmp15	16	matrix metallopeptidase 15	-14.2572	0.230541	0.000166	0.052502

Table 4.1, continued

Snrpd1	19	small nuclear ribonucleoprotein D2 polypeptide 16.5kDa	-13.1576	0.189321	0.000112	0.039944
Cacna1a	19	calcium channel, voltage-dependent, P/Q type,alpha 1A subunit	-16.2249	-0.41273	0.000195	0.054019
Gpcpd1	20	glycerophosphocholine phosphodiesterase GDE1 homolog	-14.7663	-0.43191	2.23E-05	0.018553
Sez6l	22	seizure related 6 homolog (mouse)-like	-17.7091	-0.85455	0.000112	0.039944
Prps2	X	phosphoribosyl pyrophosphate synthetase 2	-13.3607	-0.20733	3.97E-05	0.020333
Rab33a	X	RAB33A, member RAS oncogene family	-19.7235	1.514429	4.73E-05	0.022662
Arhgap36	X	Rho GTPase activating protein 36	-19.1589	-1.21519	8.94E-05	0.036428
Abca8b		ATP-binding cassette, sub-family A (ABC1), member 8b	-18.6885	-1.14695	1.23E-05	0.017076
9530091C08Rik		misc RNA RefSeq import	-17.4606	-1.18283	2.45E-05	0.018553
5830418K08Rik		RIKEN cDNA 5830418K08 gene	-12.5791	-0.17943	4.00E-05	0.020333
Zfp639		zinc finger protein 639	-14.9305	-0.29308	9.18E-05	0.036428
2610020H08Rik		RIKEN cDNA 2610020H08	-16.0046	-0.39361	0.000157	0.050586

Genes with no listed human chromosome homologue were genes found only in mouse.

Table 4.2: Differential Expression Analysis of Trisomic and Euploid E9.5 PA1

Mmu Gene	Human Chromosome Homologue	Description	logConc	logFC	P.Value	adj.P.Val
Tnnt2	1	troponin T2, cardia	-19.3943	-3.71116	4.28E-10	4.50E-07
Obscn	1	obscurin, cytoskeletal calmodulin and titin-interacting RhoGEF	-20.3212	-2.98365	1.55E-07	4.95E-05
Cited4	1	Cbp/p300-interacting transactivator, with Glu/Asp-rich carboxy-terminal domain, 4	-16.7008	1.346293	1.90E-07	5.91E-05
Nexn	1	nexilin (F actin binding protein)	-19.2088	-1.95298	2.18E-07	6.48E-05
Ryr2	1	ryanodine receptor 2 (cardiac)	-17.3056	-1.68824	3.42E-07	9.86E-05
Pklr	1	pyruvate kinase, liver and RBC	-15.098	1.092896	3.46E-07	9.86E-05
Dnm3os	1	DNM3 opposite strand/antisense RNA (non-protein coding)	-13.3269	-1.38649	7.53E-07	0.000189
Ermap	1	erythroblast membrane-associated protein (Scianna blood group)	-14.6365	1.010909	1.54E-06	0.000323
Rassf5	1	Ras association (RalGDS/AF-6) domain family member 5	-20.1291	-2.74136	1.75E-06	0.000361
Snord45c	1	small nucleolar RNA, C/D box 45C	-14.5217	-2.03633	1.96E-06	0.000386

Table 4.2, continued

Npr1	1	natriuretic peptide receptor A/guanylate cyclase A (atrionatriuretic peptide receptor A)	-17.0636	-1.17861	2.05E-06	0.000399
Actn2	1	actinin, alpha 2	-19.4995	-2.14574	2.19E-06	0.000412
Pdzk1ip1	1	PDZK1 interacting protein 1	-19.752	1.864615	7.91E-06	0.001084
Asb17	1	ankyrin repeat and SOCS box containing 17	-20.7567	2.653425	8.43E-06	0.001084
Tgfb2	1	transforming growth factor, beta 2	-17.146	-1.1013	8.63E-06	0.001091
Prkaa2	1	protein kinase, AMP-activated, alpha 2 catalytic subunit	-17.2456	-1.28588	1.44E-05	0.00167
Snord55	1	small nucleolar RNA, C/D box 55	-9.81852	-0.91157	1.98E-05	0.002182
Snord47	1	small nucleolar RNA, C/D box 47	-10.3862	-1.17075	2.25E-05	0.002437
Plekha6	1	pleckstrin homology domain containing, family A member 6	-17.4452	-1.22831	2.47E-05	0.002595
Rgs5	1	regulator of G-protein signaling 5	-16.0702	-1.18922	2.87E-05	0.002891
Mir199a-2	1	microRNA 199a-2	-18.9134	-1.56161	2.95E-05	0.002927
Snora16a	1	small nucleolar RNA, H/ACA box 16A	-15.2166	-1.10507	6.06E-05	0.005112
Ppfia4	1	protein tyrosine phosphatase, receptor type, f polypeptide (PTPRF), interacting protein (liprin), alpha 4	-17.114	-0.98584	6.75E-05	0.005586

Table 4.2, continued

Casq1	1	calsequestrin 1 (fast-twitch, skeletal muscle)	-20.1266	-1.9884	7.14E-05	0.005835
Tnni1	1	troponin I type 1 (skeletal, slow)	-17.8237	-1.57281	8.65E-05	0.006704
Mir214	1	microRNA 214	-18.0589	-1.17483	9.37E-05	0.00708
Ero1lb	1	ERO1-like beta (S. cerevisiae)	-18.7867	1.26908	0.000168	0.010778
Mgst3	1	microsomal glutathione S-transferase 3	-14.4252	0.87071	0.000203	0.012569
Mir664	1	small nucleolar RNA, H/ACA box 36B	-20.5081	-1.98906	0.000266	0.01556
Snora36b	1	small nucleolar RNA, H/ACA box 36B	-20.5283	-1.94876	0.000389	0.020779
Snora61	1	small nucleolar RNA, H/ACA box 61	-10.1994	-0.969	0.000428	0.022485
Tlr5	1	toll-like receptor 5	-19.8554	-1.58241	0.000438	0.022838
Gja5	1	gap junction protein, alpha 5, 40kDa	-15.9404	-0.96439	0.000617	0.02984
Tspan2	1	tetraspanin 2	-15.8409	-0.79725	0.000638	0.030426
Lmx1a	1	LIM homeobox transcription factor 1 alpha	-16.9828	0.839984	0.000655	0.030993
Spata1	1	Spermatogenesis-associated protein 1	-18.9247	-1.16716	0.000676	0.031598
Atp1b1	1	ATPase, Na+/K+ transporting, beta 1 polypeptide	-17.58	-1.03405	0.000791	0.035745
Nfia	1	nuclear factor I/A	-18.5734	-1.04941	0.00085	0.037465

Table 4.2, continued

Klhdc8a	1	kelch domain containing 8A	-19.6062	-1.38369	0.000865	0.037889
Lmod1	1	leiomodin 1 (smooth muscle)	-20.1146	-1.59609	0.001008	0.042475
Tmod4	1	tropomodulin 4 (muscle)	-19.5201	-1.32415	0.001044	0.04366
Rgs4	1	regulator of G-protein signaling 4	-20.0033	-1.62651	0.001054	0.043902
Rwdd3	1	RWD domain containing 3	-18.6117	-1.06331	0.001077	0.04444
Brdt	1	bromodomain, testis-specific	-19.4323	-1.2811	0.001176	0.047338
Smyd1	2	SET and MYND domain containing 1	-16.7078	-3.15762	3.85E-09	2.46E-06
Ttn	2	titin	-14.5844	-3.27642	4.78E-09	2.79E-06
Epas1	2	endothelial PAS domain protein 1	-16.5024	-1.32746	2.21E-06	0.000412
Zc3h6	2	zinc finger CCCH-type containing 6	-19.0458	-1.48007	2.36E-05	0.002512
Bcl11a	2	B cell CLL/lymphoma 11A (zinc finger protein)	-18.8831	-1.3616	6.71E-05	0.005586
Kcnh7	2	potassium voltage-gated channel, subfamily H (eag-related), member 7	-19.7507	-1.66942	0.0001	0.007328
Scn2a1	2	sodium channel, voltage-gated, type II, alpha subunit	-19.8241	-1.64911	0.00014	0.009486
Adcy3	2	adenylate cyclase 3	-16.3586	-0.86867	0.000146	0.009609

Table 4.2, continued

Kif1a	2	kinesin family member 1A	-16.4582	-0.82254	0.000158	0.010302
Neurod1	2	neurogenic differentiation 1	-20.4275	-1.86875	0.000273	0.015788
Nrxn1	2	neurexin 1	-18.2937	-1.39655	0.000303	0.016845
Snord53	2	small nucleolar RNA, C/D box 53	-12.5501	-0.77546	0.00031	0.017169
Rsad2	2	radical S-adenosyl methionine domain containing 2	-18.0235	-1.03751	0.000379	0.020333
Add2	2	adducin 2 (beta)	-14.9901	0.694501	0.000443	0.022998
Snord92	2	small nucleolar RNA, C/D box 92	-14.1181	-0.85214	0.000509	0.026026
Snord70	2	small nucleolar RNA, C/D box 70	-14.6665	-0.8487	0.000613	0.02984
Ifih1	2	interferon induced with helicase C domain 1	-20.3804	-1.71895	0.000805	0.036095
Dusp28	2	dual specificity phosphatase 28	-16.8363	-0.88277	0.000833	0.036998
Sphkap	2	SPHK1 interactor, AKAP domain containing	-17.6319	-1.3177	0.000955	0.041173
Pou3f3	2	POU class 3 homeobox 3	-17.4994	-1.02026	0.000989	0.042032
Sned1	2	sushi, nidogen and EGF-like domains 1	-18.6901	-1.04018	0.001306	0.05118
Slc8a1	2	solute carrier family 8 (sodium/calcium exchanger), member 1	-15.5574	-0.99185	0.001368	0.052806

Table 4.2, continued

Erbb4	2	v-erb-a erythroblastic leukemia viral oncogene homolog 4 (avian)	-20.2093	-1.61767	0.001433	0.053815
Xirp1	3	xin actin-binding repeat containing 1	-21.7953	-6.04913	8.33E-12	2.79E-08
Tdgf1	3	teratocarcinoma-derived growth factor 1	-21.5431	-4.54989	1.95E-08	9.03E-06
Kcnab1	3	potassium voltage-gated channel, shaker-related subfamily, beta member 1	-20.4192	-2.47088	1.24E-06	0.000277
Snora7a	3	small nucleolar RNA, H/ACA box 7A	-12.0668	-1.6092	2.79E-06	0.000505
Tnnc1	3	troponin C type 1 (slow)	-19.7577	-2.32334	5.20E-06	0.00082
Hesx1	3	HESX homeobox 1	-19.8931	2.128801	5.31E-06	0.000821
Snord61	3	Small nucleolar RNA SNORD61	-15.4615	-1.19682	7.28E-06	0.001049
Popdc2	3	popeye domain containing 2	-17.6838	-1.47734	8.93E-06	0.001119
Cpne4	3	copine IV	-20.0537	-2.14422	1.04E-05	0.001268
Cspg5	3	chondroitin sulfate proteoglycan 5 (neuroglycan C)	-19.4511	1.657913	3.16E-05	0.003088
Sema3b	3	sema domain, immunoglobulin domain (Ig), short basic domain, secreted, (semaphorin) 3B	-18.6522	-1.22154	0.000142	0.009536
Snord2	3	eukaryotic translation initiation factor 4A2	-14.4243	-0.96997	0.000179	0.011221

Table 4.2, continued

Adamts9	3	ADAM metallopeptidase with thrombospondin type 1 motif, 9	-14.8123	-0.83347	0.000183	0.01138
Cacna1d	3	calcium channel, voltage-dependent, L type, alpha 1D subunit	-16.743	-0.86018	0.000577	0.028343
Manf	3	mesencephalic astrocyte-derived neurotrophic factor	-13.0539	0.639832	0.00063	0.030277
Slc15a2	3	solute carrier family 15 (H+/peptide transporter), member 2	-17.2903	-1.0718	0.001073	0.0444
Rpl29	3	ribosomal protein L29	-13.9511	0.70219	0.001272	0.050454
Gypa	4	glycophorin A (MNS blood group)	-14.5644	0.947541	5.62E-06	0.000846
Fam198b	4	family with sequence similarity 198, member B	-16.437	-1.0855	4.92E-05	0.004488
Afp	4	alpha-fetoprotein	-20.1511	2.107951	7.68E-05	0.006244
Spp1	4	secreted phosphoprotein 1	-19.358	1.714514	0.000102	0.007352
Cpeb2	4	cytoplasmic polyadenylation element binding protein 2	-17.4279	-0.98508	0.000434	0.02273
Ppargc1a	4	peroxisome proliferator-activated receptor gamma, coactivator 1 alpha	-18.8714	-1.13089	0.000898	0.039198
Mrps18c	4	mitochondrial ribosomal protein S18C	-15.7633	0.678695	0.000953	0.041173

Table 4.2, continued

Manba	4	mannosidase, beta A, lysosomal	-18.4001	-1.0402	0.000979	0.041784
Synpo2	4	synaptopodin 2	-16.4335	-0.78473	0.001146	0.046356
Rnf150	4	ring finger protein 150	-16.1423	-0.67562	0.001383	0.052806
Prlr	5	prolactin receptor	-20.1183	-1.81043	0.000109	0.007665
Uqcrq	5	ubiquinol-cytochrome c reductase, complex III subunit VII, 9.5kDa	-15.1972	0.909517	0.000133	0.009072
Gpr98	5	G protein-coupled receptor 98	-15.3883	-0.81406	0.000158	0.010302
Lyrm7	5	Lyrm7 homolog (mouse)	-18.481	-1.27124	0.000314	0.017347
Gm2a	5	GM2 ganglioside activator	-17.6991	-0.93009	0.000818	0.036555
Ppp2r2b	5	protein phosphatase 2, regulatory subunit B, beta	-18.6281	-1.05693	0.001324	0.051581
Pdzd2	5	PDZ domain containing 2	-17.2126	-0.83746	0.001375	0.052806
Col12a1	6	collagen, type XII, alpha 1	-16.5265	-2.07908	7.53E-11	1.68E-07
Rhag	6	Rh-associated glycoprotein	-15.6944	1.025598	4.20E-06	0.0007
Syne1	6	spectrin repeat containing, nuclear envelope 1	-15.8698	-1.12388	5.06E-06	0.000807
Psmg4	6	proteasome (prosome, macropain) assembly chaperone 4	-16.6822	1.00291	2.54E-05	0.002622

Table 4.2, continued

Gata5	6	protein phosphatase 1, regulatory (inhibitor) subunit 14C	-17.9052	-1.36242	3.07E-05	0.003028
Pde7b	6	phosphodiesterase 7B	-17.9421	-1.13017	5.92E-05	0.005052
Phactr1	6	phosphatase and actin regulator 1	-16.8714	-0.94974	8.62E-05	0.006704
Hist1h3a	6	histone cluster 1, H3a	-12.4587	0.711003	0.000134	0.009115
Hist1h3g	6	histone cluster 1, H3g	-12.3733	0.682107	0.000246	0.014658
Fam65b	6	family with sequence similarity 65, member B	-19.5741	-1.44754	0.000303	0.016845
Synj2	6	synaptojanin 2	-16.6093	-0.79155	0.000379	0.020333
Hist1h2bn	6	histone cluster 1, H2bn	-13.329	0.653368	0.000511	0.026035
Klhl31	6	kelch-like 31 (Drosophila)	-20.2386	-1.77631	0.00057	0.028278
Snord66	6	Small nucleolar RNA SNORD66	-12.0523	-0.66791	0.000855	0.037595
Syncrip	6	synaptotagmin binding, cytoplasmic RNA interacting protein	-12.3561	-0.78791	0.001045	0.04366
Rps18	6	ribosomal protein S18	-15.0631	-0.89117	0.001093	0.044964
Hspa1b	6	heat shock 70kDa protein 1B	-18.4259	1.026991	0.001098	0.044996
Slc25a27	6	solute carrier family 25, member 27	-16.8749	-0.76603	0.001465	0.054774
Cap2	6	CAP, adenylate cyclase-associated protein,	-17.6622	-1.02046	0.001467	0.054774

Table 4.2, continued

		2 (yeast)				
Myl7	7	myosin, light chain 7, regulatory	-18.3004	-3.22894	4.06E-09	2.48E-06
Upk3b	7	uroplakin 3B	-19.4924	-2.33063	9.85E-08	3.33E-05
Tbx20	7	T-box 20	-16.961	-1.79452	2.08E-07	6.33E-05
Snord93	7	small nucleolar RNA, C/D box 93	-16.1858	-1.46131	4.91E-06	0.000793
Ikzf1	7	IKAROS family zinc finger 1 (Ikaros)	-16.0441	1.029381	2.07E-05	0.002253
Smarcd3	7	SWI/SNF related, matrix associated, actin dependent regulator of chromatin, subfamily d, member 3	-16.8105	-0.94729	8.07E-05	0.006516
Mrps24	7	mitochondrial ribosomal protein S24	-16.0475	0.883296	8.53E-05	0.00669
Kcp	7	kielin/chordin-like protein	-17.5511	-1.08004	8.86E-05	0.00679
Hoxa2	7	homeobox A2	-18.3598	-1.65873	0.000109	0.007665
Serpine1	7	serpin peptidase inhibitor, clade E (nexin, plasminogen activator inhibitor type 1), member 1	-18.1725	-1.09404	0.000177	0.011153
Zpbp	7	zona pellucida binding protein	-20.4236	-1.87945	0.000273	0.015788
Tspan33	7	tetraspanin 33	-16.3572	0.847488	0.000279	0.016033
Cacna2d1	7	calcium channel, voltage-dependent, alpha 2/delta subunit 1	-16.4657	-0.77395	0.000415	0.022011

Table 4.2, continued

Magi2	7	membrane associated guanylate kinase, WW and PDZ domain containing 2	-19.0241	-1.18505	0.000656	0.030993
Kel	7	Kell blood group, metallo-endopeptidase	-15.6864	0.745265	0.000792	0.035745
Nrbp2	8	nuclear receptor binding protein 2	-17.2452	-1.34411	1.30E-07	4.26E-05
Trim55	8	tripartite motif containing 55	-19.6456	-2.18783	6.95E-07	0.000183
Nkx2-6	8	NK2 homeobox 6	-18.5756	-1.85234	1.50E-06	0.000323
Car2	8	carbonic anhydrase II	-13.2247	0.828071	1.13E-05	0.00135
Gata4	8	GATA binding protein 4	-18.9711	-1.76994	1.54E-05	0.001768
Foxh1	8	forkhead box H1	-18.5924	1.402238	2.35E-05	0.002512
Sla	8	Src-like-adaptor	-19.5881	1.65995	9.84E-05	0.007247
Snord87	8	small nucleolar RNA, C/D box 87	-10.3935	-0.94958	0.000164	0.010626
Pkhd1l1	8	polycystic kidney and hepatic disease 1 (autosomal recessive)-like 1	-15.5258	0.782422	0.000358	0.019488
Cebpd	8	CCAAT/enhancer binding protein (C/EBP), delta	-19.6996	-1.45498	0.000554	0.027829
Plekha2	8	pleckstrin homology domain containing, family A (phosphoinositide binding specific) member 2	-15.6334	-0.77929	0.000728	0.033189

Table 4.2, continued

Scara3	8	scavenger receptor class A, member 3	-16.6706	-0.82181	0.000978	0.041784
Tnc	9	tenascin C	-15.504	-1.94483	2.04E-08	9.13E-06
Ddx58	9	DEAD (Asp-Glu-Ala-Asp) box polypeptide 58	-18.4821	-1.51925	1.13E-06	0.000261
Pgm5	9	phosphoglucomutase 5	-18.6455	-1.81956	3.17E-06	0.000566
Snora65	9	small nucleolar RNA, H/ACA box 65	-13.9262	-1.56057	3.30E-06	0.000575
Gfi1b	9	growth factor independent 1B transcription repressor	-17.8965	1.268166	1.15E-05	0.001359
Snord90	9	small nucleolar RNA, C/D box 90	-19.4455	-1.46398	0.000219	0.013411
Aqp3	9	aquaporin 3 (Gill blood group)	-17.5192	1.030949	0.000289	0.016365
Rusc2	9	RUN and SH3 domain containing 2	-18.0341	-0.97586	0.00052	0.026373
Ldb3	10	LIM domain binding 3	-20.7898	-4.89824	1.74E-13	1.17E-09
Ankrd1	10	ankyrin repeat domain 1 (cardiac muscle)	-19.7468	-3.79277	1.16E-10	2.21E-07
Acta2	10	actin, alpha 2, smooth muscle, aorta	-14.9387	-2.29823	6.11E-08	2.27E-05
Anubl1	10	zinc finger, AN1-type domain 4	-18.3849	-1.31915	1.44E-05	0.00167
Usmg5	10	up-regulated during skeletal muscle growth 5 homolog (mouse)	-16.3156	1.027089	1.99E-05	0.002182
Ppp1r14c	10	protein phosphatase 1, regulatory	-19.4963	-1.89405	2.91E-05	0.002912

Table 4.2, continued

		(inhibitor) subunit 14c				
Nebl	10	nebulette	-17.3285	-1.29096	3.48E-05	0.003353
Ret	10	ret proto-oncogene	-20.0676	-1.88951	8.34E-05	0.006653
Ptpre	10	protein tyrosine phosphatase, receptor type, E	-19.1747	-1.4849	9.51E-05	0.007119
Asah2	10	N-acylsphingosine amidohydrolase (non-lysosomal ceramidase) 2	-17.129	-0.9413	0.000343	0.018743
Sfxn3	10	sideroflexin 3	-18.2395	-0.96483	0.001101	0.044996
Uros	10	uroporphyrinogen III synthase	-15.0043	0.626338	0.001521	0.056547
Mybpc3	11	myosin binding protein C, cardiac	-18.8463	-4.30097	2.24E-10	3.10E-07
Eps8l2	11	EPS8-like 2	-16.337	-1.14236	6.74E-07	0.000181
Neat1	11	nuclear paraspeckle assembly transcript 1 (non-protein coding)	-18.2393	-1.71351	7.60E-07	0.000189
Tagln	11	transgelin	-15.2906	-1.50629	5.33E-06	0.000821
Snora3	11	small nucleolar RNA, H/ACA box 3	-16.1779	-1.53361	6.62E-06	0.000975
Snord15a	11	small nucleolar RNA, C/D box 15A	-11.5747	-1.53881	7.00E-06	0.00102
Cd44	11	CD44 molecule (Indian blood group)	-16.7495	-1.19218	1.40E-05	0.001648

Table 4.2, continued

Hmbs	11	hydroxymethylbilane synthase	-13.5345	0.759467	6.04E-05	0.005112
Mical2	11	microtubule associated monoxygenase, calponin and LIM domain containing 2	-17.9721	-1.1143	0.000209	0.01285
Slc1a2	11	solute carrier family 1 (glial high affinity glutamate transporter), member 2	-17.8241	-1.18071	0.0003	0.016803
Tspan18	11	tetraspanin 18	-15.9822	-0.83139	0.000391	0.020781
Naalad2	11	N-acetylated alpha-linked acidic dipeptidase 2	-19.2215	-1.29067	0.000711	0.032745
Scarna9	11	small Cajal body-specific RNA 9	-15.8258	-0.81474	0.000918	0.039974
Wt1	11	Wilms tumor 1	-20.0854	-1.47569	0.00131	0.051185
Abcg4	11	ATP-binding cassette, sub-family G (WHITE), member 4	-17.4508	0.851724	0.001411	0.053302
Snord67	11	Small nucleolar RNA SNORD67	-16.0266	-0.71269	0.001523	0.056547
Dhh	12	desert hedgehog	-20.3135	2.728132	5.16E-08	2.10E-05
Tbx5	12	T-box 5	-20.8049	-2.87231	4.43E-07	0.000124
Snora34	12	small nucleolar RNA, H/ACA box 34	-15.7914	-1.45704	7.84E-06	0.001084
Pde3a	12	phosphodiesterase 3A, cGMP-inhibited	-18.1716	-1.43315	8.38E-06	0.001084
Kcna5	12	potassium voltage-gated channel, shaker-related subfamily, member 5	-17.4065	-1.09018	2.53E-05	0.002622

Table 4.2, continued

Art4	12	ADP-ribosyltransferase 4	-16.9158	0.986679	5.51E-05	0.00486
Scarna10	12	small Cajal body-specific RNA 10	-15.1643	-0.82933	0.000102	0.007352
Tdg	12	thymine-DNA glycosylase	-15.6073	0.843566	0.000106	0.007483
Nfe2	12	nuclear factor (erythroid-derived 2), 45kDa	-16.531	0.860287	0.000266	0.01556
Snora2b	12	small nucleolar RNA, H/ACA box 2B	-17.88	-1.04011	0.000521	0.026373
Esyt1	12	extended synaptotagmin-like protein 1	-15.9231	-0.80105	0.000659	0.030993
Hebp1	12	heme binding protein 1	-15.8889	0.717942	0.001288	0.050791
Snord22	13	Small nucleolar RNA SNORD22	-9.79836	-1.59489	7.45E-07	0.000189
Mir15a	13	microRNA 15a	-20.1032	-1.83316	0.000141	0.009487
Mtus2	13	microtubule associated tumor suppressor candidate 2	-18.2659	-1.22508	0.000169	0.010812
Myh6	14	myosin, heavy chain 6, cardiac muscle, alpha	-19.7578	-5.49998	1.46E-16	1.96E-12
Myh7	14	myosin, heavy chain 7, cardiac muscle, beta	-16.0569	-2.95322	1.59E-09	1.18E-06
Nkx2-1	14	NK2 homeobox 1	-20.4824	-3.07691	2.60E-08	1.12E-05
Snord8	14	small nucleolar RNA, C/D box 8	-14.0862	-1.08644	9.65E-06	0.001198

Table 4.2, continued

Mir654	14	microRNA 654	-20.2893	-1.89894	0.000166	0.010681
Fos	14	FBJ murine osteosarcoma viral oncogene homolog	-15.6817	1.021225	0.00056	0.028003
Mir770	14	microRNA 770	-17.0986	-0.85874	0.000591	0.028923
Mir1193	14	microRNA 1193	-18.6441	-1.08073	0.000708	0.032744
Zfhx2	14	zinc finger homeobox 2	-16.944	-0.87184	0.000992	0.042032
Adcy4	14	adenylate cyclase 4	-17.3132	-0.83797	0.001045	0.04366
Glrx5	14	glutaredoxin 5	-13.6719	0.665232	0.001106	0.045061
Cdh24	14	cadherin 24, type 2	-15.4914	-0.64444	0.001411	0.053302
Mir369	14	microRNA 369	-19.2576	-1.21017	0.00143	0.053815
Mir134	14	microRNA 134	-19.1782	-1.19733	0.00155	0.057092
Actc1	15	actin, alpha, cardiac muscle	-16.6388	-4.14917	8.04E-12	2.79E-08
Aldh1a3	15	aldehyde dehydrogenase 1 family, member A3	-19.7399	-2.15043	1.92E-06	0.000384
Snora24	15	Small nucleolar RNA SNORA24	-14.5695	-1.59453	2.45E-06	0.000451
Cyp11a1	15	cytochrome P450, family 11, subfamily A, polypeptide 1	-19.3938	-1.95518	9.98E-06	0.001228

Table 4.2, continued

Mtap1a	15	microtubule-associated protein 1A	-17.3688	-1.09265	4.64E-05	0.004317
Cspg4	15	chondroitin sulfate proteoglycan 4	-18.9071	-1.40771	5.59E-05	0.00486
Alpk3	15	alpha-kinase 3	-18.6611	-1.20991	0.000723	0.03306
Gatm	15	glycine amidinotransferase (L-arginine:glycine amidinotransferase)	-17.3979	-0.8511	0.001356	0.052672
Snora30	16	small nucleolar RNA, H/ACA box 30	-15.027	-1.55106	1.23E-06	0.000277
Prss22	16	protease, serine, 22	-19.5145	-1.56822	9.84E-05	0.007247
Maf	16	v-maf musculoaponeurotic fibrosarcoma oncogene homolog (avian)	-19.4696	-1.52805	0.000101	0.007352
Crispld2	16	cysteine-rich secretory protein LCCL domain containing 2	-18.6821	-1.23494	0.000116	0.008081
Slc6a2	16	solute carrier family 6 (neurotransmitter transporter, noradrenalin), member 2	-19.4005	-1.45123	0.000223	0.013589
Snord68	16	small nucleolar RNA, C/D box 68	-12.5653	-0.84071	0.000486	0.02506
Cldn9	16	claudin 9	-19.9406	-1.5883	0.000493	0.02533
Emp2	16	epithelial membrane protein 2	-18.416	-1.06638	0.000574	0.028296
Snora21	17	Small nucleolar RNA SNORA21	-12.4768	-1.99596	3.46E-09	2.32E-06
Col1a1	17	collagen, type I, alpha 1	-15.7799	-1.61354	1.30E-08	6.23E-06

Table 4.2, continued

Unc45b	17	unc-45 homolog B (C. elegans)	-18.553	-2.76615	9.93E-08	3.33E-05
Meox1	17	mesenchyme homeobox 1	-19.0625	-1.89839	5.53E-07	0.000151
Myocd	17	myocardin	-18.5487	-2.19579	1.10E-06	0.000259
Snord104	17	small nucleolar RNA, C/D box 104	-10.2146	-1.10626	4.23E-06	0.0007
Myl4	17	myosin, light chain 4, alkali; atrial, embryonic	-18.7853	-2.53523	6.12E-06	0.000912
Ace	17	angiotensin I converting enzyme (peptidyl-dipeptidase A) 1	-19.2534	-1.63179	1.08E-05	0.001304
Krt20	17	keratin 20	-20.3096	-2.11016	1.98E-05	0.002182
Hoxb3	17	homeobox B3	-19.8492	-1.76852	5.34E-05	0.004773
Sdk2	17	sidekick cell adhesion molecule 2	-16.8093	-0.96234	5.57E-05	0.00486
Dhrs11	17	dehydrogenase/reductase (SDR family) member 11	-16.2865	0.912026	8.48E-05	0.006685
Hoxb2	17	homeobox B2	-18.9097	-1.42459	0.000173	0.010975
Lrrc48	17	leucine rich repeat containing 48	-19.7083	-1.57399	0.000182	0.011375
Srcin1	17	SRC kinase signaling inhibitor 1	-18.2753	-1.09537	0.000246	0.014658
Zbtb4	17	zinc finger and BTB domain containing 4	-17.716	-1.03904	0.000272	0.015788
Slc4a1	17	solute carrier family 4, anion exchanger,	-11.6811	0.698117	0.000485	0.02506

Table 4.2, continued

		member 1 (erythrocyte membrane protein band 3, Diego blood group)				
Pnpo	17	pyridoxamine 5'-phosphate oxidase	-13.8165	0.697429	0.000658	0.030993
Snord7	17	small nucleolar RNA, C/D box 7	-14.3611	-1.06298	0.000691	0.032155
Snord49a	17	small nucleolar RNA, C/D box 49A	-11.8254	-0.91994	0.000843	0.037314
Smtnl2	17	smoothelin-like 2	-17.6135	-0.8729	0.000994	0.042032
Vamp2	17	Vesicle-associated membrane protein 2	-16.4967	-0.75869	0.001111	0.045139
Kdm6b	17	lysine (K)-specific demethylase 6B	-14.488	-0.75868	0.001148	0.046356
Shpk	17	sedoheptulokinase	-20.5893	1.80572	0.001179	0.047338
Myom1	18	myomesin 1, 185k	-17.8351	-1.87926	9.89E-08	3.33E-05
Snord58b	18	small nucleolar RNA, C/D box 58B	-15.7358	-1.20173	3.21E-06	0.000566
Klhl14	18	kelch-like 14 (Drosophila)	-19.4027	-1.80878	1.63E-05	0.001856
Gata6	18	GATA binding protein 6	-17.7275	-1.26719	4.48E-05	0.004227
Ccbe1	18	collagen and calcium binding EGF domains 1	-16.9422	-0.99822	0.000174	0.011018
Fosb	19	FBJ murine osteosarcoma viral oncogene homolog B	-15.1277	1.536375	1.02E-08	5.04E-06

Table 4.2, continued

Cnn1	19	calponin 1, basic, smooth muscle	-19.5138	-3.20421	2.67E-08	1.12E-05
Blvrb	19	biliverdin reductase B (flavin reductase (NADPH))	-16.3525	1.086488	3.61E-06	0.000613
Lgi4	19	leucine-rich repeat LGI family, member 4	-19.3967	-1.81308	4.89E-06	0.000793
Acp5	19	acid phosphatase 5, tartrate resistant	-15.2369	0.965548	7.68E-06	0.001084
Epor	19	erythropoietin receptor	-16.2868	0.942723	5.24E-05	0.004713
Klf1	19	Kruppel-like factor 1 (erythroid)	-16.8095	1.088061	5.72E-05	0.00492
Rps19	19	ribosomal protein S19	-13.1258	0.793089	9.11E-05	0.00694
Snord111	19	Small Nucleolar RNA SNORD111	-15.2534	-0.93757	9.62E-05	0.007166
Matk	19	megakaryocyte-associated tyrosine kinase	-20.713	-2.22046	0.000104	0.007401
Kcnn4	19	potassium intermediate/small conductance calcium-activated channel, subfamily N, member 4	-17.362	1.011583	0.000123	0.008576
Gdf1	19	growth differentiation factor 1	-17.7558	-0.99711	0.000144	0.009565
Lass1	19	ceramide synthase 1	-17.7558	-0.99711	0.000144	0.009565
Icam4	19	intercellular adhesion molecule 4 (Landsteiner-Wiener blood group)	-19.7537	1.630118	0.000244	0.014658
Snord35a	19	small nucleolar RNA, C/D box 35A	-10.6831	-0.924	0.000245	0.014658

Table 4.2, continued

Prr12	19	proline rich 12	-14.6841	-0.85625	0.000261	0.01543
Snord34	19	small nucleolar RNA, C/D box 34	-10.9436	-0.71732	0.000775	0.035204
Rps28	19	ribosomal protein S28	-15.271	0.775647	0.001197	0.047899
Zglp1	19	zinc finger, GATA-like protein 1	-19.7026	1.323064	0.001275	0.050454
Rps11	19	ribosomal protein S11	-11.1502	0.642368	0.001276	0.050454
Mrpl34	19	mitochondrial ribosomal protein L34	-15.4658	0.691345	0.00139	0.052806
Snord12	20	small nucleolar RNA, C/D box 12	-14.4493	-1.31812	1.27E-06	0.00028
Trib3	20	tribbles homolog 3 (Drosophila)	-18.0105	1.463354	1.79E-06	0.000364
Snord17	20	Small nucleolar RNA, c/d box 17	-12.9254	-1.01915	6.20E-05	0.005199
Prokr2	20	prokineticin receptor 2	-20.7105	-2.22245	6.85E-05	0.00563
Snord110	20	small nucleolar RNA, C/D box 110	-13.0942	-0.96188	0.000155	0.010178
Ahcy	20	adenosylhomocysteinase	-14.2912	-0.92902	0.000566	0.028209
Myl9	20	myosin, light chain 9, regulatory	-15.7858	-0.91342	0.000663	0.03109
Snhg11	20	small nucleolar RNA host gene 11	-16.849	-0.76732	0.001536	0.056742
Sh3bgr	21	SH3 domain binding glutamic acid-rich protein	-20.2103	-4.0535	4.78E-10	4.58E-07
Snora81	21	Small nucleolar RNA SNORA81	-14.2374	-1.44847	2.79E-05	0.002834

Table 4.2, continued

Mrap	21	melanocortin 2 receptor accessory protein	-18.2549	1.263949	4.80E-05	0.004436
Ubash3a	21	ubiquitin associated and SH3 domain containing A	-19.098	1.487342	0.000131	0.008989
Col6a2	21	collagen, type VI, alpha 2	-18.5626	-1.16626	0.000254	0.015089
Cldn8	21	claudin 8	-17.1882	-0.95183	0.000282	0.016074
Erg	21	v-ets erythroblastosis virus E26 oncogene homolog (avian)	-16.626	-0.80155	0.001238	0.049402
Tiam1	21	T-cell lymphoma invasion and metastasis 1	-13.9473	-0.69161	0.001528	0.05657
Myo18b	22	myosin XVIIIB	-20.3054	-2.39451	7.47E-06	0.001065
Sox10	22	SRY (sex determining region Y)-box 10	-19.4735	-1.77688	8.08E-06	0.001084
Grap2	22	GRB2-related adaptor protein 2	-18.5699	1.342658	3.40E-05	0.003307
Snora15	22	Small nucleolar RNA SNORA15	-15.114	-0.84291	0.0013	0.051124
Snora31	1,2,5,7,11,17, X	Small nucleolar RNA SNORA31	-14.1166	-1.09201	5.06E-05	0.004582
Snora68	5,13,17,19,X	Small nucleolar RNA SNORA68	-11.463	-1.11328	5.62E-05	0.00486
Scarna6	6,15	Small Cajal body specific RNA 6	-15.1266	-1.76637	1.21E-09	9.51E-07
Slc38a5	X	solute carrier family 38, member 5	-17.6398	1.361652	8.63E-07	0.000206

Table 4.2, continued

Gata1	X	GATA binding protein 1 (globin transcription factor 1)	-15.8758	1.071303	1.54E-06	0.000323
Alas2	X	aminolevulinate, delta-, synthase 2	-13.0776	0.966691	8.37E-06	0.001084
5730405O15Rik	X	RIKEN cDNA 5730405O15 gene	-20.7408	-2.54656	1.95E-05	0.002182
Dcx	X	doublecortin	-18.5436	-1.20738	0.000226	0.01372
Nrk	X	Nik related kinase	-15.9088	-0.80339	0.000572	0.028278
L1cam	X	L1 cell adhesion molecule	-19.0181	-1.27982	0.000713	0.032745
Prl7a1		prolactin family 7, subfamily a, member 1	-19.3097	-3.63051	2.62E-11	7.04E-08
Scarna3b		small Cajal body-specific RNA 3B	-16.899	-2.93309	2.24E-10	3.10E-07
Psg29		pregnancy-specific glycoprotein 29	-20.2687	-3.50461	2.40E-10	3.10E-07
2610203C20Rik		RIKEN cDNA 2610203C20 gene	-16.8671	-1.63036	2.55E-10	3.10E-07
Mir1843		small Cajal body-specific RNA 3B	-16.9266	-2.94422	4.36E-10	4.50E-07
Mir5117		growth arrest specific 5	-12.4139	-1.88468	6.57E-10	5.87E-07
Hbb-bh1		hemoglobin Z, beta-like embryonic chain	-8.50035	1.222477	1.12E-09	9.41E-07
C430049B03Rik		RIKEN cDNA C430049B03 gene	-15.8243	-1.48415	2.47E-09	1.74E-06
Mir1843b		small Cajal body-specific RNA 3A	-15.5633	-2.14558	6.34E-09	3.54E-06

Table 4.2, continued

Snord16a	Small nucleolar RNA SNORD16	-12.3603	-2.01119	7.51E-09	3.95E-06
Scarna3a	small Cajal body-specific RNA 3A	-15.5348	-2.13221	7.66E-09	3.95E-06
Prl2c3	prolactin family 2, subfamily c, member 3	-19.154	-2.72545	6.08E-08	2.27E-05
Prl2c4	prolactin family 2, subfamily c, member 3	-19.154	-2.72545	6.08E-08	2.27E-05
Epb4.2	erythrocyte protein band 4.2	-15.2304	1.161039	7.73E-08	2.80E-05
Rps19-ps3	ribosomal protein S19, pseudogene 3	-17.4107	1.327991	7.89E-07	0.000192
4732471J01Rik	RIKEN cDNA 4732471J01 gene	-19.6669	-1.98292	2.15E-06	0.000412
1190007F08Rik	RIKEN cDNA 1190007F08 gene	-15.8117	1.099543	3.39E-06	0.000583
Mir3066	microRNA 3066	-20.3478	-2.31155	5.43E-06	0.000827
3632451O06Rik	RIKEN cDNA 3632451O06 gene	-14.8471	-1.51158	8.07E-06	0.001084
Mir666	microRNA 666	-19.1832	-1.65825	8.40E-06	0.001084
2900060B14Rik	RIKEN cDNA 2900060B14 gene	-15.1019	-1.27834	8.46E-06	0.001084
Mir3096b	misc RNA RefSeq import	-16.1132	-1.41513	8.49E-06	0.001084
Gm98	predicted gene 98	-15.5691	-0.96993	2.48E-05	0.002595
Hist1h4n	histone cluster 1, H4n	-14.3459	1.084602	2.76E-05	0.002829
5730408K05Rik	Small nucleolar RNA SNORA57	-12.166	0.940994	3.72E-05	0.003565

Table 4.2, continued

Snhg8	small nucleolar RNA, H/ACA box 24	-14.1852	-1.23896	4.43E-05	0.004209
Iigp1	interferon inducible GTPase 1	-20.695	-2.25334	4.51E-05	0.004228
Mir3068	Small nucleolar RNA SNORA58	-16.9569	-1.54999	4.84E-05	0.004441
Gm9855	predicted pseudogene 9855	-15.6426	0.877228	5.58E-05	0.00486
Hba-x	hemoglobin X, alpha-like embryonic chain in Hba complex	-8.92932	0.784263	8.17E-05	0.006559
Prl3d1	prolactin family 3, subfamily d, member 1	-19.3368	-1.80992	8.43E-05	0.006684
Hbb-y	hemoglobin Y, beta-like embryonic chain	-7.70578	0.721147	8.85E-05	0.00679
Tex16	testis expressed gene 16	-20.2618	-1.94091	9.40E-05	0.00708
Mir667 ,	microRNA 667	-20.7321	-2.19009	0.000104	0.007401
Car7	carbonic anhydrase 7	-20.2674	-1.95244	0.000126	0.008704
Mir1931	microRNA 1931	-18.6918	-1.23285	0.000281	0.016074
2610507I01Rik	RIKEN cDNA 2610507I01 gene	-17.7527	-1.03234	0.000289	0.016365
Mir3091	microRNA 3091	-17.3273	0.927263	0.000299	0.016803
Hbq1b	hemoglobin, theta 1B	-19.1536	1.375773	0.000316	0.017375
2010300C02Rik	RIKEN cDNA 2010300C02 gene	-19.2387	-1.355	0.000368	0.01996
1700012D14Rik	RNA RefSeq import	-19.9594	-1.56384	0.000372	0.020116

Table 4.2, continued

Mtrnr2l	Mtrnr2-like	-14.6859	0.786393	0.00042	0.022153
1300017J02Rik	RIKEN cDNA 1300017J02 gene	-17.1708	0.880019	0.000554	0.027829
2410015M20Rik	RIKEN cDNA 2410015M20 gene	-15.8287	0.754478	0.000617	0.02984
Zfp78	zinc finger protein 78	-19.4938	-1.3719	0.000619	0.02984
Gm5177	pseudogene RefSeq import	-17.5387	-0.96141	0.000633	0.030299
AI450353	misc RNA RefSeq import	-14.0505	-0.94812	0.000703	0.032631
Cdk3-ps	cyclin-dependent kinase 3, pseudogene	-20.3686	-1.74357	0.000805	0.036095
Mir686	microRNA 686	-15.8143	0.857422	0.00083	0.03697
5730508B09Rik	RIKEN cDNA 5730508B09 gene	-18.2607	1.018964	0.000949	0.041159
H2-D1	histocompatibility 2, D region locus 1	-18.6465	-1.121	0.000968	0.041592
Mirlet7a-1	microRNA let7a-1	-17.5976	-0.88458	0.001061	0.044025
C78339	expressed sequence C78339	-15.3114	-0.76824	0.00137	0.052806
2210403K04Rik	RIKEN cDNA 2210403K04 gene	-19.4081	-1.2185	0.001382	0.052806
Gm6251	ribosomal protein L32	-16.5523	0.798314	0.001383	0.052806
AF357355	snoRNA AF357355	-13.2361	-0.81269	0.00139	0.052806

Genes with no listed human chromosome were genes only found in mosue.

Table 4.3: Number of Unique Mmu 16 Transcript Variants of Genes with Homologues on Hsa21 found Using Ensembl and NCBI/GenBank Databases

Gene	Ensembl	NCBI/GenBank
Dyrk1a	6	2
Rcan1	2	2
Tiam1	15	3
Erg	9	1
Sh3bgr	8	1
Cldn8	1	1
Mrap	4	1

Table 4.4: List of Mmu Genes Containing Alternative Splicing Events between Trisomic and Euploid E9.5 PA1 and E9.25 NT Tissue

Comparison 1		Comparison 2		Comparison 3		Comparison 4	
Euploid PA1 (E9.5) and Trisomic PA1 (E9.5)		**Euploid NT (E9.25) and Trisomic NT (E9.25)**		**Euploid PA1 (E9.5) and Euploid NT (E9.25)**		**Trisomic PA1 (E9.5) and Trisomic NT (E9.25)**	
Sumo1	Rbms3	Rpl13a		Zcchc17	Snf8	Atp5l	Ccnl1
Ccnl1	Gpbp1	Snord32a		Uap1	Uqcrh	Cttn	Pex2
Rpl11	Tlk1	Brd8		Eif4a2	Tomm70a	Srsf7	Acot8
Nop56	Cab39l	Klhl26		Brd8	Ttc3	Rpl11	Cd59a
Ccnl1	Btrc	Abl2		Uap1	Ankrd10	Pes1	
Ctbp2	Ttbk2	Pex2		Mtch2	Tk2	Zmym3	
Tpp2	Ccbl1	Timm9		Nop56	Apobec3	Fgfr1op2	
Zmym3	Dtx2	Cdc14b		Tpp2	Sipa1	Ccnl1	
Fam76a	Rab3il1	Top3b		Bin1	Nadk2	Arl16	
Tecr	C330007P0	Chpf		Fgfr1op2	Trub2	Fgfr2	
Nbr1	Tomm22	Tmem198		Fam76a	Foxk2	2810474O19Rik	
Sun1	Pcmt1	Esd		Hnrnpr	Srr	Xpnpep3	
Tomm70a	Ctage5	Dph3		Tmem164	Repin1	Dph3	
Foxk2	Ttc3	Oxnad1		Cab39l	Car2	Oxnad1	
Parp11	Eif4enif1	Rhot1		Acly	Pnpo	Tsr3	
Arl16	Mdm4	Dhfr		Dph3	Timm9	Slc29a1	
Klhl18	4632434I1	Msh3		Oxnad1	Mtss1	Git2	
Tex30	Fam220a	C2cd5		Zfand3	Gprasp1	Mboat7	
Srp19	Dlg1	Tm2d3		Slc22a17	Armcx5	Klhl26	
Ankrd10	Tcof1	Xpnpep3		Hnrnpr	Rdh13	Wnk1	
Tmem57	Golm1	Cnot4		Meg3	Timm9	Dpm1	
Blcap	Zfand3	Eif4g3		Mir1906-2	Ttc13	Zfp454	
Nnat	Csnk1g1	Repin1		Mir1906-1	Pxdn	Tmem222	
Rbck1		Kif1c		Ndufs1	Map2	Asap2	
Ppp4r1l-p				Hnrnpa2b	Kif1c	Rbck1	
Ddit3				Suv39h2	Sec24b	Nbr1	
Lrp8				Pnpo	Tlk1	Slc29a1	
Cdc14b				Top3b	Stk19	Ccbl1	

FIGURES

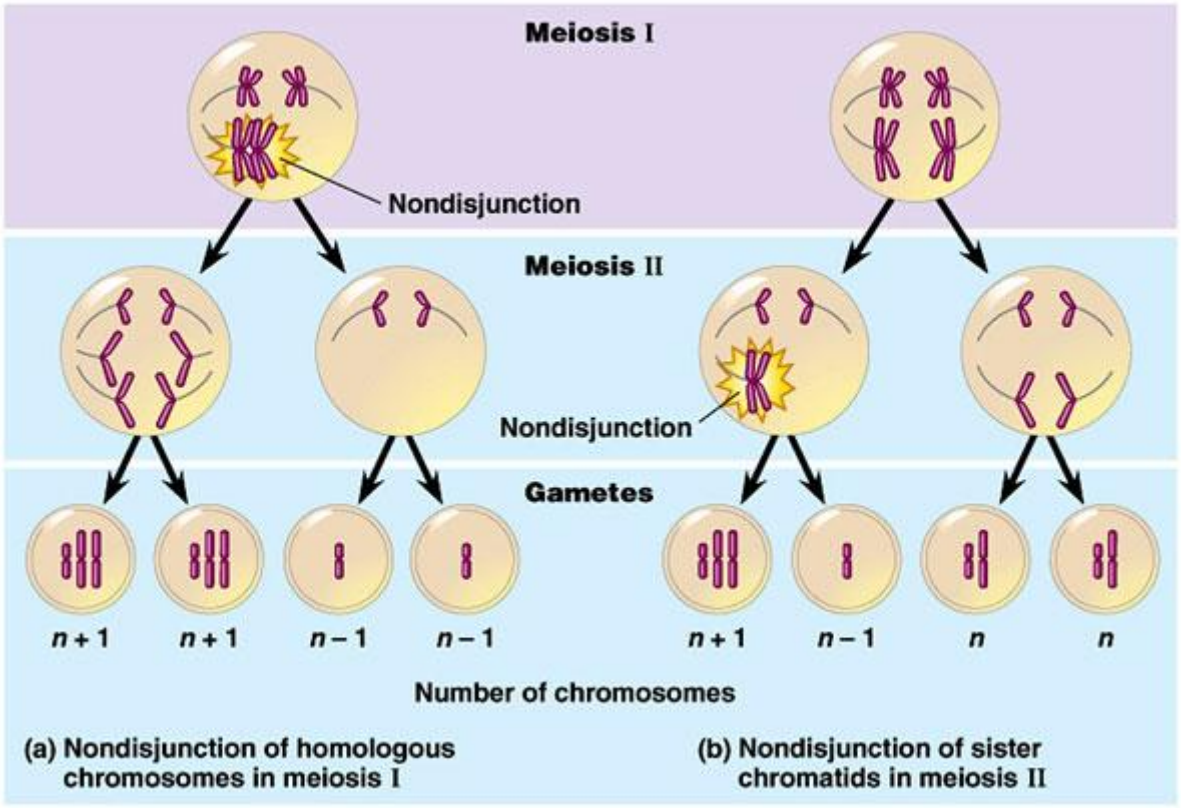

Figure 1.1: Nondisjunction in Meiosis I and Meiosis II causes Trisomy 21. Trisomy 21 in humans is caused by nondisjunction of chromosome 21 during Meiosis I or II. (a) In Meiosis I when homologous chromsomes fail to separate, one daughter cell will contain an extra chromosome 21, while the other will lack a chromosome. After division of sister chromatids in Meiosis II, the resulting gametes from the first daughter cell will contain the extra chromosome (n+1), while the set of gametes from the second daughter cell will lack the chromosome (n-1). (b) When Meiosis I proceeds normally, but sister chromatids fail to separate during Meiosis II, the gametes from the cell with the extra chromatid will divide unevenly into a gamete containing an extra chromosome 21 (n+1) and a gamete lacking a chromosome 21 (n-1). When any (n+1) gametes are united with a normal gamete from another parent, the resulting zygote will contain the normal chromosome compliment for each chromosome except for an extra copy of chromosome 21 (2n+1). This occurrence is referred to as Trisomy 21, referring to the three copies of chromosome 21 relative to the normal two copies of all other autosomal chromosomes. 88% of cases of DS arise from nondisjunction of Hsa21 in the oocyte, rather than the sperm (http://www.bio.miami.edu/~cmallery/150/mendel/c15x11nondisjunction.jpg).

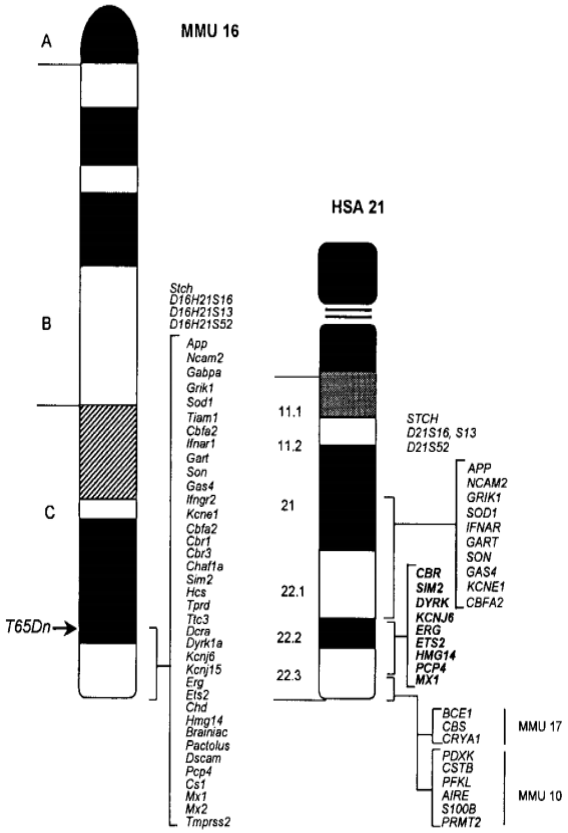

Figure 1.2: Gene Homology between Mmu16 and Hsa21. Diagram detailing gene homology between the extra chromosome 16 in mouse (Mmu16) displayed in segmental trisomy in Ts65Dn mice and Hsa21. The extra Mmu16 chromosome in Ts65Dn mice contains ~50% of the genes on Hsa21.

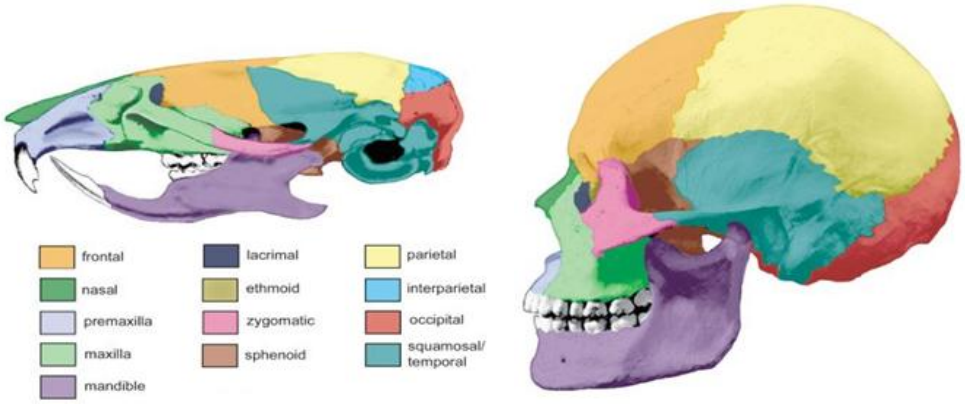

Figure 1.3: Regional Cranial Homology of the Ts65Dn and Human Skull. Ts65Dn mice contain ~50% of the gene homologues found on Hsa21 and mirror many of the craniofacial and other phenotypes displayed in DS including the reduced size of the maxilla (pink) and mandible (purple), a flattened occiput (red), flattened nasal bridge (green), and reduced bizygomatic breadth (pink) (RICHTSMEIER *et al.* 2000; RICHTSMEIER *et al.* 2002; SHOTT 2006; STARBUCK *et al.* 2013).

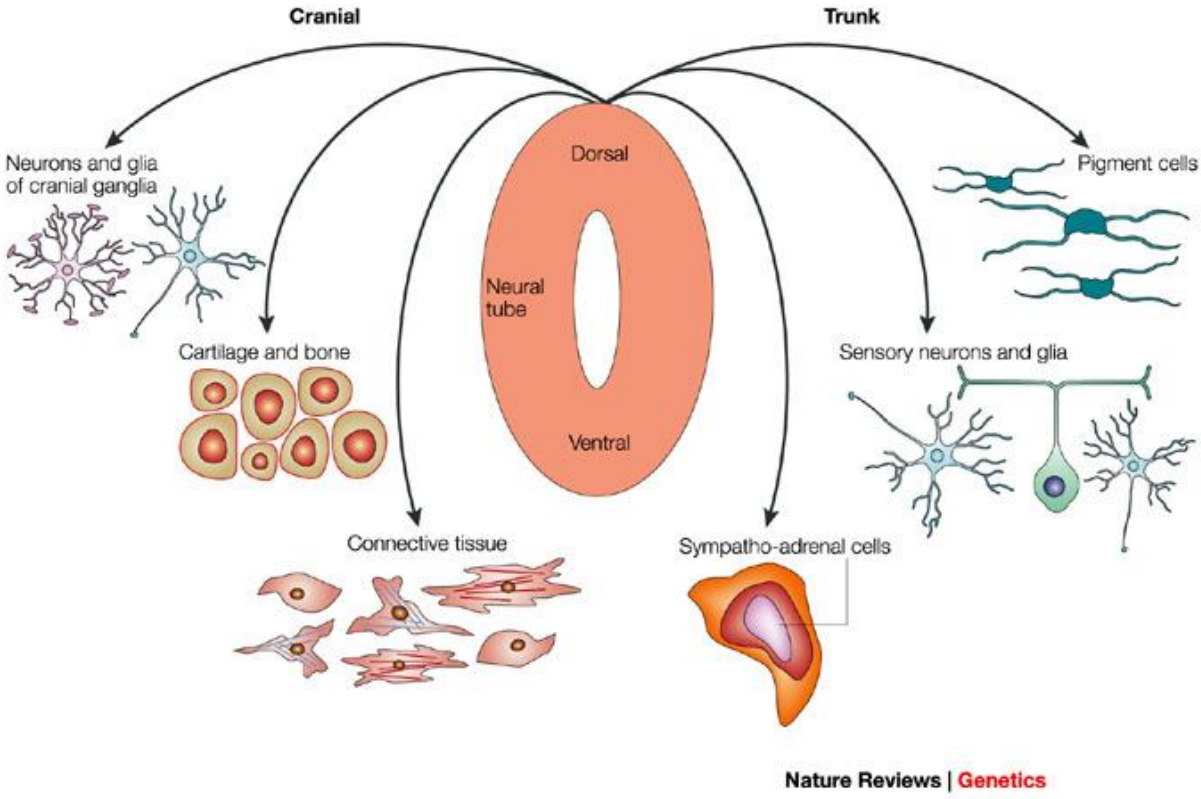

Figure 1.4: Differentiation Potential of Neural Crest Cells in the Neural Tube. Neural crest cells originating from the dorsal side of the neural tube may become either cranial neural crest cells or trunk neural crest cells. Cranial neural crest cells differentiate into the neurons and glia of the cranial ganglia, cartilage, bone, and connective tissue of the head, face, and neck. Trunk neural crest cells differentiate into a variety of cell types including, sympahto-adrenal cells, sensory neurons and glia, and pigment cells. Cranial neural crest and the building of the vertebrate head (KNECHT and BRONNER-FRASER 2002).

Figure 1.5: Whole mount Ts65Dn, Wnt1lacZ/+ Euploid E9.5 Embryo with Labeled Neural Crest Cells. Picture of a whole E9.5 euploid embryo with neural crest cell-derived structures labeled in blue with β-galactosidase. The developing first pharyngeal arch (PA1), visible just below the head (circled in red), will contribute to the bones and connective tissue, and musculature of the jaw and lower face (ROPER *et al.* 2009).

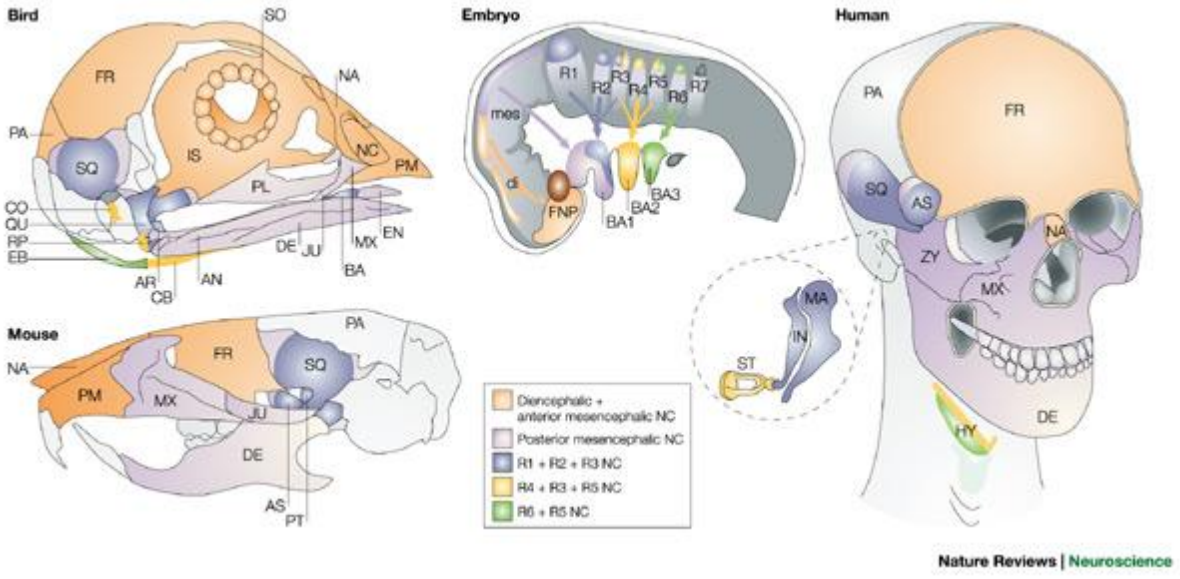

Figure 1.6: Developmental Homology of the Bird, Mouse, and Human Skull. The skull of bird, mouse, and humans show similar homologous structures which originate from near identical early embryonic patterns of development in the head in addition to migration of neural crest cells to populate the BA1, BA2, and BA3 (also known as PA1, PA2, and PA3 respectively) from their respective rhombomeres (SANTAGATI and RIJLI 2003).

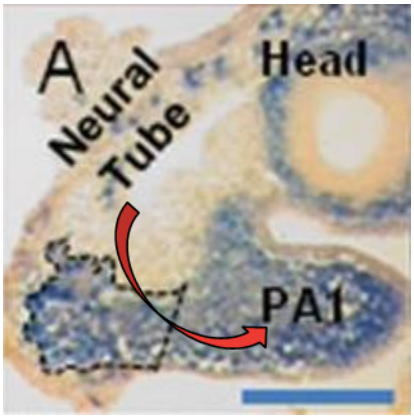

Figure 1.7: Migration Path of Neural Crest in the Formation of the First Pharyngeal Arch . Section of E9.5 Ts65Dn embryo showing the migration path (red arrow) of neural crest cells (NCC) delaminating from the neural tube to migrate to the developing first pharyngeal arch (PA1) in pre-mandible formation. Ts65Dn embryos show deficits in the migration of NCC to the PA1, and failure of NCC to proliferate once in the PA1. This leads to a smaller, hypocellular PA1 deficient in NCC which persists throughout development, and contributes to the undersized mandible in Ts65Dn mice (ROPER *et al.* 2009).

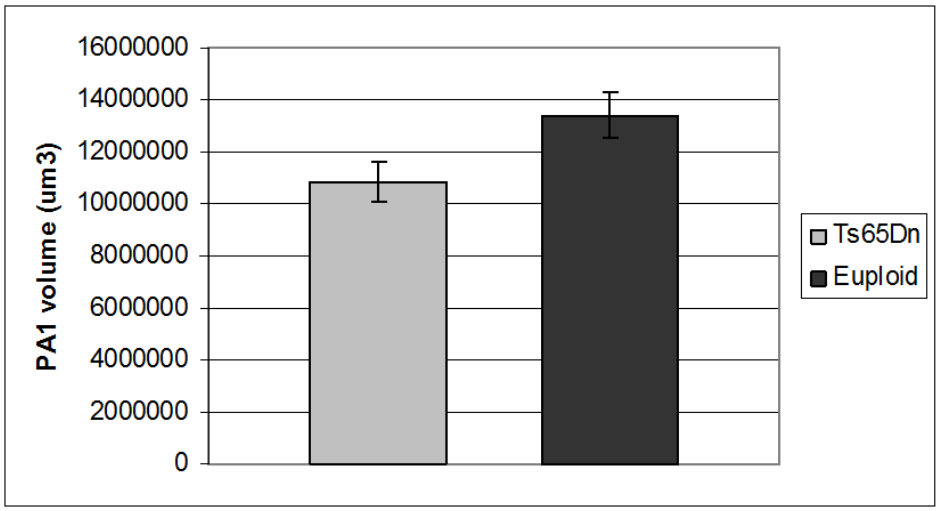

Figure 1.8: PA1 Volume of Ts65Dn and Euploid E9.5 Embryos. Trisomic Ts65Dn embryos have a smaller PA1 volume than euploid littermates at E9.5 (ROPER *et al.* 2009).

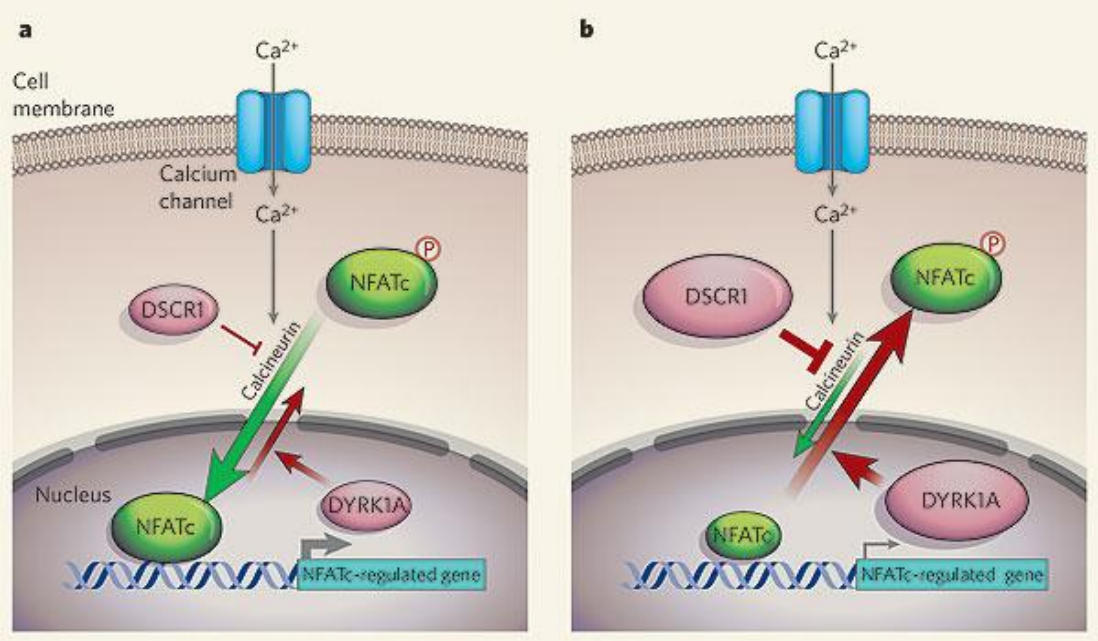

Figure 1.9: Overexpression of Dyrk1A Alters the Mechanism of the NFATc Pathway. (a) Shows the equilibrium of cytosolic and nuclear NFATc under normal expression of Dyrk1a. NFATc is a transcription factor that regulates many genes involved in development and the cell cycle. When phosphorylated, it is localized in the cytosol, and when not phosphorylated is localized in the nucleus where it is able to transcribe downstream genes. Under normal conditions, there is an equilibrium between nuclear and cytosolic NFATc. This equilibrium is maintained by Dyrk1a, Dscr1 (also named Rcan1), and Calceneurin. Dyrk1a phosphorylates NFATc, causing its removal from the nucleus to the cytosol. Calceneurin dephosphorylates NFATc, relocalizing it to the nucleus where it is able to transcribe downstream genes. Dscr1 is an inhibitor of Calceneurin that indirectly prevents dephosphorylation of NFATc, keeping it localized in the cytosol. (b) Shows how overexpression of Dyrk1a causes removal of NFATc from the nucleus, lowering expression of NFATc-regulated genes. In Trisomy 21, Dyrk1a and Dscr1 are overexpressed, disrupting the equilibrium between nuclear and cytosolic NFATc. Overexpression of Dyrk1a causes excess phosphorylation of NFATc , causing higher levels of NFATc to be removed from the nucleus. Excess Dscr1 prevents the cytosolic NFATc from being dephosphorylated, keeping it localized in the cytosol. With higher levels of cytosolic NFATc and lowered levels of nuclear NFATc, transcription is hindered, lowering expression of downstream target genes. It is hypothesized that this downregulation of NFATc target genes may be a mechanism whereby overexpression of Dyrk1a causes dysregulation of specific genes leading to an altered phenotype in DS (ARRON *et al.* 2006).

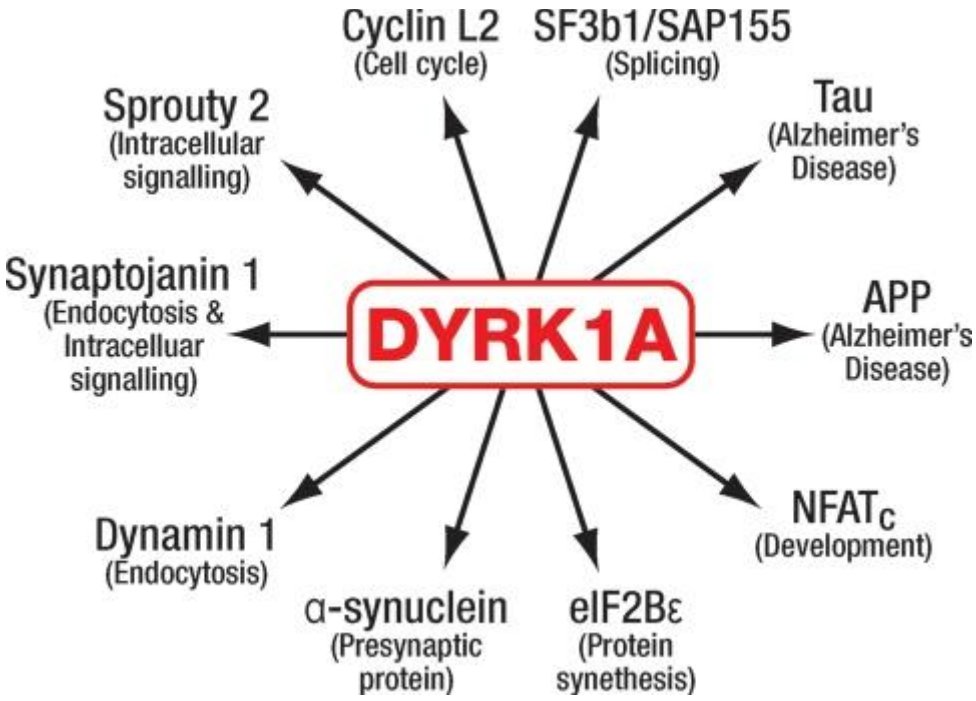

Figure 1.10: Downstream Targets of the DYRK1A Protein. Through particular downstream targets, including those listed above, DYRK1A plays an role important role in regulating development, the cell cycle, signaling, and protein synthesis. Changes in the expression of DYRK1A could potentially alter these functions and lead to altered phenotypes (WISEMAN *et al.* 2009).

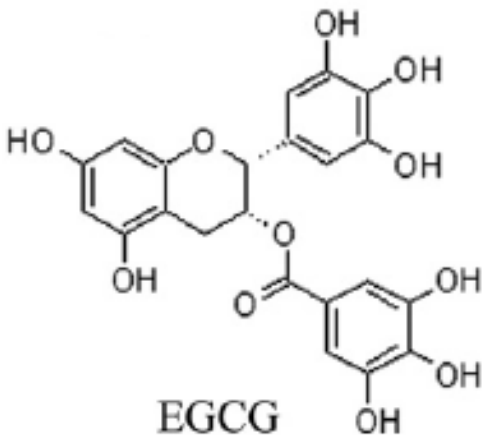

Figure 1.11: Molecular Structure of Epigallo-catechin-(3')-gallate (EGCG). EGCG is a green tea polyphenol and a known small molecule inhibitor of the DYRK1A protein (WANG *et al.* 2012). EGCG has been tested as a clinically translatable way to normalize DYRK1A overexpression and correct phenotypes associated with DS (BAIN *et al.* 2003).

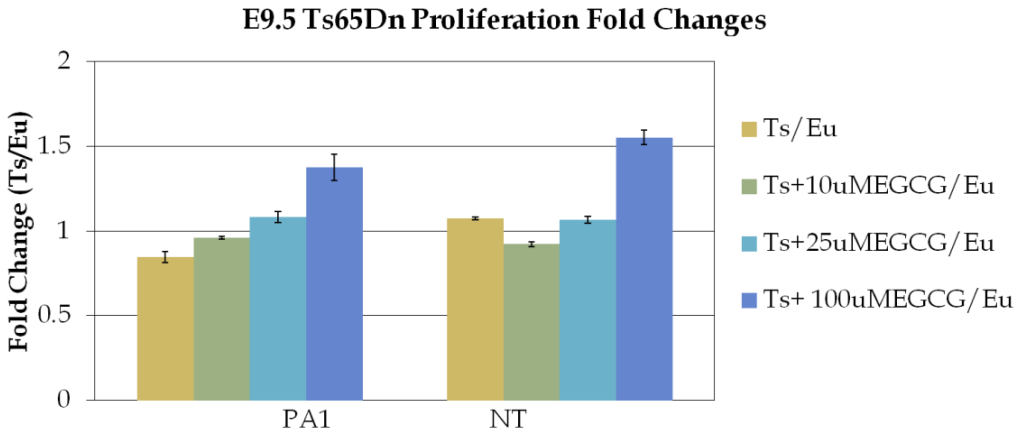

Figure 3.1: *In vitro* Proliferation Assay of E9.5 PA1 and NT cells Show a Dose-Dependent Response to EGCG. In a proliferation assay, PA1 and NT cells extracted from E9.5 euploid and Ts65Dn embryos were plated and grown in cell culture. Cells were treated with 10µM, 25µM, or 100µM of EGCG or given no treatment. Both PA1 and NT cells showed increases in proliferation which increase with EGCG concentration. These results suggest that EGCG is able to promote proliferation *in vitro*, providing evidence for the ability of EGCG to promote proliferation for *in vitro* studies (Deitz, *Unpublished data*).

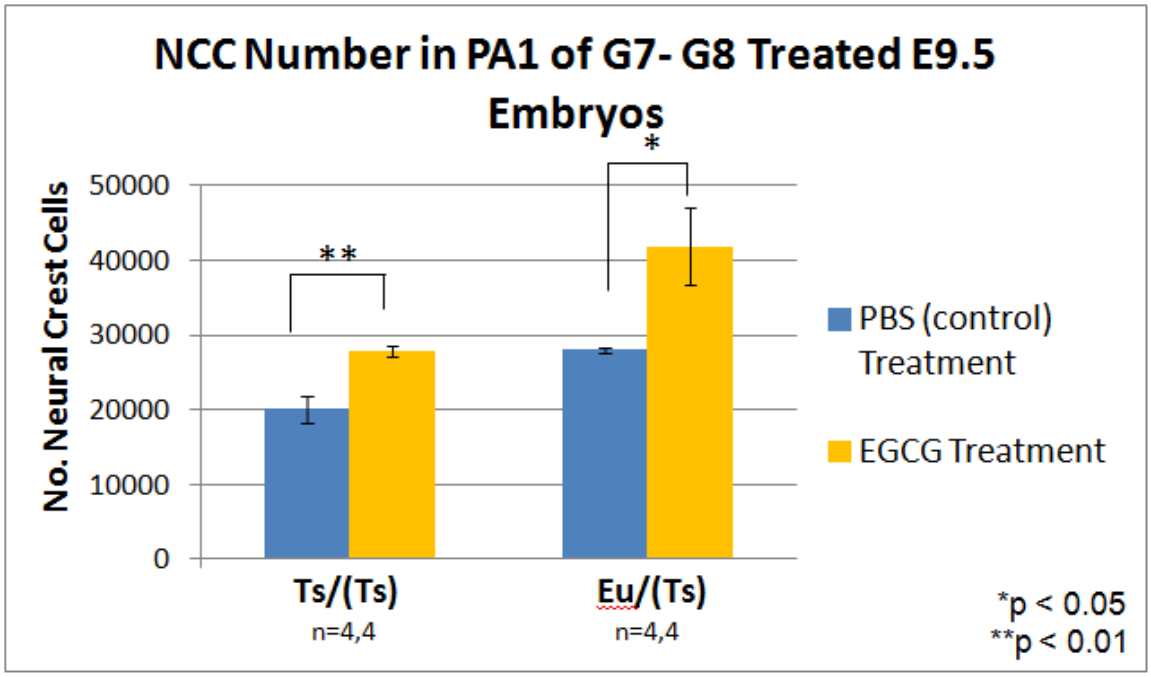

Figure 3.2: Number of Neural Crest Cells in the E9.5 PA1 of G7-G8 Treated Embryos. The NCC number of E9.5 embryos (staged 21-24 somites; Wnt1-LacZ euploid fathers) whose mothers were treated with EGCG or PBS as control from G7-G8. Trisomic embryos treated with EGCG show a significant increase in the number of NCC compared to untreated trisomic embryos (**p=0.0029). Euploid embryos treated with EGCG also show increased number of NCC compared to untreated euploid embryos (*p=0.017) indicating observed EGCG-dependent increases in NCC may not be genotype specific. Ts/(Ts): trisomic embryo from trisomic mother, Eu/(Ts): euploid embryo from trisomic mother.

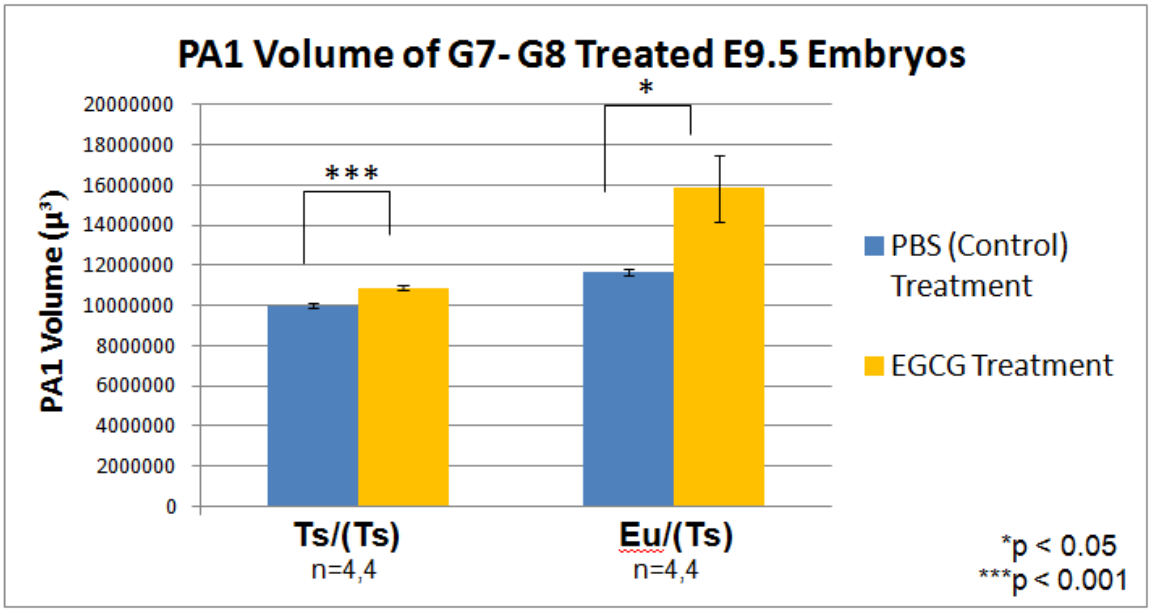

Figure 3.3: PA1 Volume of E9.5 PA1 of G7-G8 Treated Embryos. The PA1 volume of E9.5 embryos (staged 21-24 somites; Wnt1-LacZ euploid fathers) whose mothers were treated with EGCG or PBS as a control from G7-G8. Trisomic embryos treated with EGCG show a significant increase in PA1 volume compared to untreated embryos (***p=0.0009). There was also a significant difference between treated and untreated euploid embryos (*p=0.022) suggesting that the effects of EGCG may not be genotype specific. Ts/(Ts): trisomic embryo from trisomic mother, Eu/(Ts): euploid embryo from trisomic mother.

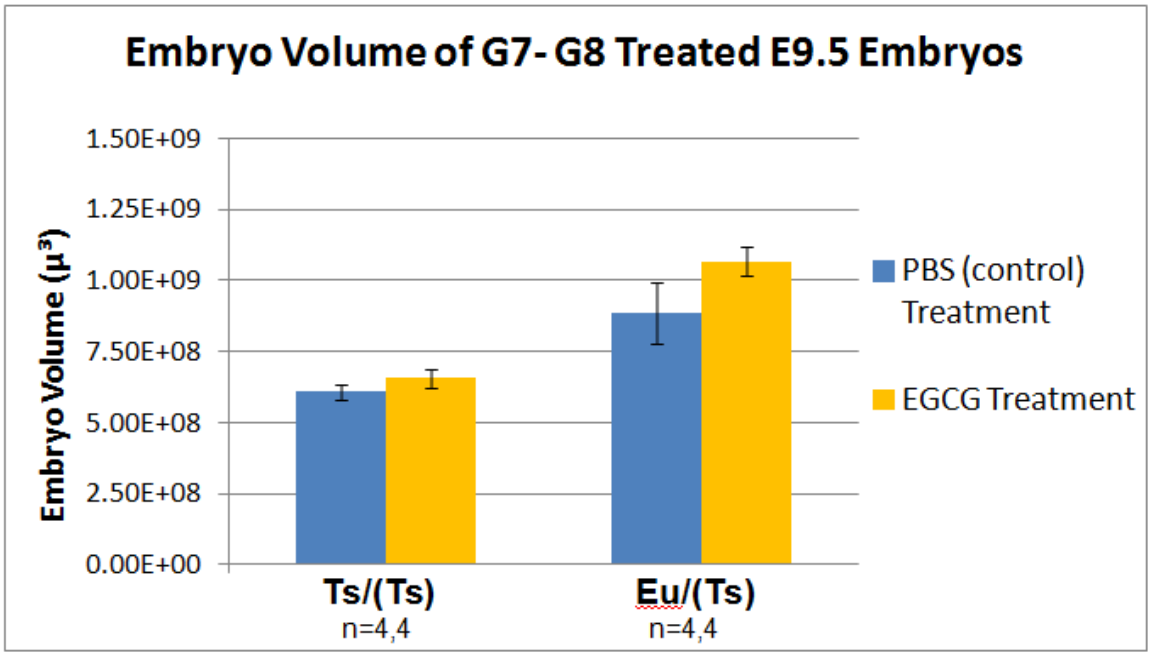

Figure 3.4: Embryo Volume of E9.5 PA1 of G7-G8 Treated Embryos. The total embryo volume of E9.5 embryos (staged 21-24 somites; Wnt1-LacZ euploid fathers) whose mothers were treated with EGCG of PBS as control from G7-G8. This EGCG treatment did not significantly increase the embryo volume of trisomic (p=0.14) or euploid embryos (p=0.092). Ts/(Ts): trisomic embryo from trisomic mother, Eu/(Ts): euploid embryo from trisomic mother.

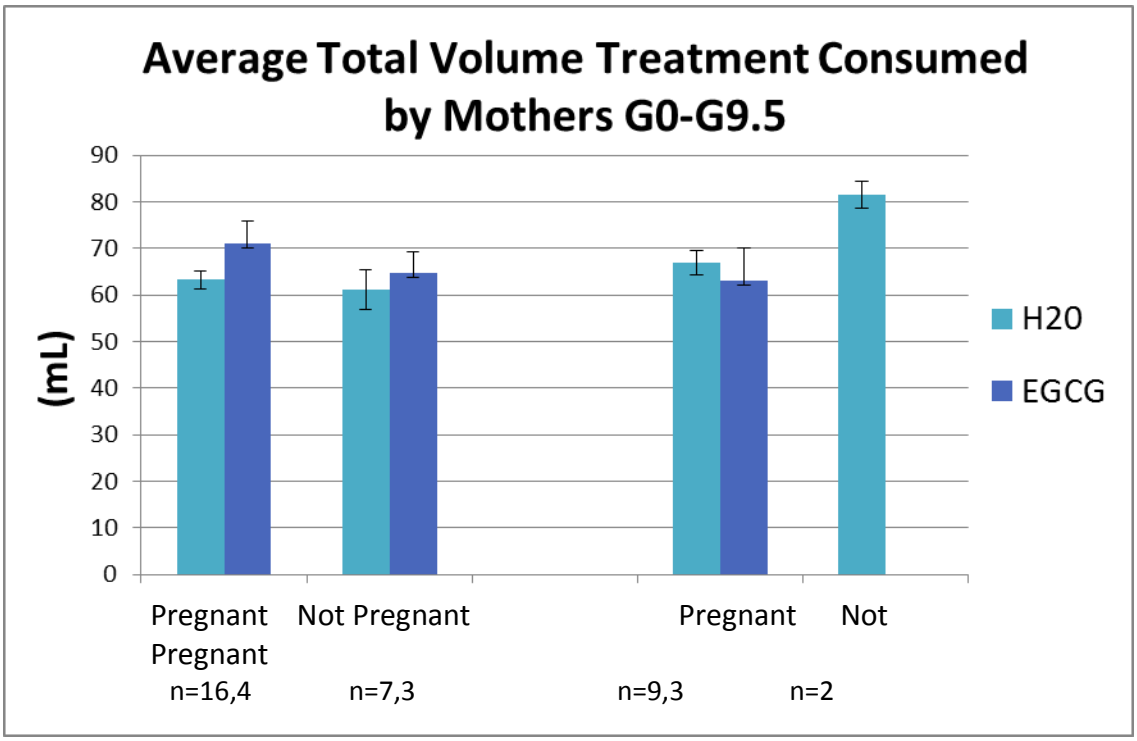

Figure 3.5: Average Total Volume Treatment Consumed by Mothers G0-G9.5. Ts65Dn (trisomic) or euploid mouse mothers (B6C3F1 euploid fathers) suspected to be pregnant after breeding were treated *ad libitum* with either H_2O or EGCG dissolved in H_2O from G0-G9.5. Volume of treatment consumed was measured every other day and recorded. There were no significant differences ($p \leq 0.05$) in the total volume of treatment consumed between pregnant or non-pregnant mice, trisomic or euploid mice, or between treatment groups.

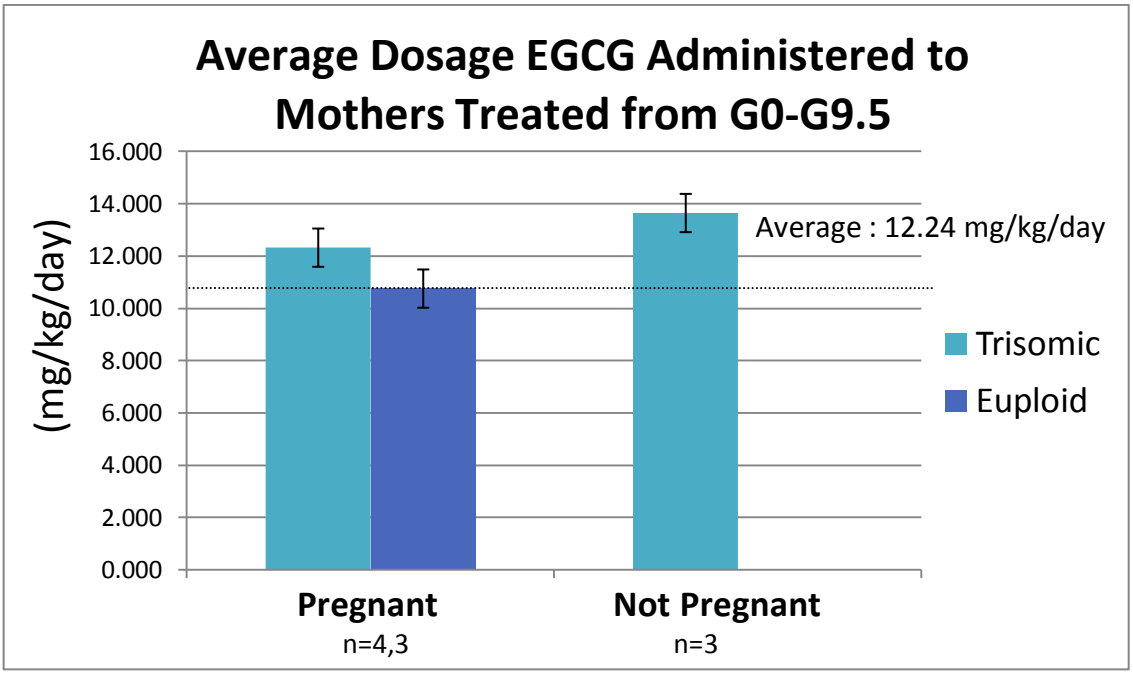

Figure 3.6: Average Dosage of EGCG Administered to Mothers Treated from G0 – G9.5. Ts65Dn (trisomic) or euploid mouse mothers (B6C3F1 euploid fathers) suspected to be pregnant after breeding were treated *ad libitum* with either H_2O or EGCG dissolved in H_2O from G0-G9.5. Volume of treatment consumed was measured every other day, recorded, and intake dose of EGCG calculated for each mouse. There were no significant differences between doses of EGCG for any test group. Average dose of EGCG for all three groups was ~12.238 ± 0.732 mg EGCG/kg body weight/day (mg/kg/day).

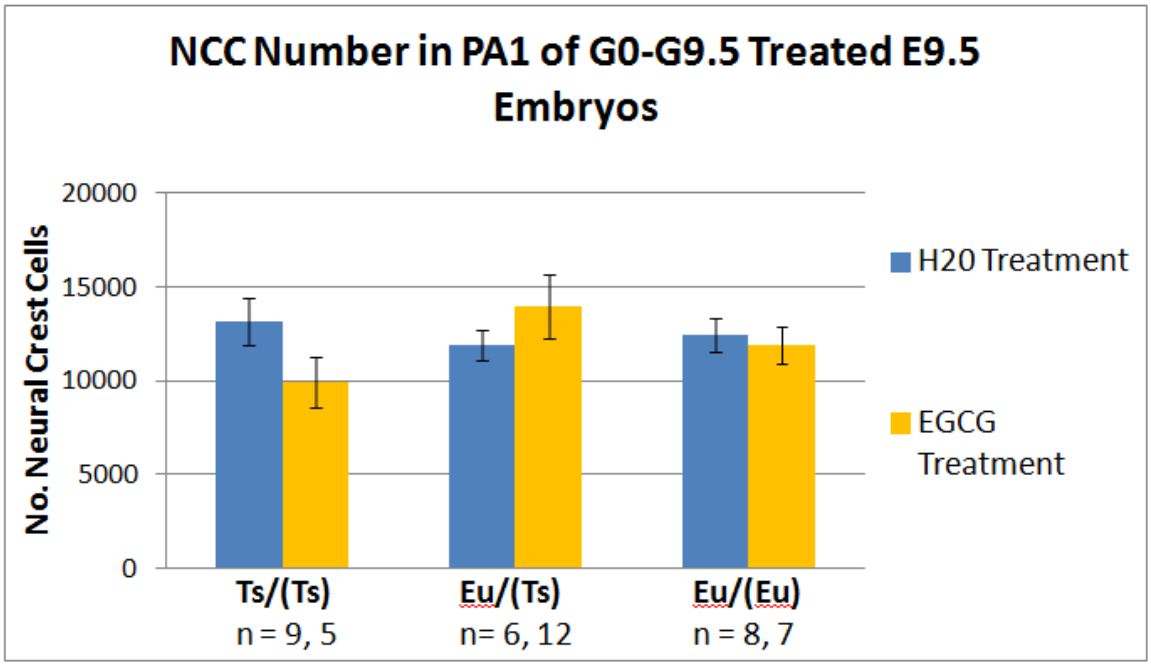

Figure 3.7: Number of Neural Crest Cells in the PA1 of G0-G9.5 Treated E9.5 Embryos. The NCC number of E9.5 embryos (staged 21-24 somites; B6C3F1 euploid fathers) whose mothers were treated with EGCG or water from G0-G9.5. EGCG treatment from G0-G9.5 at ~12.2 mg/kg/day did not significantly alter the number of NCC in E9.5 euploid embryos compared to untreated embryos. The slight but non-significant decrease in NCC in EGCG-treated Ts/(Ts) embryos was likely due to a lower average somite number in this group compared to water treated embryos (p=0.0613). Ts/(Ts): trisomic embryo from trisomic mother, Eu/(Ts): euploid embryo from trisomic mother, Eu/(Eu): euploid embryo from euploid mother.

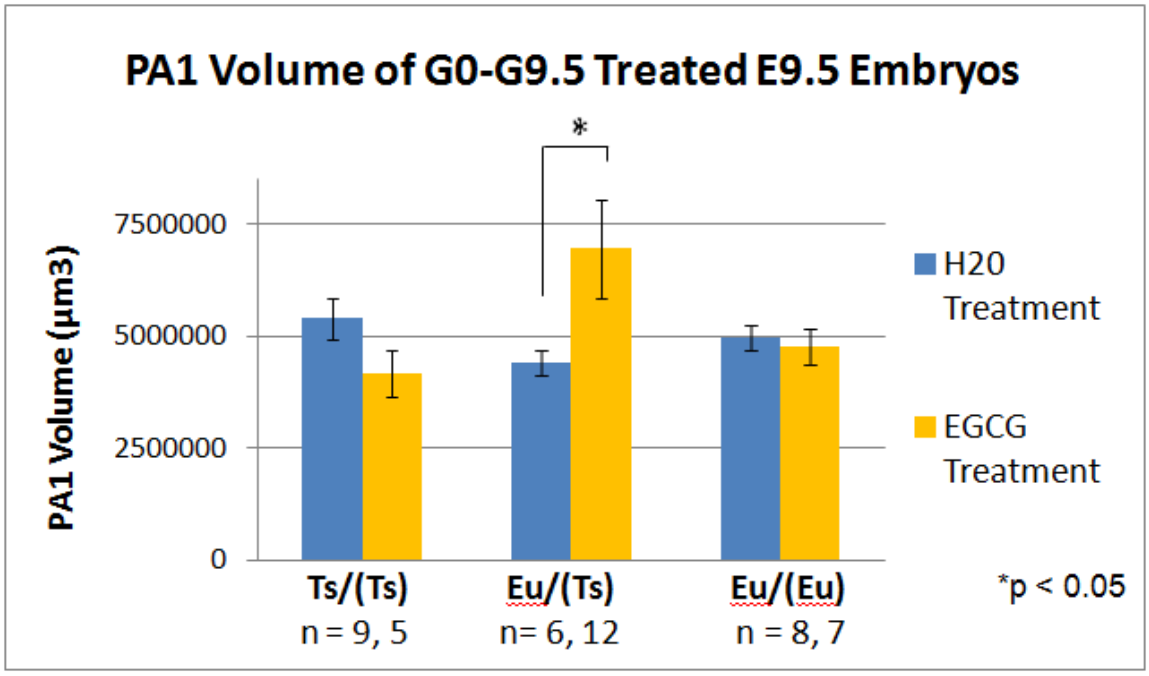

Figure 3.8: PA1 Volume of G0-G9.5 Treated E9.5 Embryos. The PA1 volume of E9.5 embryos (staged 21-24 somites; B6C3F1 euploid fathers) whose mothers were treated with EGCG or water from G0-G9.5. No significant differences in PA1 volume were attributed to G0-G9.5 EGCG treatment (p=0.058). PA1 volume was significantly increased in EGCG-treated Eu/(Ts) embryos compared to untreated embryos (*p=0.046). Ts/(Ts): trisomic embryo from trisomic mother, Eu/(Ts): euploid embryo from trisomic mother, Eu/(Eu): euploid embryo from euploid mother.

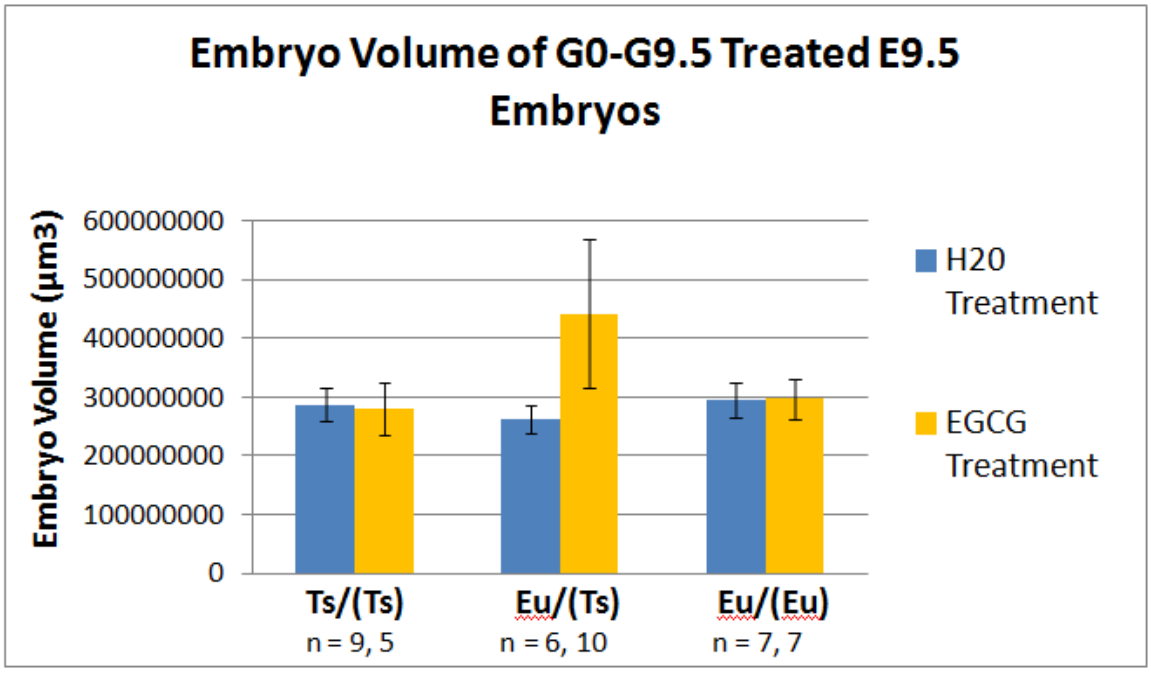

Figure 3.9: Embryo Volume of G0-G9.5 Treated E9.5 Embryos. The total embryo volume of E9.5 embryos (staged 21-24 somites; B6C3F1 euploid fathers) whose mothers were treated with EGCG or water from G0-G9.5. There were no differences between treated and untreated embryo volume of any trisomic or euploid embryos. Eu/(Ts) embryos treated with EGCG had slightly but not significantly larger embryo volume than embryos of all other treatment groups (p=0.089). Ts/(Ts): trisomic embryo from trisomic mother, Eu/(Ts): euploid embryo from trisomic mother, Eu/(Eu): euploid embryo from euploid mother.

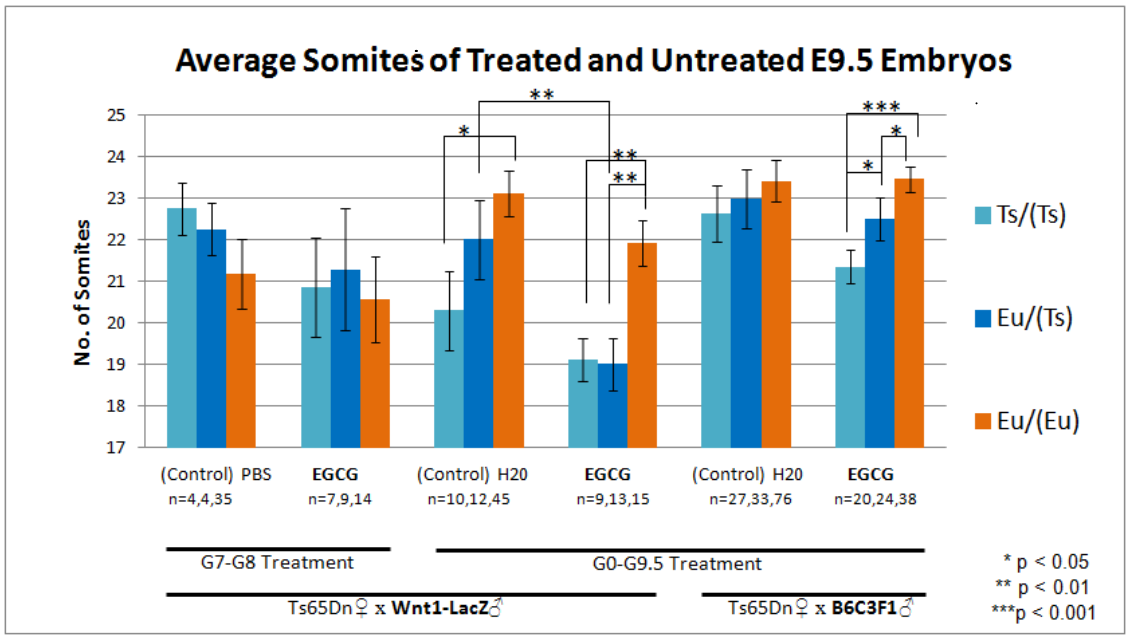

Figure 3.10: E9.5 Embryos from Trisomic Mothers Treated with G0-G9.5 EGCG Display Decreased Somite Numbers. Ts/(Ts) and Eu/(Ts) embryos from both Wnt1-LacZ and B6C3F1 fathers treated with EGCG G0-G9.5 displayed lower somite numbers on average compared to untreated embryos of the same genotype and Eu/(Eu) embryos in the same treatment group. This effect was more pronounced in embryos with Wnt1-LacZ fathers (average ~19 somites) than in embryos with B6C3F1 fathers (average ~21.5-22.5 somites). No significant differences were observed in somite numbers of embryos treated with PBS or EGCG from G7-G8. Ts/(Ts): trisomic embryos from trisomic mothers, Eu/(Ts): euploid embryos from trisomic mothers, Eu/(Eu): euploid embryos from euploid mothers). (*p≤0.05, **p≤0.01, ***p≤0.001).

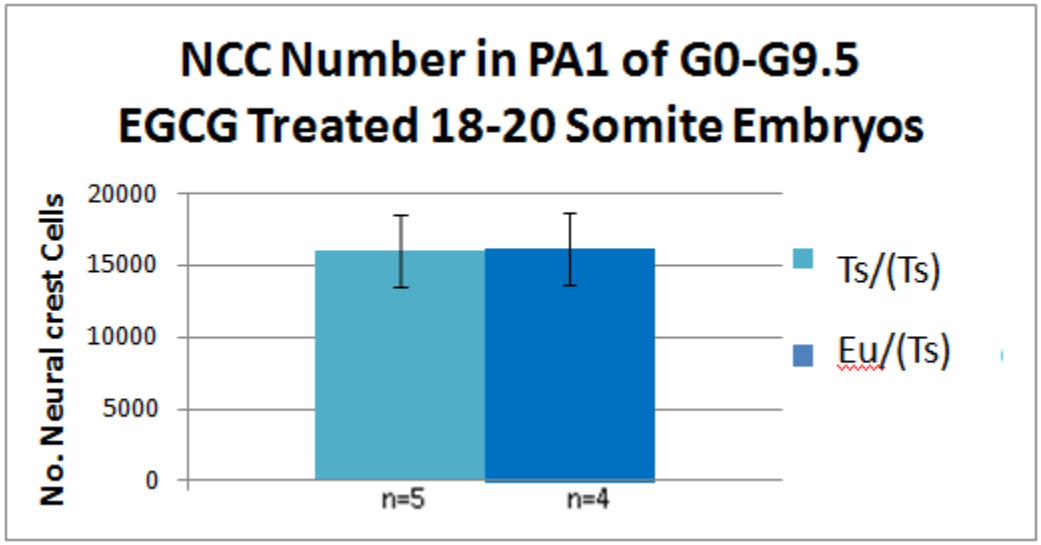

Figure 3.11: Number of Neural Crest Cells in PA1 of G0-G9.5 Treated 18-20 Somite Embryos. The NCC number of E9.5 embryos with Wnt1-LacZ fathers whose trisomic mothers were treated with EGCG from G0-G9.5. There are no differences in NCC number between trisomic and euploid embryos at this time point. These findings suggest that the NCC deficits in the PA1 in trisomic embryos occur after, but not during the 18-20 somite stage. Ts/(Ts): trisomic embryos from trisomic mothers, Eu/(Ts): euploid embryos from trisomic mothers.

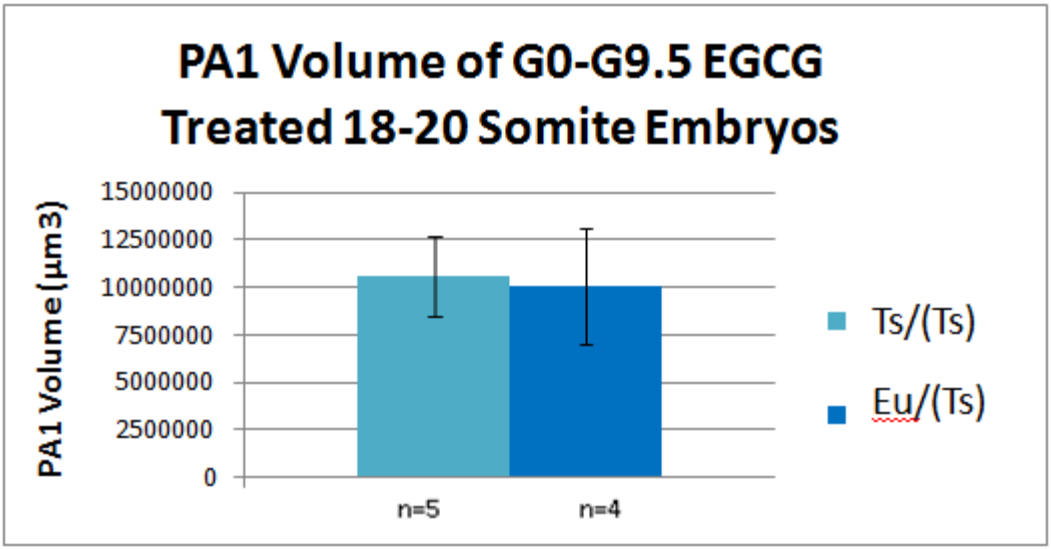

Figure 3.12: PA1 Volume of G0-G9.5 Treated 18-20 Somite Embryos. The PA1 volume of E9.5 embryos with Wnt1-LacZ fathers whose trisomic mothers were treated with EGCG from G0-G9.5. There are no differences in PA1 volume between trisomic and euploid embryos at this time point. These findings provide further evidence that the deficits in PA1 volume in trisomic embryos likely occur after, but not during the 18-20 somite stage. Ts/(Ts): trisomic embryos from trisomic mothers, Eu/(Ts): euploid embryos from trisomic mothers.

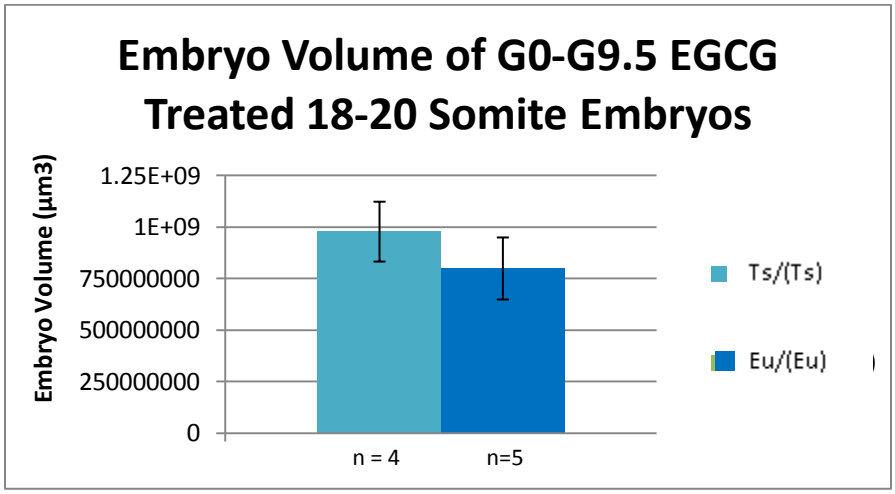

Figure 3.13: Embryo Volume of G0-G9.5 Treated 18-20 Somite Embryos. The embryo volume of E9.5 embryos with Wnt1-LacZ fathers whose trisomic mothers were treated with EGCG from G0-G9.5. There are no differences in total embryo volume between trisomic and euploid embryos at this time point. This suggests that trisomic embryos reach a statistically significant deficit in embryo volume compared to euploid littermates after, but not during the 18-20 somite stage. Ts/(Ts): trisomic embryos from trisomic mothers, Eu/(Ts): euploid embryos from trisomic mothers.

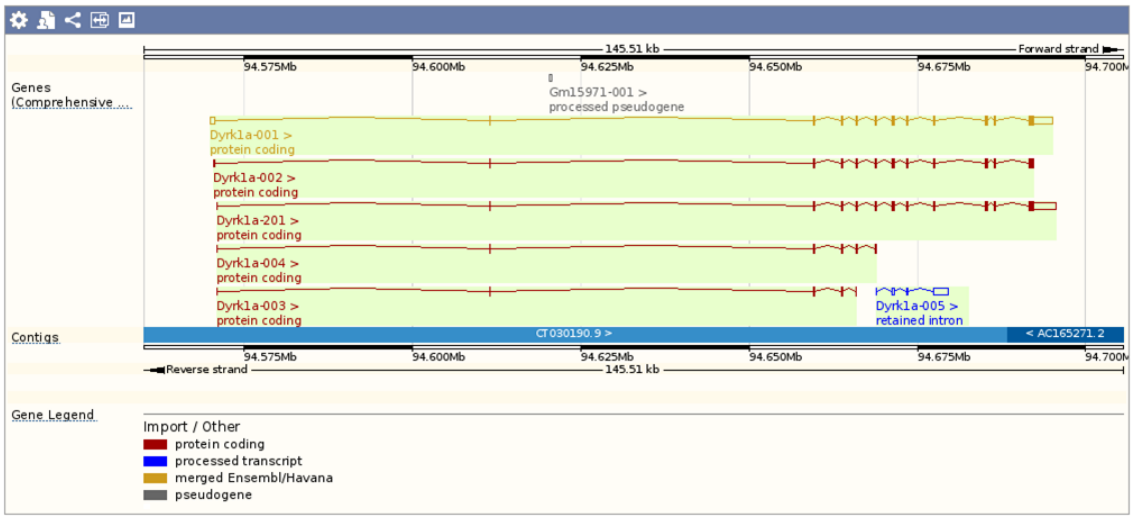

Figure 4.1: Comparison of *Dyrk1a* Transcript Variants from the Ensembl Genome Database. Screenshot from the Ensembl Genome Database of 5 aligned protein-coding and 1 non-protein coding transcript variant of the *Dyrk1a* gene on Mmu 16. (http://ueast.ensembl.org/Mus_musculus/Gene/Summary?db=core;g=ENSMUSG00000022897;r=16:94570010-94695517). Last accessed October 15, 2014

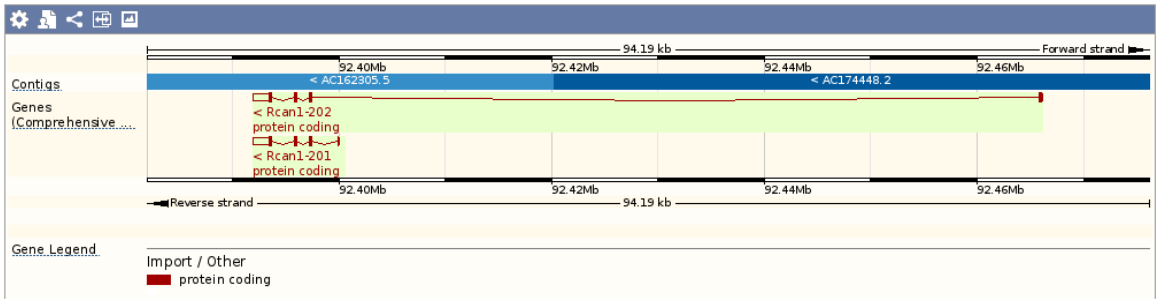

Figure 4.2: Comparison of *Rcan1* Transcript Variants from the Ensembl Genome Database. Screenshot from the Ensembl Genome Database of 2 aligned protein-coding transcript variants of the *Rcan1* gene on Mmu 16 (http://ueast.ensembl.org/Mus_musculus/Gene/Summary?db=core;g=ENSMUSG00000022951;r=16:92391953-92466146). Last accessed October 15, 2014

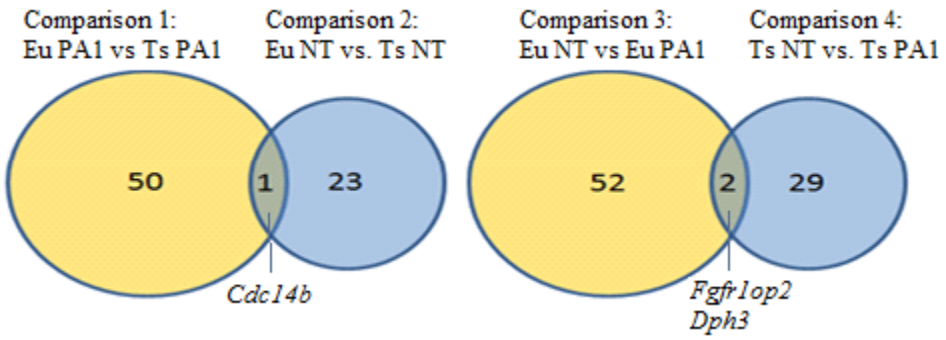

Figure 4.3: Detection of Alternative Splicing Events in Euploid and Trisomic E9.25 Neural Tube and E9.5 PA1 Tissue. Diagram shows the number of alternative splicing events detected using MISO when comparing RNA sequence data from either euploid (Eu) or trisomic/Ts65Dn (Ts) E9.5 first pharyngeal arch (PA1) or E9.25 neural tube (NT) tissue. Genes with alternative splicing events detected in multiple comparisons are numbered in the overlap of the yellow and blue circles and listed below. Data show approximately twice the number of alternative splicing events in PA1 tissue compared to NT tissue and in euploid NT and PA1 compared to trisomic NT and PA1. This shows that more alternative splicing is occurring in euploid tissues and in E9.5 PA1 tissue suggesting trisomy may decrease the number of alternative splicing events. This provides a further mechanism whereby trisomy may lead to an altered phenotype.

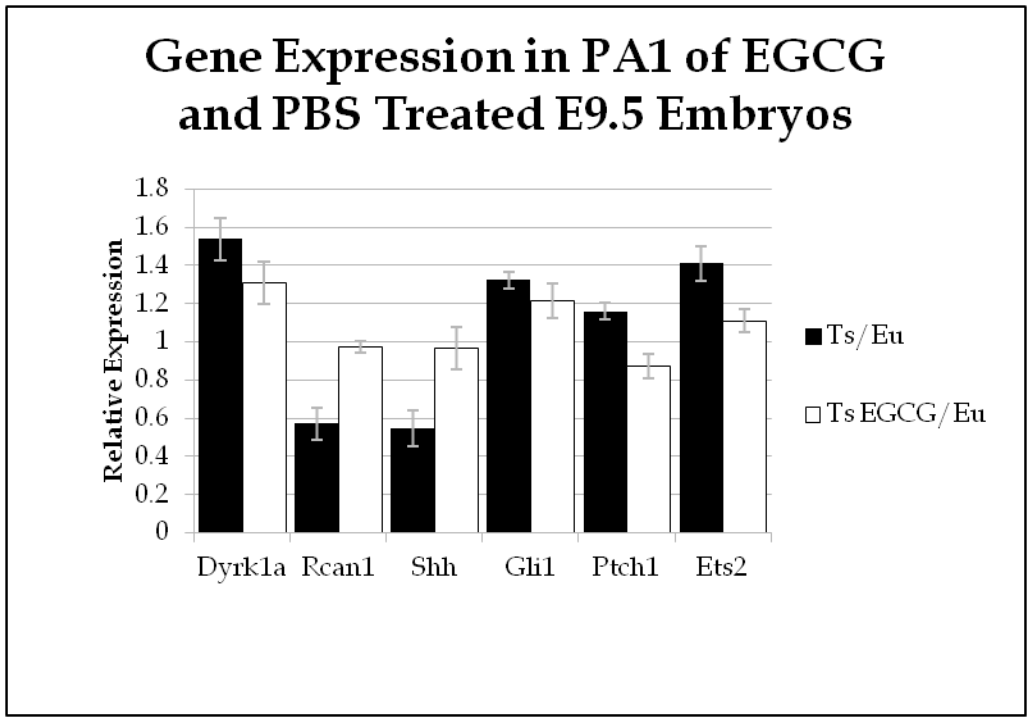

Figure 5.1: Relative Trisomic to Euploid Gene Expression in E9.5 PA1 with EGCG Treatment. Pregnant Ts65Dn mothers were treated with PBS or 400mg/kg/day EGCG twice per day on G7 and G8. Embryos were removed at G9.5 and PA1 tissue collected from embryos. qPCR was performed on RNA isolated taken from the E9.5 PA1 tissue. Expression levels of common developmental genes with a known role in DS were quantified. Gene expression of *Rcan1* and *Shh was* lower in EGCG treated samples compared to untreated samples. Expression of *Gli1, Ptch1, and Ets2* was elevated in EGCG treated samples compared to untreated samples (Unpublished data, Roper).